A STABLE DICATIONIC SALT IN REACTIVE DESI-MS IMAGING IN POSITIVE ION MODE TO ANALYZE BIOLOGICAL SAMPLES

DRAGOS LOSTUN

A THESIS SUBMITTED TO
THE FACULTY OF GRADUATE STUDIES
IN PARTIAL FULFILLMENT OF THE REQUIREMENTS
FOR THE DEGREE OF MASTERS OF SCIENCE

GRADUATE PROGRAM IN CHEMISTRY
YORK UNIVERSITY
TORONTO, ONTARIO
MAY 2015

Abstract

The main project of my master's thesis involved the application of a dicationic salt for imaging in reactive desorption electrospray ionization mass spectrometry (DESI-MS) on biological samples. The samples interrogated in this experiment were whole body zebrafish tissues and rat brain tissue. The stable dictation salt forms a stable bond with biological tissue fatty acids and lipids and allows detection in positive ion mode. Tandem mass spectrometry (MS/MS) was used to characterize the dication salt (DC9) and to identify linked lipid-dication compounds in rat brain and zebrafsh tissues. The fragmentation energy of dication-lipid bound compounds indicate a stabilizing effect of the dication which could be applied in other mass spectrometry methods. Reactive DESI-MS imaging in positive ion mode of rat brain and zebrafish tissues allowed enhanced detection of certain compounds commonly observed in negative ion mode. Variance in intensity between negative and positive mode indicate that the ionization process could be affected by matrix effects of various tissues, leading to different overall intensity which could provide new information on the same compounds when compared between negative ion mode images and reactive DESI positive ion mode images.

Another project involved a comparative study between DESI and easy ambient ionization (EASI) mass spectrometry methods. The study compared the methods in terms of spatial resolution, limits of detection, and overall imaging differences. Under similar conditions spray spatial resolution dictated mainly by spray spot size was found to have little to no variance between both methods. Limits of detection were one order of magnitude better for DESI for most compounds, but was matched by EASI in some cases. In terms of imaging capabilities both methods have similar chemical specificity and resolution, however DESI has a lower limit of detection.

Acknowledgements

I would like to thank my supervisor Professor Demian R. Ifa for the guidance and support provided. This experience gave me the opportunity to learn, practice, and further my understanding of chemistry. I would also like to thank the other members of my defence and supervisory committee, Professor Derek J. Wilson, Professor Diethard K. Bohme, and Professor Roger R. Lew for providing valuable feedback and insight.

I would also like to extend my gratitude to Dr. Elaine Cabral and Dr. Alessandra Tata for sharing their experience and providing guidance and advice in my work.

The assistance and help of Consuelo Perez has been a tremendous help with the dicationic experiments. All aspects of the experiment from the tissue slicing to pushing the paper into swift publication has been possible due to Consuelo Perez assistance.

I would like to extend my gratitude and recognize the efforts of David A. Barrett's group and Peter Licence from the University of Nottingham, for synthesizing and providing the dications for our group, their collaboration made the reactive DESI-MS experiments possible.

I would also like to thank my colleague Tanam Sanjana Hamid who I worked with on the DESI vs EASI comparison project for allowing me to practice and fully understand how DESI truly works. I am grateful for all my colleagues at the Center for Research in Mass Spectrometry for assistance and advice throughout my stay.

Table of Contents

List of Tables

List of Figures

CHAPTER 1

1. INTRODUCTION

1.1 Mass spectrometry – Fundamentals and background

Mass spectrometry is a well-established science field with a long history. Fundamentally a mass spectrometer is an instrument designed to measure the mass of a charged particle, it does so by correlating the speed of the charged particle moving through a magnetic field to its mass. An increase in charge on a particle results in a speed increase through the magnetic field therefore measurements obtained on a mass spectrometer are reported as mass to charge values (*m/z*). [1] The first mass spectrometer was created by J.J. Thomson in 1912 and was used to discover the existence of the stable isotopes of Neon-20 and Neon-22. [2]. In order to detect the mass of a compound it needs to have a charge whether negative or positive is not important as long as the compound has a charge. The process of converting a neutral compound into charged particle, also called an ion, is referred to as the ionization process and how well this process converts the compounds to ions is referred as ionization efficiency. [1] While the analyzers have improved exponentially over the last few decades, the ionization of compounds together with sample preparation is the principal challenge for many mass spectrometry techniques.

Traditionally mass spectrometry instruments required the sample to be introduced in a low pressure 10^{-6} torr environment in order to be ionized. Electron ionization (EI) was the first ionization source used on an organic compound in 1918. The sample is introduced into a low pressure chamber where a heated filament emits electrons accelerated towards the sample. The energy used to bombard the sample has with a broad maximum ionization efficiency around 70 electron volts (eV), causing the sample to fragment into smaller ions. This method is still being used today since it generates extensive and reproducible fragmentation useful in identification of compounds. [3]

Chemical ionization (CI) was introduced in 1966 as an alternative to EI, where the sample is collided with an ions of reagent gas, typically methane, in order to achieve less fragmentation. [4]. These early ionization techniques called “hard ionization” techniques resulted in numerous fragments making the detection of the main ion of the compounds difficult and created complex spectra which were often difficult to interpret. Over time innovation in instrumentation and ionization processes led to the so called “soft ionization” techniques which are able to ionize the compound with little to no fragmentation. [1].

1.2 Ambient Ionization Mass Spectrometry

While detection of compounds still require the sample to pass to the instrument detector at low pressure, ionization techniques have been developed to ionize the sample outside the instrument at standard atmospheric pressure before it is introduced in the mass spectrometer; this type of ionization techniques are called ambient ionization techniques. Electrospray Ionization (ESI) is one of the most common ionization techniques which is both a “soft ionization” technique and an ambient ionization technique, it was first introduced by Masamichi Yamashita and John B. Fenn in 1984[5]. ESI employs a charged solvent to ionize the sample allowing formation multiple charged ions without fragmentation. [5] ESI paved the way for several new developments among them Desorption Electrospray Ionization (DESI) and easy ambient sonic spray ionization (EASI). These methods are both ambient ionization methods and are spray based ionization techniques.

1.3 Imaging Mass Spectrometry & Ambient Imaging Mass spectrometry

Imaging mass spectrometry (IMS) works by compiling spectra obtained at different spatial coordinates, in order to generate an ion intensity distribution map of the sample. Several techniques such as (DESI-MS), Matrix-assisted laser desorption/ionization (MALDI-MS), and secondary ion mass spectrometry (SIMS) among many others, have used this procedure to create ion images over

a broad spectrum of samples. [6-8] Imaging mass spectrometry can be used to identify analytes of interest in localized regions, and taken together with ion spatial distribution and ion intensity map, representing relative abundance, can provide vital new in-situ information. [9-12] Ambient ionization IMS methods ionize the sample at atmospheric pressure, this allows for insertion of ions into the analyzer and not the entire sample, [13] due to this procedure ambient IMS based techniques require minimal or no sample preparation, and are generally fast analysis techniques.[14] To give an example of how powerful imaging mass spectrometry techniques can be, DESI-MS imaging has been implemented for cancer diagnostic in human prostate tissue[15] DESI-MS has been used for imaging mass spectrometry since 2006, for discriminating forgeries, and for analysis of a variety of biological tissue samples, such as, rat brain tissue, adrenal gland, and bladder tissues for cancer diagnostic research, to name a few [6, 16-24]

1.4 DESI-MS

DESI-MS technique was introduced in 2004 by professor Graham Cooks and coworkers at Purdue University. This technique is an ambient and soft ionization technique and unlike traditional ESI, a charged solvent spray is nebulized via high gas pressure onto the sample adding a desorption step to the process of analysis. DESI has been implemented in a wide range of fields such as metabolomics [20], pharmaceuticals[20], forensics[16-18] and analysis of polymers [19].

1.4.1 DESI Ionization mechanisms

DESI works via a “droplet pickup mechanism”, where a charged solvent spray is nebulized, with the assistance of a nebulizing gas, generating charged microdroplets. These charged droplets hit the sample surface generating small area with a thin liquid film. Subsequent droplets impacting the thin liquid interface desorb progeny droplets containing sample analytes. DESI ionization follows one of two processes, for small molecules ionization occurs via charge transfer typically

an electron or a proton charge transfer occurs in the gas phase; while high mass molecules tend to have multiple charges transferred from the charged solvent droplet, the transfer of charge occurs in liquid phase.[25] Gas phase ions are generated from the drying of the progeny droplets with analytes, which then proceed towards the MS inlet to be analyzed by the mass spectrometer.[26]

1.4.2 DESI – setup parameters, factors and experimental considerations for imaging

A typical schematic is presented in Figure 1 along with a picture of the custom DESI source used in the experiments for reference.The DESI ionization source assembly is composed of an inner silica capillary through which the charged solvent passes, an outer silica capillary through which Nitrogen gas passes. The gas nebulizes the solvent onto the sample and is typically set to 100 psi, it can be used at a higher pressure however at very high pressures sample can be damaged by high pressure resulting in poor ion images. The DESI spray assembly is mounted on a XYZ platform which allows adjustments in distance and angle of the spray tip relative to the instrument inlet and the sample surface, a XYZ motor on the sample platform allows for imaging experiments. A metal clamp on the solvent syringe needle charges the solvent, typically applying 4-5 kV. Solvent flow rate for DESI imaging is typically ranges between 1-5µL/min, higher flow rates result in sample smearing and are avoided in imaging experiments. Solvent composition of MeOH/H2O mix is generally preferred due to its ionization efficiency and rapid evaporation, often resulting in high quality images however DESI is a versatile method and the solvent is often varied based on experimental requirements. Sample surface is another important factor, a surface which allows easy desorption and enhance ionization such as, porous polytetrafluoroethylene (PTFE). For optimum DESI imaging analysis a hard and flat surface is required for efficient desorption and signal stability. Many other surfaces have been used based on sample experimental needs such as TLC plates, filter paper, microscopic glass slides, however nonconductive surfaces are preferred.

Based on the distance and angle of the spray, the pressure and the solvent composition, sample surface, spray spot size on the sample will vary and in turn it affects minimum distance required in order to differentiate two neighboring spectra in space, often referred to as spatial resolution. Typical lateral spatial resolution, which is the capability to clearly distinguish between two adjacent spots on the surface, is typically 200 µm. However, the spatial resolution can be reduced to 40 µm under specific conditions [27]. Typical limits of detection (LOD) have been reported in the range of picograms (pg) to femtograms (fg) making DESI-MS a sensitive method useful for trace amount detection.[28, 29]

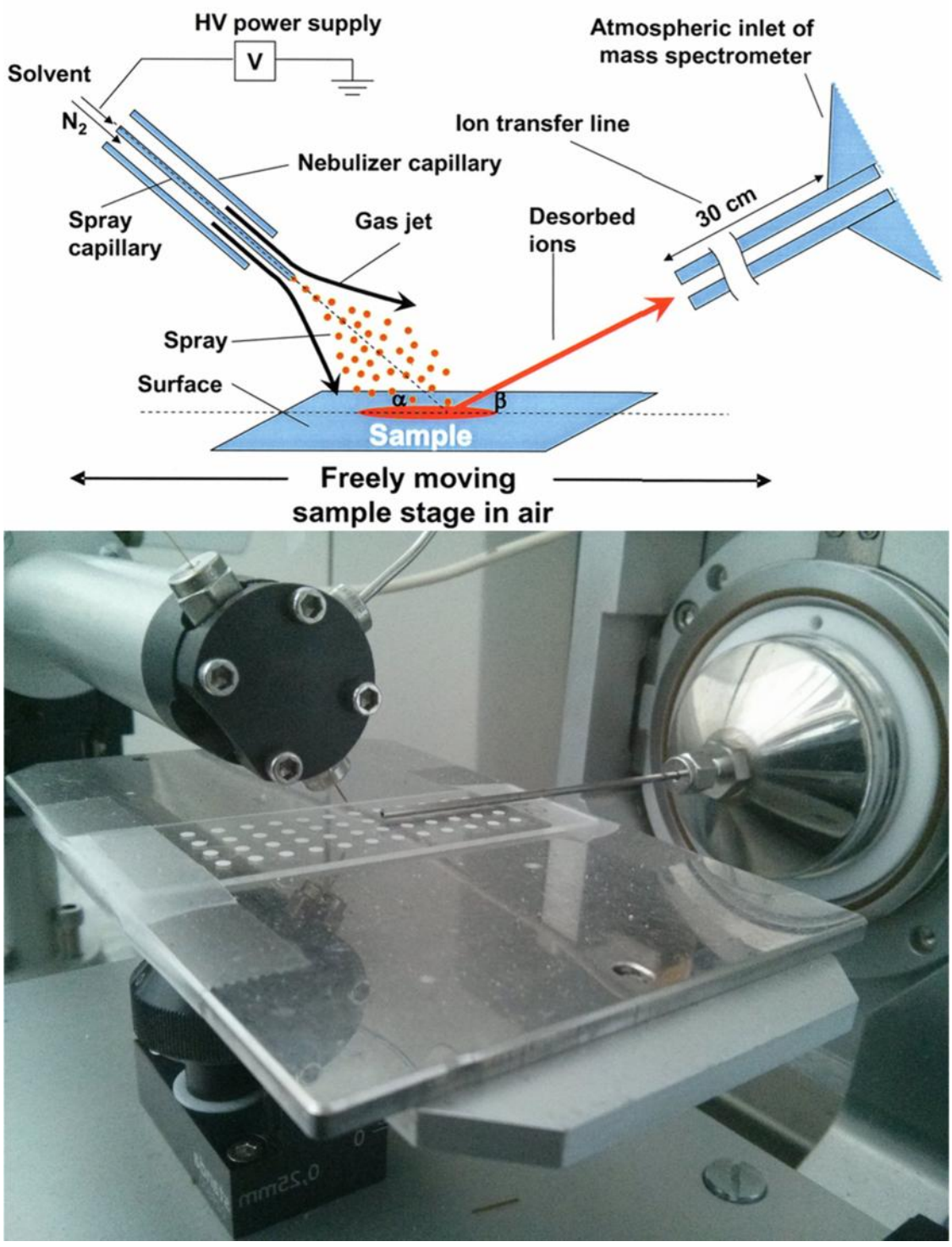

Figure 1. Schematic of a typical DESI-MS setup at the top.[30] Bottom is a picture of custom lab built DESI source used.

1.4.3 Reactive DESI-MS

Reactive DESI-MS is a variant of the DESI-MS technique, in which a reactant is included in the spray solvent. When the solution is sprayed on the sample surface it reacts with the sample analyte, the resulting product is analyzed by the mass spectrometer. Reactive DESI-MS has been used when working with samples that are hard to ionize, typically via simple adduct formation, such as complexation of RDX with the anion CF_3COO^-, or TNT with the methoxide anion[28, 30]. Hao Chen et al. introduced bond-forming reactions using reactive DESI. The experiment used cyclization with benzeneboronate anions $PhB(OH)_3^-$ on biomolecules containing aliphatic diols and aromatic diols, compounds which are not ionized efficiently via ESI and MALDI.[31] Reactive DESI is a powerful tool due to its capabilities to be able to target molecules of interest or compounds which are difficult to ionize, in order to detect and/or enhance ionization efficiency.[24, 28, 32, 33]

1.5 EASI-MS

Easy ambient sonic spray ionization (EASI) technique was introduced in 2006 initially under the name of desorption sonic spray ionization (DeSSI), [21] and it was later renamed from 2008 onwards as EASI[34]. This technique is similar in setup but it doesn't apply voltage to the solvent thus undergoing a different ionization mechanism claimed to be an even softer alternative to ESI. EASI has been successfully applied to quality control and forensic analysis.[21, 35, 36] It has been also applied to check for the purity of biodiesel, among other applications. [37, 38].

1.5.1 EASI ionization mechanism

EASI uses sonic spray ionization in order to generate ions. This mechanism involves generation of unbalanced charged distribution in solvent droplets under high gas flow rate (>3.0L/min) and high nebulizing gas backpressure, typically 400 psi. This results in a small percentage of droplets

having either a negative or positive charge due to an uneven evaporation and distribution of solvent. The intensity of the ions produced in the sonic spray is strongly depended on the nebulizing gas velocity [39] The low amount of unbalanced solvent droplets required for efficient ionization is compensated using an high solvent flow rate, typically 20 µL/min. [21] The EASI-MS setup used is virtually identical to that of the DESI-MS setup, the difference being the absence of a voltage applied to the solvent, and different pressure and solvent flow rate.

Chapter 2

2. Reactive DESI-MS imaging of biological tissues with dicationic ion-pairing compounds

2.1 Introduction

This work illustrates application of a stable dicationic reactant in reactive desorption electrospray ionization mode mass spectrometry (DESI-MS) on rat brain and zebrafish tissues.

The dicationic reactant used is an ionic salt. Ionic salts have been traditionally used in organic synthesis and more recently in mass spectrometry to ionize difficult samples, target specific compounds, and/or to generally enhance ionization efficiency. [40-44] Barrett's group recently published a work involving nine dicationic ion-pairing compounds using DESI-MS for enhanced lipid detection, naming such compounds: DC1 to DC9. From the nine dicationic compounds tested against lipid standards, most compounds were able to form stable ion-pairs with the tested negatively charged lipid species. The dications have a similar structure of two rings of 5-6 atoms,

linked by a hydrocarbon chain with varying length and a positive charge on each nitrogen atom on the two rings. Of the compounds tested, DC2 and DC9 demonstrated signal enhancement and DC9 attained superior signal intensity over a broader range of compounds than DC2, therefore DC9 has been chosen for the imaging experiments. [40] DC9 has the molecular formula $[C_6(C_1Pyrr)_2][Br]_2$ and is a stable dicationic salt able to bind to a negatively charged compound, a figure of the structure of DC9 without the bromide counter ions can be seen in Figure 2.

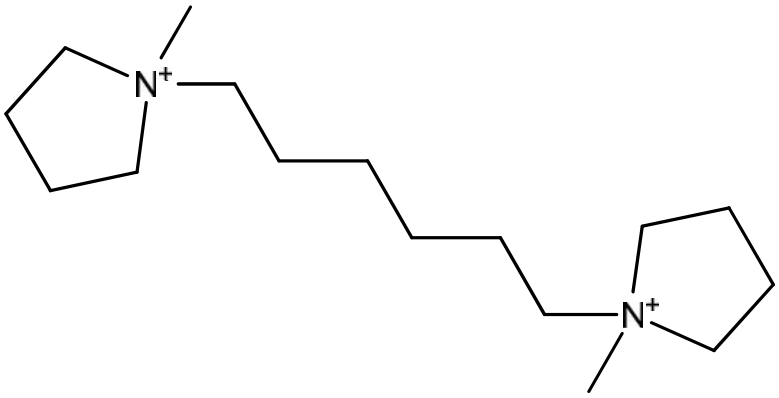

1,1'-(hexane-1,6-diyl)bis(1-methylpyrrolidin-1-ium)

Figure 2. DC9 dication compound structure with the formal name, depicted without the two bromide counter ions.

DC9 has a mass of 254.4 Da consisting of two positive charges on the nitrogen atoms from which it can be observed at *m/z* 127.2 by DESI-MS. The dication salt can bind to lipids, the net charge of the complex becomes positive which permits imaging of compounds, more importantly, lipids in positive ion mode. Fatty acids and certain classes of lipids are detected in negative ion mode however, DC9 is capable of creating an ion-pair changing the polarity of the compounds for DESI-MS analysis. Analyses with DC9 in positive ion mode allows for higher signal to noise ratio and increased sensitivity for selected lipids when compared to negative ion mode. These new compounds are not fully understood and factors such as steric hindrance, structural flexibility and

charge localization affect the binding of the ionic liquid to the targeted lipid for detection in positive ion mode. [40]

This experiment uses dicationic compounds for imaging purposes for the first time in DES-IMS and evaluates the performance of the dicationic compound DC9 in complex biological tissue samples in positive ion mode by reactive DESI-MS. Enhancements of lipid signal intensity and/or signal to noise levels due to a change in polarity can allow improved imaging of biological samples. Imaging experiments were performed on whole body zebrafish and rat brain tissue slices. Zebrafish was selected since it is an important biological model commonly used to study genetics[45, 46], environmental toxicology[47-50], cancer[51, 52], and other diseases[53-55]. In addition, rat brain is another important biological model generally used to study behavioural patterns [56, 57], cancer[58, 59], and disease[60-64].

This study presents applications for imaging of lipids in positive ion mode from rat brain and whole body zebrafish tissue with enhanced intensity and ionization efficiency using reactive DESI-MS. DESI-MS has been employed in negative ion mode to discriminate normal from cancerous tissue based on lipid profiles[65-67]; using this application can lead to new avenues into cancer research and lipidomics studies on complex tissues.

2.2 Materials and Methods

2.2.1 Materials and biological samples

The HPLC grade methanol, tricainemesylate and carboxymethyl cellulose sodium (CMC) were purchased from Sigma-Aldrich (Oakville, ON, CA). Porous PTFE sheets 1.5 mm thick with a

medium porous size of 7 µm was purchased from Berghof (Eningen, Germany). Microscope slides 26 mm x 77 mm thickness 1 mm single frosted were purchased from Bionuclear diagnostics Inc. (Toronto, ON, Canada). Rat brains were purchased from Rockland Immunochemicals Inc. (Gilbertsville, PA, USA). Zebrafish were donated by Dr. Chun Peng (York University, Toronto, ON, CA). H&E staining kit was purchased from American Master Tech Scientific (Lodi, CA, USA).

2.2.2 Dicationic compound synthesis and preparation

The compound DC9 investigated in this study was synthesized using previously reported literature. [40, 68, 69] A stock solution of 1 mM was prepared by dissolving DC9 in methanol. A diluted 10 µM DC9 solution was prepared from DC9 stock solution and diluted into a 20 mL sterilized vial with methanol. All DESI-MS, imaging and tandem mass spectrometry (MS/MS) experiments with DC9 were conducted with 10 µM DC9 methanol solution in the solvent spray. For the purpose of this study dicationic compound DC9 was investigated against biological tissue samples.

2.2.3 Rat brain sample preparation and cryosectioning

Rat brain was stored in a -80°C freezer. The brain was sectioned into 20 µm size coronal cross section slices on a Shandon cryotome FE and FSE (Thermo Fischer Scientific, Nepean, ON, Canada). The sections were placed onto microscope glass slides and kept frozen in a -18°C freezer. Prior to DESI-MS analysis, the rat brain tissue slices were defrosted and dried for 30 minutes at room temperature. H&E staining was conducted on adjacent tissue sections after DESI-MS analysis.

2.2.4 Zebrafish tissue sample preparation and cryosectioning

Four zebrafish were euthanized in a container with tricainemesylate solution at 300 mg/L. The deceased fish were placed into flexible moulds to provide support and prevent deformation while cryosectioning. A 5% CMC solution was prepared with distilled water and poured into each mould containing a whole body zebrafish. The moulds were immediately frozen at -18°C overnight before sectioning. For cryosectioning, the plastic mould was removed and CMC frozen zebrafish blocks were used to prepare 20-50 µm sagittal tissue sections. The fish slices were placed on glass microscopic glass slides and kept in -18°C freezer until use. Prior to DESI-MS analysis, the zebrafish slices were defrosted and dried for 30 minutes at room temperature. H&E was conducted on adjacent tissue sections after DESI-MS analysis.

2.2.5 Tandem mass spectrometry (MS/MS) analysis

For the DC9 characterization, 2µL of a 10µM solution was spotted on a PTFE surface and sprayed with pure methanol. For the characterization in reactive DESI-MS, a methanol solvent containing 10µM DC9 was sprayed directly onto the biological tissue samples. The MS/MS collision energy was set to 90 (arbitrary units) for DC9 and 12 (arbitrary units) for the DC9-lipid compounds.

2.2.6 DESI-MS parameters for rat brain and zebrafish tissue

The nebulizing nitrogen gas back pressure was 120 psi, the solvent voltage was set at 5 kV, the spray capillary to surface angle was 52°, the spray capillary to surface distance was ~0.5-2 mm, spray capillary to inlet distance was 4-5mm. The solvent flow rate was set at 3 µL/min and solvent composition was pure MeOH for negative ion and positive ion modes control, and MeOH spiked to 10 µM DC9 for reactive DESI-MS positive ion mode. The injection time was set at 30 ms and 40 ms for rat brain and zebrafish respectively. Imaging spatial resolution was set at 150µm for both rat brain and zebrafish. The mass range for negative ion mode scanned in the range of *m/z*

200-800, and for positive ion mode control and reactive DESI-MS positive ion mode in the range of *m/z* 454-1254. The data was acquired on a Thermo Finnigan LTQ using Xcalibur™ and was processed using Biomap (freeware, www.msi.maldi.org) to generate ion images of signal intensity versus spatial coordinates.

2.3 Results and Discussion

The dication, DC9, is a new compound without previous fragmentation data available in the literature. The first step was to obtain tandem mass spectrometry data by fragmenting the DC9 compound. This was achieved by spotting 2uL of 10 µM of DC9 onto a PTFE surface and spraying with a pure methanol solvent solution. A concentration of 10 µM was chosen because is the same concentration as in the experiments performed by Barret et al. with lipid standards. PTFE was chosen due to its chemically inert surface to ensure the sample did not react with the surface. In the full spectrum the predominant peak was observed at *m/z* 127.2, this corresponds to the doubly charged DC9 compound. The double charge of the molecule is confirmed by observing the natural isotope at *m/z* 127.70 which is calculated at 17.7% of the main peak and is observed about 18% on the tested compound spectra. (Figure 3 inset) A slight mass shift of 0.1 *m/z* is observed in (Figure 3) when looking at the full scan and it was taken into account for all experiments.

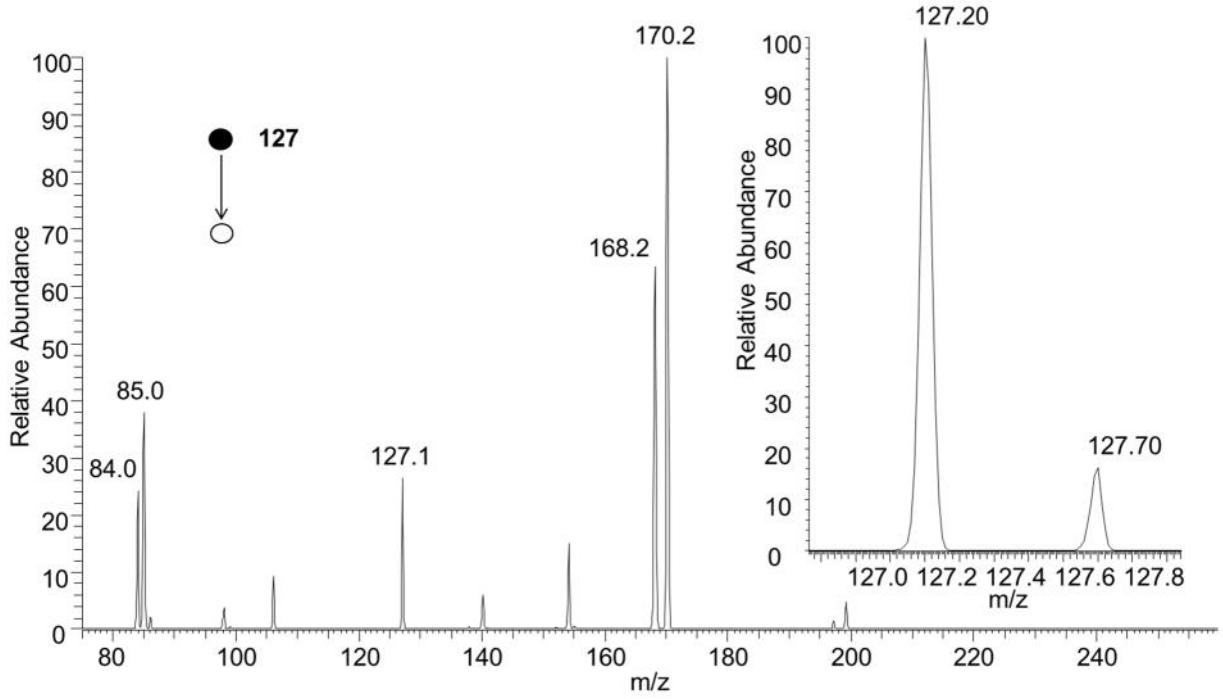

Figure 3. Tandem mass spectrometry (MS/MS) analysis of dicationic compound DC9 observed at *m/z* 127. Inset is a zoom scan (a feature of Thermo Finnigan instrument, a scan with a higher resolution and longer acquisition time) which shows the natural abundance isotope of the doubly charged species.

The ion at 127 was selected for fragmentation, resulting in fragmentation only when subjected to high collision energy, fragmentation started to occur above (70 arbitrary units) and required ~90 arbitrary units to obtain the spectra in Figure 3. Four main fragments have been observed. An alpha cleavage of the nitrogen ring results in a fragment at *m/z* 85 corresponding to an N-methyl pyrrolidine radical cation.

The complementary radical cation at *m/z* 169 is not observed, however an ion at *m/z* 168 is observed, most likely a result of the *m/z* 169 radical losing a hydrogen to create a stable terminal double bond. A fragment at *m/z* 84 is also observed which is likely due to the *m/z* 85 methyl heterocyclic ring cation undergoing rearrangement to create a double bond. A complementary

cation to *m/z* 84 is also observed at *m/z* 170, most likely a result of the *m/z* 169 radical cation gaining a hydrogen on the terminal chain to stabilize the radical charge.

2.3.1 Rat brain DESI-MS analysis

Rat brain is an important biological model that has been used to study behavioural patterns [56, 57], cancer[58, 59], and disease[60-64]. Different solvent systems were investigated briefly in a previous study[40]. It was found that a mix of pure methanol gave a superior signal than methanol/chloroform. All experiments involving DESI-MS in negative and positive ion mode controls were performed under optimum solvent conditions of pure methanol. The rat brain tissue was submitted to three analyses for compound identification and comparison: DESI-MS in positive ion mode control, DESI-MS in negative ion mode, and reactive DESI-MS with DC9 in positive ion mode. Imaging was performed with reactive DESI positive ion mode and negative ion mode to obtain *in situ* information on the compounds identified.

In the positive ion mode control (Figure 5a) a cluster of phosphatidylcholines between *m/z* 700-900 was observed. MS/MS analysis was conducted on the peaks in the cluster and several of the highest intensity compounds: *m/z* 782, 798 and 848 were identified as phosphatidylcholines. Phosphatidylcholines have a main fragment neutral loss of 59 Da associated with trimethylamine and a neutral loss of 183 Da corresponding to the choline head group which was observed in the peaks between *m/z* 700-900 (Figure 4). [70-72] The cluster of phosphatidylcholines is observed also in the reactive DESI-MS experiments on rat brain tissue (Figure 5c).

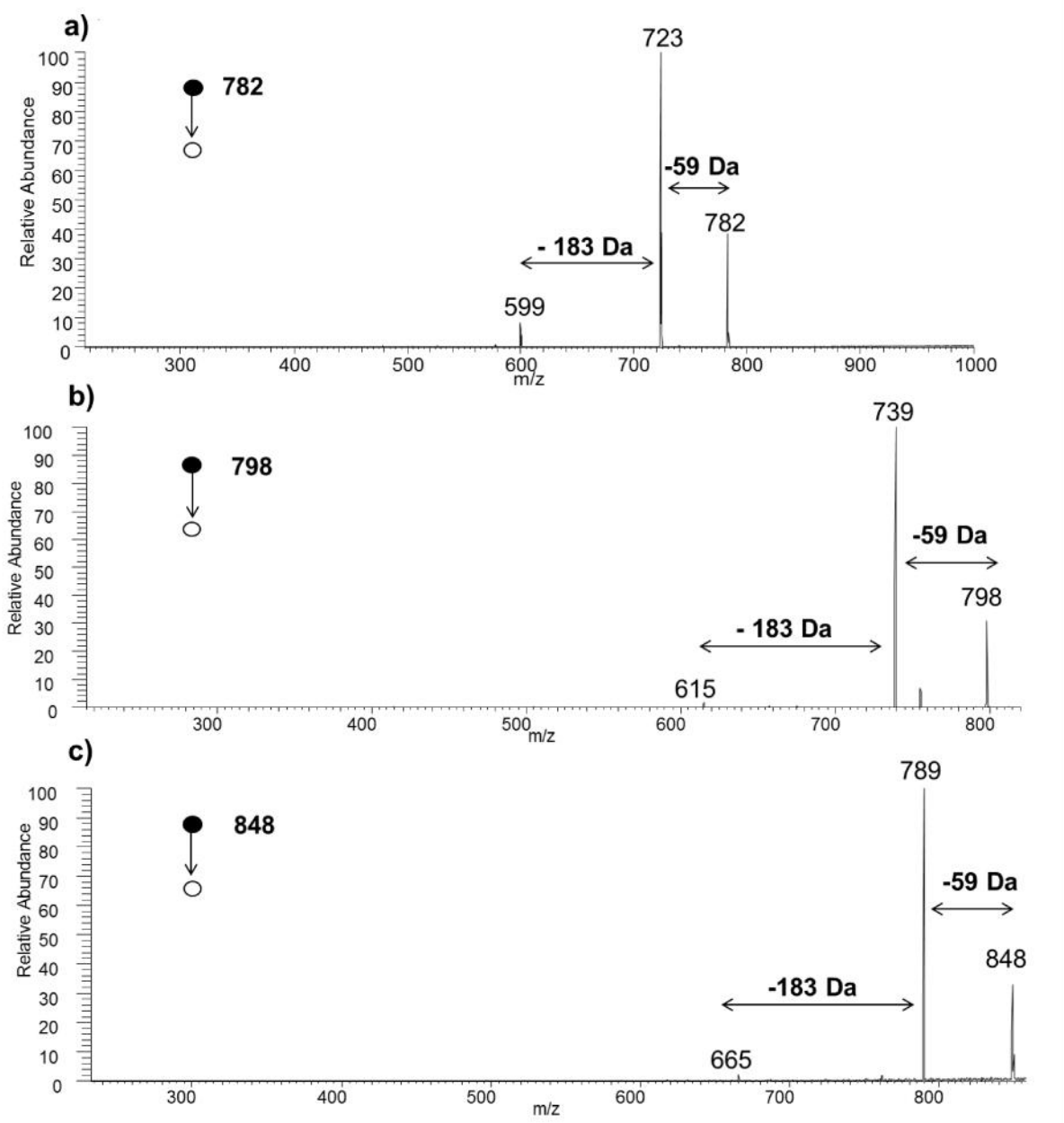

Figure 4. Tandem mass spectrometry MS/MS spectra of selected phosphatidylcholines in the full scan DESI-MS spectrum of rat brain in positive mode with common losses of 59 Da and 183 Da corresponding to trimethylamine and the choline head group, respectively. (a) MS/MS spectrum of potassiated phosphatidylcholine, PC (16:0/18:1) at *m/z* 782 (b) MS/MS spectrum of potassiated phosphatidylcholine, PC(16:0/18:1) at *m/z* 798 (c) MS/MS spectrum of potassiated phosphatidylcholine, PC (18:0/20:4) at *m/z* 848.

A negative ion mode scan was done in order to identify possible candidates for complexation with the DC9 dication. Analysis of fatty acids and phospholipids in negative ion mode on rat brain tissue has been previously studied, therefore these compounds were assigned according to literature.[73-76] In the negative ion mode, two distinct cluster of ions were present in the rat brain tissue (Figure 5b). In the first cluster of ions, between *m/z* range of 250-350, palmitoleic acid (16:1) at *m/z* 253, palmitic acid (16:0) at *m/z* 255, oleic acid (18:1) at *m/z* 281 and arachidonic acid (20:4) at *m/z* 303 were identified (Table 1). While the second cluster was observed between *m/z* range of 700-900 consisting of phosphoethanolamine (PE 36:1) at *m/z* 700 (not labelled on Figure 5), phosphoethanolamine (PE 36:2) at *m/z* 726, phosphoethanolamine (PE 38:4) at *m/z* 766 (not shown), phosphoethanolamine (PE 40:6) at *m/z* 774 and phosphoethanolamine (PE 40:6) at *m/z* 790 (Figure 5b and Table 1).

Small molecules that bind to DC9 would give peaks between *m/z* 254 – 350, and would give rise to strong peaks that supress ionization. DC9 has a permanent charge and a very strong signal intensity. The mass range around 254 displays a very strong peak supressing the signal and leading to broad peaks and unstable signals, therefore it is necessary to choose a mass range above this peak to acquire quality data with DC9, due to these constrains the mass range for reactive DESI-MS was selected to start at *m/z* 454 to align the negative and positive ions and allow for easy visual comparison. Figure 5 has a DC9 mass shift range of + *m/z* 254 for the positive ion mode in order to align the ions bound to DC9 with the observed negative ions.

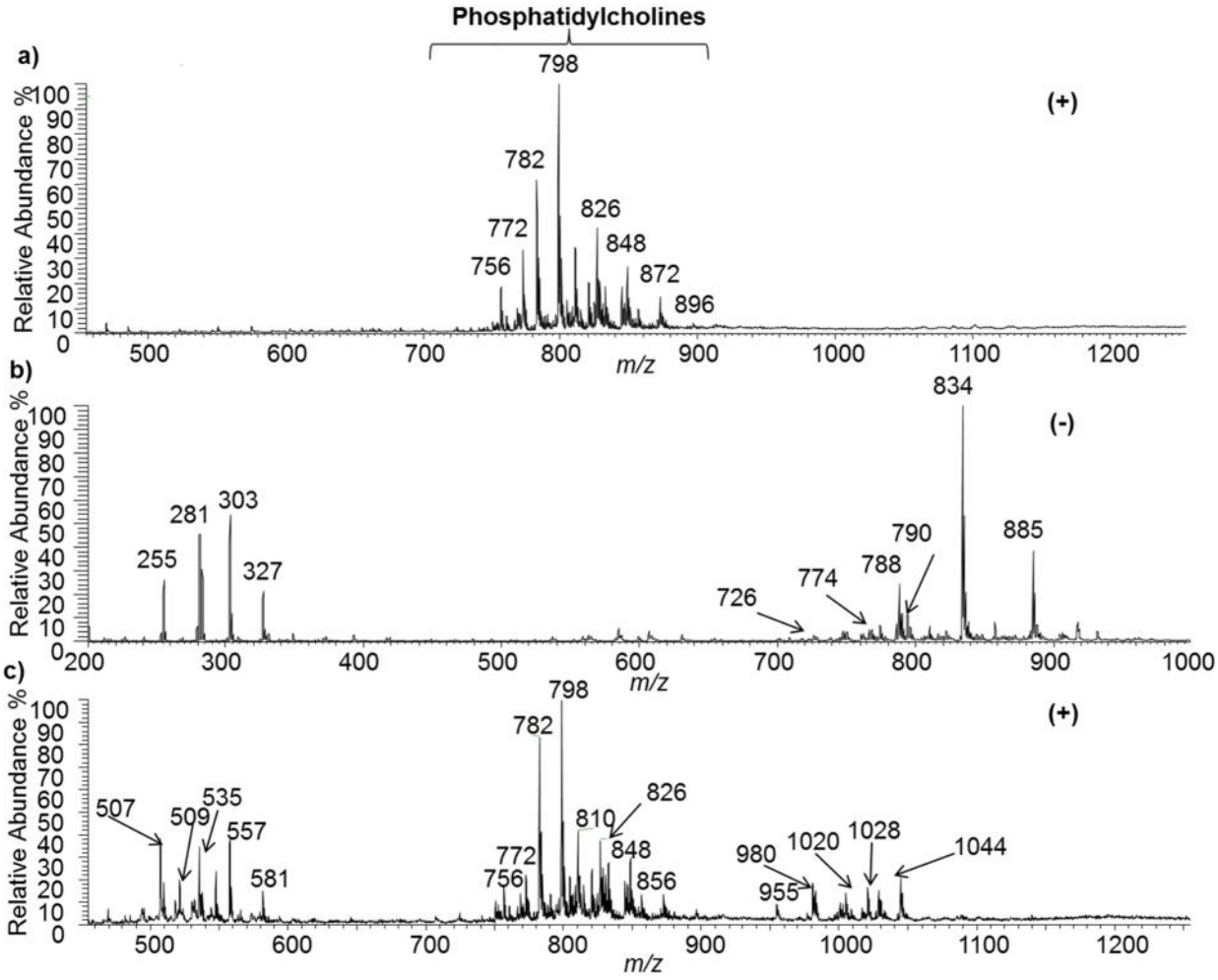

Figure 5. Representative DESI-MS mass spectra of lipids in rat brain (a) phosphatidylcholines present in rat brain in the positive ion mode control (b) lipids in rat brain in negative ion mode control (c) Reactive DESI-MS spectrum of enhanced intensity DC9-lipid ion pairs in rat brain in positive ion mode

Analysis of the reactive DESI scan was compared to the positive control and the negative control scans in order to assign which lipid ions were present in the reactive DESI spectra as DC9-lipid ion pairs. Several fatty acids and lipids present in DESI-MS negative ion mode are observed in the

positive DC9 spectra. In positive ion mode reactive DESI-MS with compound DC9, three distinct clusters of ions can be observed (Figure 5c). The first cluster of ions between the range of *m/z* 500-600 are the lipid bound to DC9 complex corresponding to the first cluster in negative ion mode. DC9-palmitoleic acid (16:1) at *m/z* 507 was enhanced compared to the negative ion mode spectra while other fatty acids in that range maintained their previous profile. The second cluster observed between *m/z* 700-900 belonged to the phosphatidylcholines species also found in the positive control with a similar relative abundance to the positive ion mode control. The last cluster of ions between *m/z* 950-1050 correlates to the second cluster observed in the negative ion mode. Several lipids had enhanced signal to noise and an overall increase in signal for instance PE (34:1) *m/z* 700 cannot be reasonably detected in negative ion mode since it is in the noise level and PE (36:2) *m/z* 726 has very low intensity in negative ion mode. In reactive DESI-MS positive ion mode PE (34:1) and PE (36:2) can be observed in positive ion mode as their mass plus the DC9 mass at *m/z* 955 and *m/z* 980, the relative intensity increased and became easily distinguishable from noise level (Figure 5c). Other groups however, do not bind very well with the DC9 dication, phosphatidylserine (PS 40:6) being the most intense peak in negative mode at *m/z* 834 and phosphotidylinositol (PI 38:4) at *m/z* 885 are not observed as the dication-pair in the reactive DESI spectra. These results are in accordance with the previous study that found PE groups to have enhanced signal intensity and the other higher mass compounds such as PI to have a poor binding to DC9.[40]

Table 1 summarizes the effect of reactive DESI-MS on specific fatty acids or lipids compared to the negative ion mode results. Signal intensity does not necessarily correlate with a better detection, in our case DC9 compounds detected in negative mode were seen to have higher

intensity but also higher noise levels, thus to determine how DC9 compound affects detection, the signal to noise ratio was used as an indicator. The signal to noise ratio was incorporated in order to have normalized data and compare between the reactive DESI positive ion mode scan and the negative ion mode scan. The change was reported as a percentage in the signal to noise ratio of each compound analyzed. Three average spectra taken across the entire rat brain samples were compared between positive ion mode scans with DC9 and negative ion mode scans. The three spectra chosen targeted gray and white matter and were obtained from the widest section of the brain. Table 1 reports whether the signal to noise levels of each compound increased or decreased compared to their native detection in negative ion mode. These values are provided in order to help understand the signal change using DC9; however variations between and within samples based not only on the chemical nature of this reaction but also by the small variation of the spray geometry features of DESI can occur.

Table 1. Lipids and dicationic compound DC9 forming ion-pairs in DESI-MS spectrum in positive ion mode of rat brain (DC9 m.w. 254.4 Da)

Rat brain lipids in negative ion mode	**Observed *m/z* negative ion mode**	**DC9-lipid ion pair in rat brain in positive ion mode**	**Signal to Noise change (DC9 vs negative ion mode)**
Palmitoleic acid (16:1)	253[73, 76]	507	512%
Palmitic acid (16:0)	255[73, 75, 76]	509	26%
Oleic acid (18:1)	281[73-76]	535	37%
Arachidonic acid (20:4)	303[73-76]	557	37%
Phosphoethanolamine (PE 34:1)	700[77]	955	127%
Phosphoethanolamine (PE 36:2)	726[77]	980	107%
Phosphoethanolamine (PE 38:4)	766[77]	1020	153%
Phosphoethanolamine (PE 40:6)	774[77]	1028	124%
Phosphoethanolamine (PE 40:6)	790[77]	1044	119%
Phosphatidylserine (PS 40:6)	834[73-75]	1088	Not Detected
Phosphotidylinositol (PI 38:4)	885[73-76]	1139	Not Detected

Using tandem mass spectrometry, several compounds were identified to be linked with DC9: *m/z* 507, 535, 557, 980, 1020, 1028 and 1044 consisting of DC9-lipid ion pairs. The compounds were subjected to MS/MS and a common loss of 85 Da was observed for all ions mentioned above upon fragmentation of the DC9-lipid ion pairs**.** The loss of 85 Da corresponds to the alpha cleavage of DC9 nitrogen ring Figure 2**.** A DC9 fragment was observed at *m/z* 85 which is a common loss for all lipids bound to DC9 (Figure 6). No other fragments were observed from the lipd-DC9 complex,

this indicates that the dication creates a stable compound with lipids which cannot be easily removed.

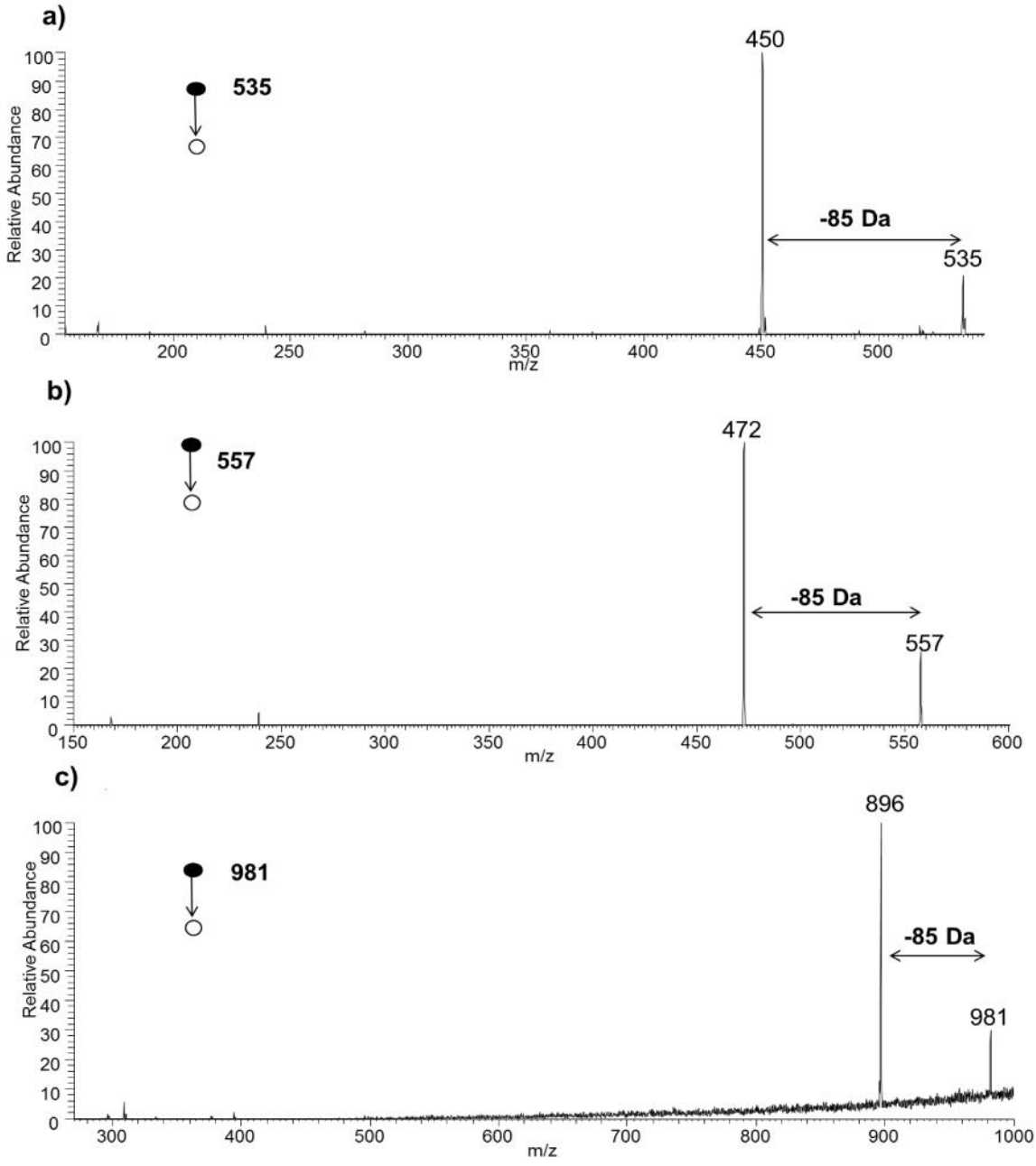

Figure 6. Tandem mass spectrometry (MS/MS) spectra of selected DC9-lipid ion pairs in the reactive full scan DESI-MS rat brain spectrum in positive mode producing a common loss of 85 Da corresponding to high intensity DC9 fragment. (a) MS/MS spectrum of *m/z* 535 ion-pair

between DC9 and oleic acid (18:1) (b) MS/MS spectrum of *m/z* 557 ion-pair between DC9 and arachidonic acid (20:4) (c) MS/MS spectrum of *m/z* 980 ion-pair between DC9 and PE (36:2).

The collision energy used to obtain the fragmentation data was set to 12 (arbitrary units), from this we can infer that DC9 becomes easier to fragment when bound rather than dissociate from the lipid adduct, but also that it can have the effect of reducing or preventing in source fragmentation. This stabilizing effect could be a factor in the overall increase of signal by reducing in source fragmentation. This opens the possibility that DC9 could be used for other techniques to increase signal intensity and stabilize lipids. For example, matrix assisted laser desorption ionization (MALDI) technique has been used to map rat brain lipids[78-81] and DC9 could be incorporated in the matrix application step to stabilize certain labile lipids, such as gangliosides, a family of glycosphingolipids, prone to lose sialic acid group upon MALDI analysis[82, 83].

Imaging on rat brain tissues were performed in negative ion mode and positive ion mode from adjacent tissue slices in order to compare and contrast the differences between ion intensity distribution and insitu signal intensity variation. Selected ions in Figure 7 illustrate the imaging of lipids using reactive DESI-MS in positive ion mode and a few lipids in negative ion mode to compare. In reactive DESI-MS lipids are present in high abundance in the gray matter, such as PE (36:2) at *m/z* 980, whereas other lipids are abundant in the white matter of the brain, such as at PE (40:6) at *m/z* 1044, when the two ions are overlapped a clear image of the structural features in white matter and gray matter can easily be distinguished (Figure 7j). Negative ion mode images of Arachidonic acid (20:4) at *m/z* 303 and Phosphoethanolamine (PE 36:2) at *m/z* 726 were added to Figure 7k and 7l for comparison.

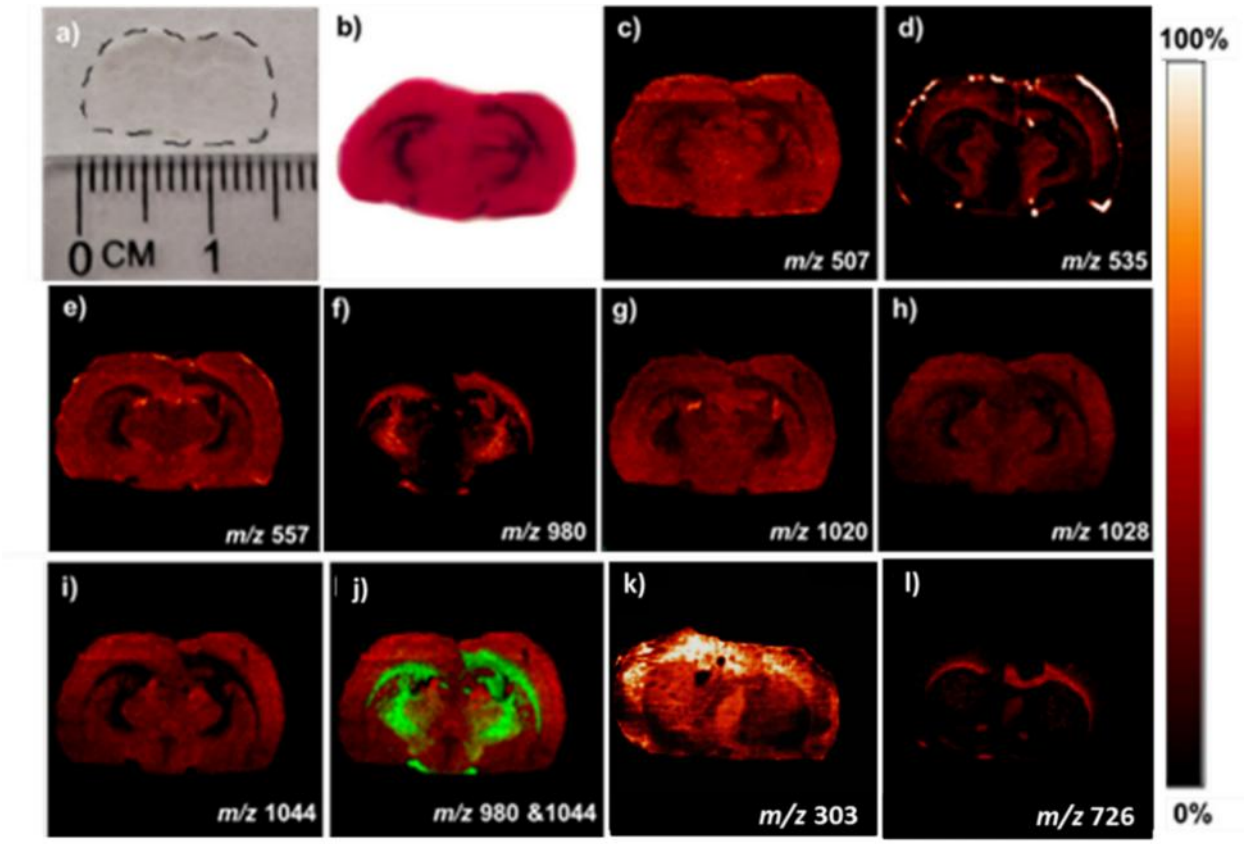

Figure 7. Panel of rat brain images analyzed by reactive DESI-MSI with compound DC9 in positive ion mode. a) Optical image of rat brain tissue slide with an outline of the tissue slice b) H&E stained rat brain tissue slide (c-i) DESI-MS images of lipids with DC9 ion-pairs in the positive ion mode c) *m/z* 507: DC9 and palmitoleic acid (16:1). d) *m/z* 535: DC9 and oleic acid (18:1). e) *m/z* 557: DC9 and arachidonic acid. f) *m/z* 980: DC9 and PE (36:2). g) *m/z* 1020: DC9 and PE (38:4). h) *m/z* 1028: DC9 and PE (40:6). (i) *m/z* 1044: DC9 and PE (40:6). (j) Overlay image of *m/z* 980 and *m/z* 1044. (k & l) DESI-MS images of lipids in the negative ion mode k) Arachidonic acid (20:4) at *m/z* 303 l) Phosphoethanolamine (PE 36:2) at *m/z* 726

With reactive DESI-MS one can visualize the same distribution of the same compounds, such as phosphoethanolamine (PE 36:2) which has a strong intensity, while in negative mode the signal intensity is low resulting in a poor quality image. The signal intensity difference could be attributed

to the ionization efficiency difference, to matrix effects from the tissue, leading to different ionization pattern when comparing the negative ion mode ionization to the reactive DESI ionization. DC9 forms a stable complex and could have a stabilizing effect on certain compounds thus leading to a more intense signal by reducing or eliminating in source fragmentation. It is difficult to definitively determine the process which gives rise to this variation, and further research on reactivity needs to be performed. Figure 7d exhibits a border effect which was later identified to be a result of the mounting glue polymer used in the tissue sectioning.

This technique can be used in order to enhance phosphoethanolamines signal and at the same time allow both the negative compounds and the positive phosphatidylcholines groups to be scanned in a single spectrum with reactive DESI in positive ion mode. The trade-off is that some compounds such as phosphatidylserines and phosphotidylinositols are not detected, but this only confirms that the information provided by this technique is not redundant information from negative mode but new and complementary chemical information.

2.3.2 Zebrafish DESI-MS analysis

Zebrafish is an important biological model commonly used to study genetics[45, 46], environmental toxicology[47-50], cancer[51, 52], and other diseases[53-55]. The specimen is also very small 2-4 cm in length, due to its small size the zebrafish allows imaging mass spectrometry experiments to be performed simultaneously on all tissue types. Spectra of zebrafish whole body were acquired in negative ion mode, in positive ion mode control and reactive DESI-MS with DC9

positive ion mode for comparison and analysis. Imaging was done with reactive DESI positive ion mode and negative ion mode to analyse *in situ* information of compounds of interest.

Similarly to the rat brain, the positive ion mode control of the zebrafish in the range of *m/z* 700-900 has a cluster of phosphatidylcholines (Figure 8a). These lipids were also confirmed via tandem mass spectrometry as described in the rat brain section. [70, 71]

Figure 8 has an *m/z* shift of 254 for the positive mode in order to align the negative ions with the positive DC9 ions.

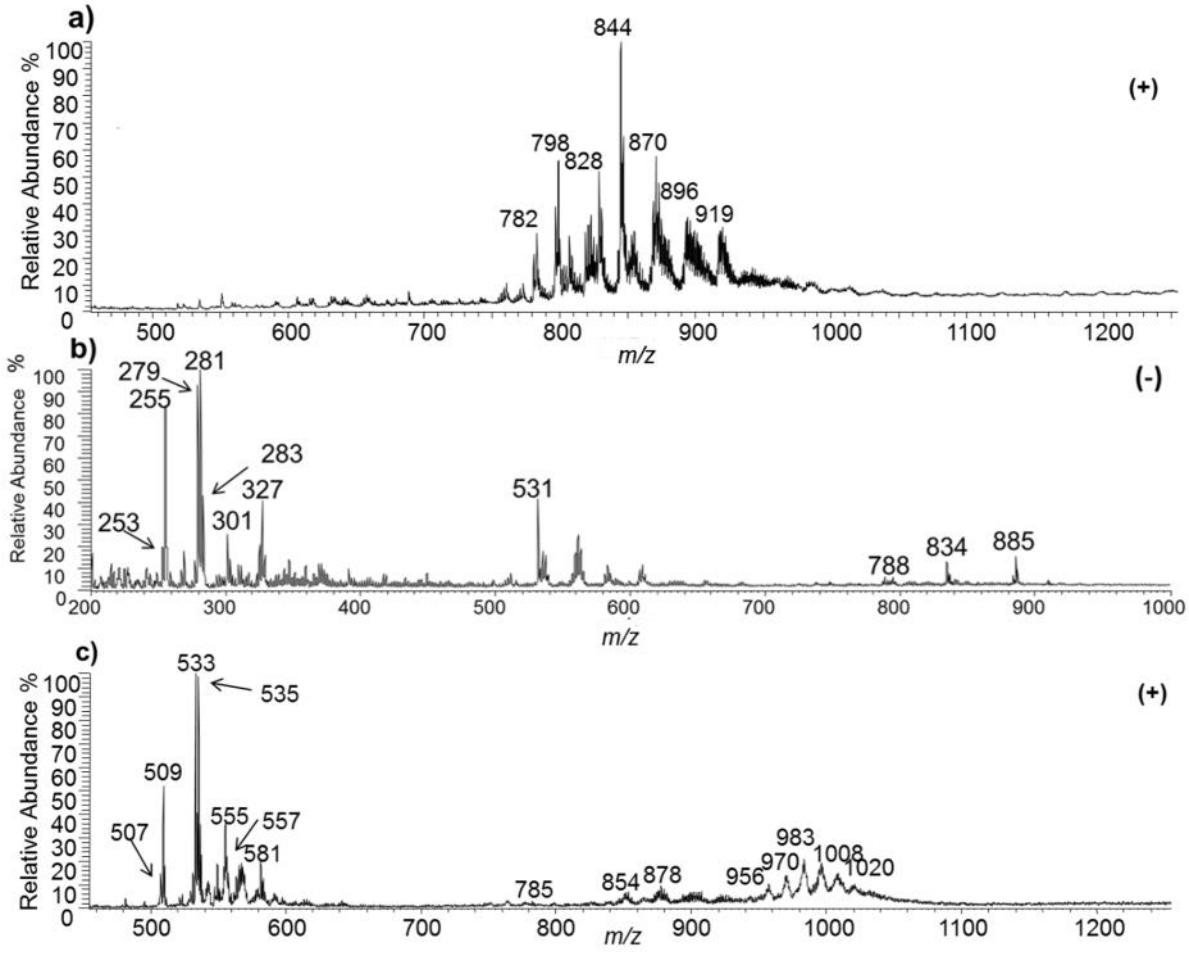

Figure 8. DESI-MS spectra of characteristic metabolites in whole body zebrafish tissue sections (a) Phosphatidylcholines in zebrafish in DESI-MS positive ion mode control (b) Control DESI-

MS spectrum of zebrafish tissue in negative ion mode (c) Positive reactive DESI-MS spectrum of enhanced intensity between DC9-metabolite ion pairs in zebrafish compared to DESI-MS spectrum negative ion mode control.

Compounds in negative ion mode have been identified and characterized in literature and were assigned accordingly. In the range between *m/z* 250-350 contains ions such as palmitic acid (16:0), linoleic acid (18:2), oleic acid (18:1), and others (Figure 8b & Table 2). 5α-cyprinol 27-sulfate, a bile salt produced in the stomach and/or intestinal system was detected at *m/z* 531.[84] Two phosphatidylserines (PS 36:1 and PS 40:6) identified at *m/z* 788 and 834, a phosphatidylinositol (PE 38:4) at *m/z* 885, and a sulfatide (ST 24:0) at *m/z* 890 were also observed.[84]

In reactive DESI-MS, (Figure 8c), lipid-DC9 bound compounds detected in the range of *m/z* 500-600 were correlated to the negative ion mode compounds in the range of *m/z* 250-350 via tandem mass spectrometry. The lipid-dication compounds had a common loss of 85 Da correspond to DC9 cleavage at the nitrogen ring, as in the rat brain experiment. The bile salt 5α-cyprinol 27-sulfate was also observed as a DC9 bound ion in the reactive DESI-MS ion mode in the stomach and intestines region. The signal intensity of the 5α-cyprinol 27-sulfate salt ion is reduced compared to the other lipid-dication bound compounds, but it demonstrates that dications can be implemented for a variety of organic compounds. Lipid compounds including phosphatidylserines (PS), phosphatidylinositols (PI), and phosphatidylglycerols (PG) have a low binding affinity to DC9 and were not detected in our reactive DESI-MS experiments. These results are in accordance with Barrett's group study conducted with lipid standards where enhancement of these types of lipids in the reactive DESI-MS spectrum was not observed.[40]

Higher mass compounds in the reactive DESI-MS in the range of *m/z* 900 and above were not possible to identify via tandem mass spectrometry due to overlapping signals of multiple ions and/or low signal intensity. Several broad peaks observed in the range of *m/z* 950-1050 could not be identified. Fragmentation was only possible when isolation window was open to *m/z* 10. Fragmentation energy required was 7 (arbitrary units), and the fragments obtained are provided in the Table 2.

Table 2. Zebra fish MS/MS using dicationic compound DC9 on unidentified broad peaks in the range *m/z* 900-1100. Parent ions selected with an isolation window width *m/z* 10. Center of peaks reported with the width of the peaks as an *m/z* ± value.

	Parent Ion				
Center peak *m/z* (Iso window ± 5)	**1020**	**1008**	**996**	**983**	**970**
	Daughter Fragments				
Fragment 1 (*m/z* ±5)	603	592	579	580	580
Fragment 2 (*m/z* ±5)	592	579	568	568	568
Fragment 3 (*m/z* ±5)	579	567	555	555	555
Fragment 4 (*m/z* ±5)	567	555	542	542	542
Fragment 5 (*m/z* ±5)	555	543	529	529	529
	Neutral Losses				
Neutral Loss 1 (*m/z* ±5)	417	416	417	403	390
Neutral Loss 2 (*m/z* ±5)	428	429	428	415	402
Neutral Loss 3 (*m/z* ±5)	441	441	441	428	415
Neutral Loss 4 (*m/z* ±5)	453	453	454	441	428
Neutral Loss 5 (*m/z* ±5)	465	465	467	454	441

The fragments obtained are very broad indicating a cluster of ions is being formed with DC9. This pattern of ions is only observed with DC9. Signal intensity was too low to perform MS^3 analysis, and although positive identification was not possible at the moment, some of these ions were mapped and images are provided in Figure 9.

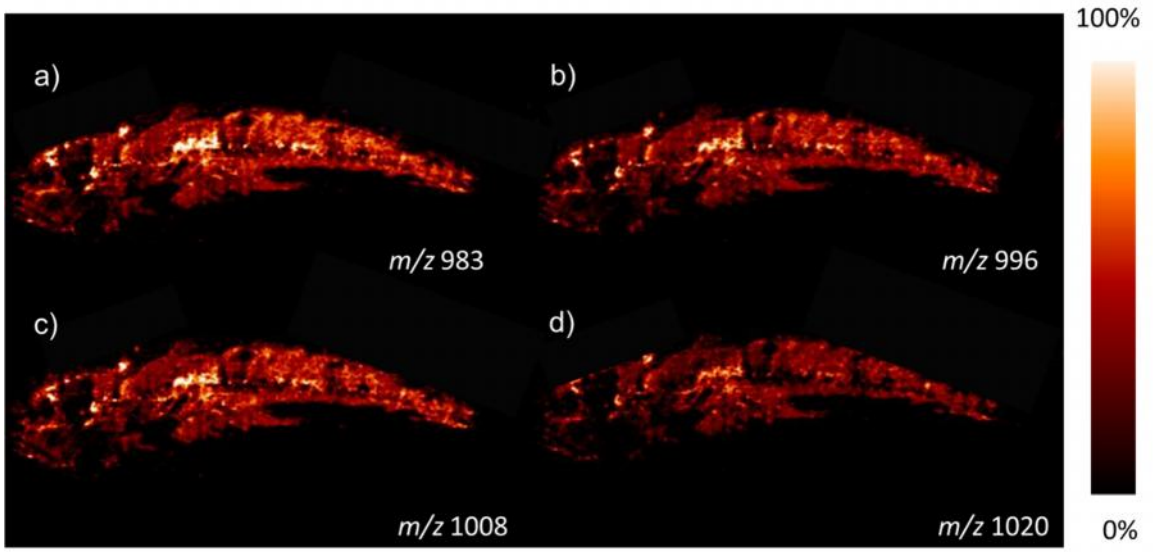

Figure 9. Panel of zebra fish images analyzed by reactive DESI-MSI with compound DC9 in positive ion of unidentified peaks, *m/z* 983, 996, 1008, and 1020 respectively.

Fragmentation of these species had overlapping ion daughters, but very broad to be useful for identification, imaging experiments revealed that these ions seem to have the same distribution, indicating that they belong to the same class of compounds. However, from the previous findings we could speculate that these peaks could correspond to phosphoethanolamine groups with DC9 or could be 3 or molecules bound loosely together due to a lower fragmentation energy required. If the molecules belong to phosphoethanolamine groups they might correspond within the range of the mass *m/z* 970 are PE (34:2) at and PE (34:1) at *m/z* 714 and *m/z* 716 in negative ion mode.

The mass range at *m/z* 983 might correspond to PE (36:2) at *m/z* 728 in negative ion mode. The mass range at *m/z* 996 might correspond to PE (36:3) at *m/z* 740. Mass range at *m/z* 1008 could correspond to PE (38:4) at *m/z* 740 in negative ion mode.[85] The ions are present throughout the body with the exception of the organs; this can be a useful starting point for further experiments.

Table 3. Zebrafish metabolites and dicationic compound DC9 ion-pairs in DESI-MS spectrum in positive ion mode (DC9 m.w. 254.4 Da)

Zebrafish metabolites in negative ion mode	**Observed *m/z* negative ion mode**[84]	**DC9-metabolite ion pair in positive ion mode**	**Signal to Noise change (DC9 vs Negative ion mode)**
Myristic acid	227	481	64%
Palmitic acid (16:0)	255	509	79%
Linoleic acid (18:2)	279	533	101%
Oleic acid (18:1)	281	535	88%
Stearic acid (18:0)	283	537	115%
Eicosapentaenoic acid (20:5)	301	555	354%
Docosahexaenoic acid (22:6)	327	581	118%
5α-cyprinol 27-sulfate	531	785	7%
Phosphatidylserine (PS 36:1)	788	1042	Not Detected
Phosphatidylserine (PS 40:6)	834	1088	Not Detected
Phosphatidylinositol (PI 38:4)	885	1139	Not Detected
Sulfatide (ST 24:0)	890	1144	Not Detected

The signal to noise was used as an indicator of the DC9 effect on detection as in the rat brain experiment. Three average spectra were taken across the entire zebrafish samples and were compared between reactive DESI positive ion mode scans and negative ion mode scans. These spectra were acquired from the eye to the tail of the zebrafish. Table 3 reports whether the signal to noise levels of each compound increased or decreased compared to their native detection in negative ion mode. These values are provided in order to help the understanding of the signal change using DC9. As previously mentioned there is great variation, especially when trying to encompass an entire specimen's body where the various organs will have different composition and may either suppress or enhance the reaction of the DC9 to varying extents.

Selected zebrafish ion images in Figure 10 illustrate the mapping of lipids using reactive DESI-MS in positive ion mode. Compound distribution varies greatly within the whole body, for example a ion can be observed throughout the entire body such as oleic acid (18:1) (Figure 10e), or with a high abundance in certain organs, such as docosahexaenoic acid (22:6) (Figure 10f) in the eye or spleen, and 5α-cyprinol 27-sulfate found in the digestive system (stomach and/or intestines) (Figure 10g) Structural features can easily be elucidated whenever using the reactive ion mode with DC9. An overlap between palmitic acid (16:0) concentrated in the fish liver and docosahexaenoic acid (22:6) concentrated in the eye and spleen is shown as an example of how reactive DESI-MS imaging can be used for biological structural differentiation. Negative ion mode images are included in the panel of Figure 10 (i-l) for comparison of corresponding reactive DESI-MS selected ions. When comparing the same ions ionized in reactive DESI-MS over the control negative mode, different signal intensity distribution between the two modes can be observed due to different tissue composition which react differently with the dicationic salt in reactive DESI-MS mode. This may result to be very advantageous since reactive DESI can provide different

imaging than the negative mode, thus offering new information and not redundant information. This phenomenon is observed strongly in the whole zebrafish body images than in the rat brain images. The tissue slices are serial slices, hence this phenomenon is indicative that DC9 coupling reaction could be suppressed to a varying degree in different organs. The dication is not binding to a specific compound but rather multiple anions available in tissue, binding competition and binding affinity becomes a factor of the intensity and overall distribution of the tissue image. This variation of how DC9 reacts across different tissue types can be an advantage since the information provided by these ion images is not redundant information from negative ion mode and can therefore be used to provide missing or complementary information. An example of this case is docosahexanoic acid (22:6) where it is observed in negative mode in organs such as, gills, liver, intestinal system, (Figure 10k) but in reactive DESI-MS it is localized mostly in the liver and bile (Figure 10f). This result does not necessarily mean that it is in a higher abundance in that particular area, but rather that the dication has less competition in this tissue and is able to bind more effectively with docosahexanoic acid (22:6). It is difficult to definitively attribute this effect to matrix suppression or facilitated reactivity from compounds in organs. This is a new compound and its general reactivity is not fully understood yet. Future reactivity work will help to better understand this phenomenon.

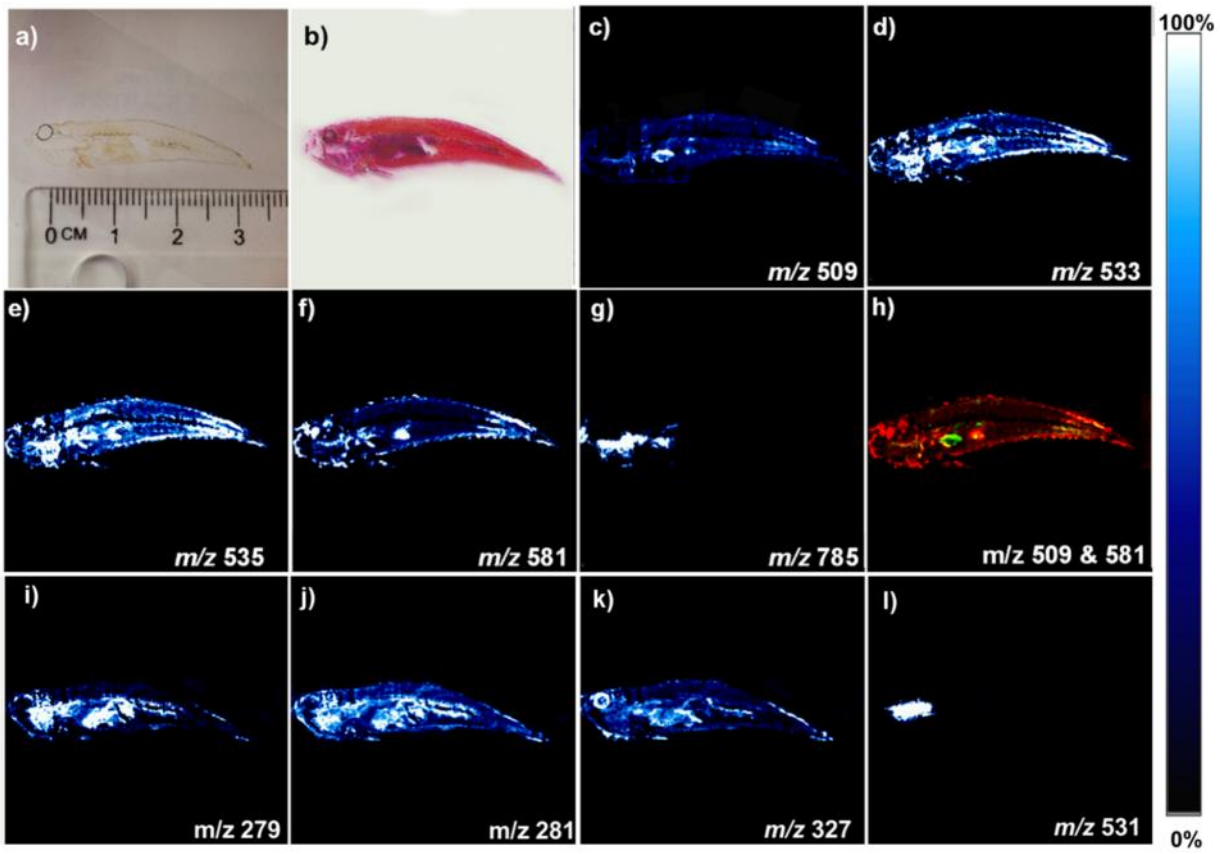

Figure 10. Panel of zebrafish images analyzed by reactive DESI-MSI with compound DC9 in positive ion mode (c-h) and negative ion mode (i-l) (a) Optical image of zebrafish tissue on a microscopic glass slide (b) H&E stained zebrafish tissue on a microscopic glass slide (c-h) DESI-MS metabolite images with DC9 ion-pairs in the positive ion mode c*) m/z* 509: DC9- Palmitic acid (16:0) d) *m/z* 533: DC9- Linoleic acid (18:2) e) *m/z* 535: DC9- Oleic acid (18:1) f) *m/z* 581: DC9-Docosahexaenoic acid (22:6) g) *m/z* 785: DC9-5α-cyprinol 27 sulfate h) Overlay image of ion pairs *m/z* 509 and *m/z* 581, DESI-MS metabolite images in the negative ion mode (i-l) (i) Linoleic acid (18:2) at *m/z* 279 (j) Oleic acid at *m/z* 281 (k) Docosahexanoic acid (22:6) at *m/z* 327 (l) a-cyprinol 27-sulfate at *m/z* 531 g)

2.4 Conclusion

Reactive DESI-MS with compound DC9 in positive ion mode was successful in increasing the intensity of certain low mass lipids in the range of *m/z* 250-350 and of phosphoethanolamines (PE) *m/z* 700-800 in rat brain and zebrafish biological tissues. Reactive DESI-MS ion images appeared to have a slight difference in distribution which could be attributed to a tissue matrix effect, competing or supressing the dication. DC9-lipid ion pairs have shown an increase in intensity in comparison to the conventional DESI-MS analysis of lipids in negative ion mode. This method allows the mapping of ions present in positive ion mode and negative ion mode in one single spectrum, decreasing imaging time and the amount of sample required to run an analysis, this can be very powerful when there is limited sample, for example biopsy samples. Positive ion mode images using reactive DESI are different than the negative ion mode for the same compound using DESI, this opens the possibility of providing new information about the sample rather than redundant information when looking at a complex sample.

Morphological elucidation and the ability to select areas of organs via Biomap, to average all the spectra in the region and compare tissue specific spectra to different sections of the body can be a very powerful tool when combined with reactive DESI-MS. This can prove advantageous when looking for tissue damage, toxin accumulation or metabolic processes by using a targeted approach with new dicationic compounds.

Since DESI-MS has been successfully employed in negative ion mode to discriminate normal from cancerous tissue based on lipid profiles.[65, 66] Reactive DESI-MS using dicationic compounds can open new avenues into cancer research, drug development, investigate metabolism, disease and generally a more targeted ionization technique.

Chapter 3

3. Desorption electrospray ionization (DESI) and easy ambient sonic-spray ionization (EASI) comparison for imaging mass spectrometry purposes.

3.1 Introduction

DESI and EASI techniques are very similar in setup with only a few parameters varying.

For imaging experiments it is important to take into account not only the ability to ionize a sample, but also the impact of the technique (spatial effects) on the sample interrogated. EASI is not fully compatible with IMS because it requires high gas flow rates (>3.0L/min) and high solvent flow rates (>20µL/min) in order to promote the ionization. These conditions cannot be applied to all kinds of sample, especially biological tissues, because they damage the sample before it can be entirely mapped. Experiments can be done under specific conditions using low gas flow rates (<3.0L/min) and low solvent flow rates (<10µL/min) as reported here. However, these conditions eliminate the "sonic spray" effect responsible for the high ionization efficiency. Indeed, the ionization under these conditions were investigated and reported as non-optimal DESI in 2005.[25] In 2012, Janfelt and Nørgaard published a comparative study between DESI and EASI in terms of spatial resolution and sensitivity by producing ion images of tissue sections[86]. In this study a pixel to pixel comparison was performed as it can distinguish between signal and noise. It was concluded that EASI can be as efficient as DESI for imaging and direct analysis of tissue sections as long as a higher solvent flow rate (10 µL/min) is maintained. Improved EASI signals were

observed as long as the pressure was kept at 10 bar which equal around 145 psi. When the pressure was above 10 bar, no further improvements in EASI signals was observed. It was found that DESI is more sensitive than EASI towards analytes that are present at low abundance for both rat brain and plant imprints deriving the fact that there must be a difference in dynamic range for both DESI and EASI.

This study expands on that work by comparing DESI and EASI techniques at nonstandard equivalent conditions for the assessment of the limit of detection (LOD) of several drugs on PTFE surface and for the determination of the spray spot size varying flow rate and solvent composition for imaging purposes. MS/MS imaging was also done with both methods as a proof of concept for imaging discrimination comparison. The experiments reported here were not under the standard conditions for either DESI[25] or EASI[21] [36], but rather similar conditions that could overlap both techniques to get comparative results. The techniques were compared in terms of the sensitivity (limits of detection), spray spot size and lateral spatial resolution in order to gauge the capabilities in terms of imaging performance.

The first experiment was used to interrogate spray spot size, directly linked to the minimum spatial resolution requirements. For spray based techniques spot size is is the main factor which restricts the resolution of the chemical image. Using water sensitive paper the spray area was analyzed for both DESI and EASI. The next step was to investigate limit of detection using various drugs on PTFE, to compare DESI and EASI ionization and transfer efficiency. As a proof of concept MS/MS imaging was done with both methods to observe how they would perform in a forensic discrimination application. The results obtained from these experiments give further insight into the capabilities of DESI and EASI, and to interrogate these techniques for IMS purposes.

3.2 Materials and methods:

3.2.1 Materials and reagents:

Solvents used in the experiments were purchased from Sigma-Aldrich Canada, solvent grade HPLC. Compounds used in the limit of detection experiment: propranolol, testosterone, dobutamine, verapamil, chloramphenicol, ibuprofen, diazepam, roxithromycin, angiotensin ii, were obtained from Sigma-Aldrich Canada, Ltd. Porous PTFE sheets 1.5 mm thick with a medium porous size of 7µm purchased from Berghof (Eningen, Germany). Microscope slides 26x77mm thickness 1mm single frosted were purchased from Bionuclear diagnostics INC, (Toronto, ON, Canada). Water sensitive paper, a paper that changes its color when exposed to water, was from TeeJet Technologies (Harrisburg, Dillsburg, PA). Red pens containing Rhodamine B and Rhodamine 6G, BIC Company, used in MS/MS experiment were purchased from the bookstore at York University.

3.2.2 Sample preparation

Water Sensitive paper: Water sensitive paper was cut to working size and was secured on the moving stage with tape on the all sides.

Limit of Detection: Standards of 1 mg/mL were prepared in methanol solvent. The spotting solutions were created from 1 mg/mL standard using serial dilution to 100, 10, 1, 0.1, and 0.01 ng/µL prepared in a 1:1 ratio of methanol to water solution. Solvent used to spray was also prepared with methanol to water ratio of 1 to 1.

MS/MS imaging: Two different red pens were used to create an attempted forgery on a piece of paper. The paper was secured to the running stage with tape and an MS imaging performed.

3.2.3 Instrumentation

All experiments were carried using an LTQ linear ion trap mass spectrometer (Thermo Fisher Scientific, San Jose, CA, USA) with a lab-built DESI ion source.

3.2.4 Water Sensitive paper:

Experiments were performed with varied solvent flow rates from 0.5 µL/min to 4.0 µL/min. Methanol to water ratios of 1:1 and 9:1 were used. Varying the nitrogen (N_2) gas backpressure from a pressure of 80 psi to 140 psi was measured while keeping the flow rate at 2.0 µL/min and 1:1, methanol: water, solvent ratio. The geometry conditions were set as: spray angle 52 degrees, capillary to inlet distance ~ 3 mm and capillary to surface ~ 2 mm. DESI conditions used 5kV spray charge, while EASI used 0kV, all other parameters were kept the same. In order to ensure the absence of residual charge in the syringe when turning off the voltage from DESI to EASI, a ground wire was connected to the syringe metal tip during EASI experiments. The moving stage was programmed to make five distinct spots; the distance between each spot was 1 mm and the spray held position on each spot for 1 second before moving to the next. This was followed by making a line of 10 mm long with continuous spray over slow movement with speed of 200 µm per second. Each line ended with a final spot sprayed for 10 seconds before moving on to the next line. After the experiment the resulting papers were scanned for visual inspection.

3.2.5 Limit of Detection (LOD):

Shallow parallel indentation lines were drawn on the porous material using a spare inlet. Volumes of one microliter were pipetted on the line in increasing concentrations from 0.01, 0.1, 1.0, 10 and 100 ng/µL respectively, delivering the same weight of compound per spot for each of the

compounds. The spots were left to dry about 20 minutes and analysis was performed by scanning across the line with a speed of 200 micrometers per second. Distance optimized under EASI conditions with capillary angle at 52 degrees, capillary to inlet distance set at ~ 3 mm and capillary to surface set at ~ 2 mm. A solvent flow rate of 1.5 µL/min of MeOH:H_2O mixture (1:1, v/v) and nebulizing gas (N_2) pressure of 140 psi were used. The limits of detection were established by doing MS/MS on parent ion and monitoring the main daughter ion.

3.2.6 MS/MS imaging:

Two red pens containing Rhodamine B and Rhodamine 6G were used one a piece of paper. One pen to write a 3 and an F and the other to convert the 3 to an 8 and the F to a B. The paper was secured to the moving stage and a MS image was obtained. The flow rate was set at 3µL/min, spray tip to inlet distance 3 mm, and spray tip to surface distance 1 mm, solvent was a 1:1 MeOH:H_2O for both DESI and EASI. Voltage was set at 5kV and pressure at 100 psi for DESI, while EASI was done at 140 psi and 0kV. Spatial resolution was set at 150 micrometers, 2 micro scans per spot, and Automatic Gain Control turned off. Experiment ran in MS/MS mode (daughter ion scan) monitoring 443 m/z fragments from 200 to 500 m/z, with collision energy of 19eV.

3.2.7 Imaging

Ion images were obtained using a lab-built software named ImgCreator that converted the mass spectra files into a format that is compatible with Biomap (freeware, www.msi.maldi.org).

3.3 Results and Discussion

3.3.1 Water sensitive paper

The first experiment was done with water sensitive paper in order to compare the size of the spray impact produced by both DESI and EASI. This type of paper changes color when water hits it, thus allowing for a visual inspection of the solvent impact area. The lines were created by alternating DESI and EASI conditions created to minimize variation due to sample surface, such as previous exposure to moisture or geometry fluctuation. By alternating each line this ensures both methods are comparable even if setup errors arise. DESI was expected to give a different spray pattern since the solvent droplets were charged, if the charge on the droplet is sufficient, approaching the Reilegh limit, this could lead to a columbic explosion of the droplets resulting in much smaller solvent droplets.

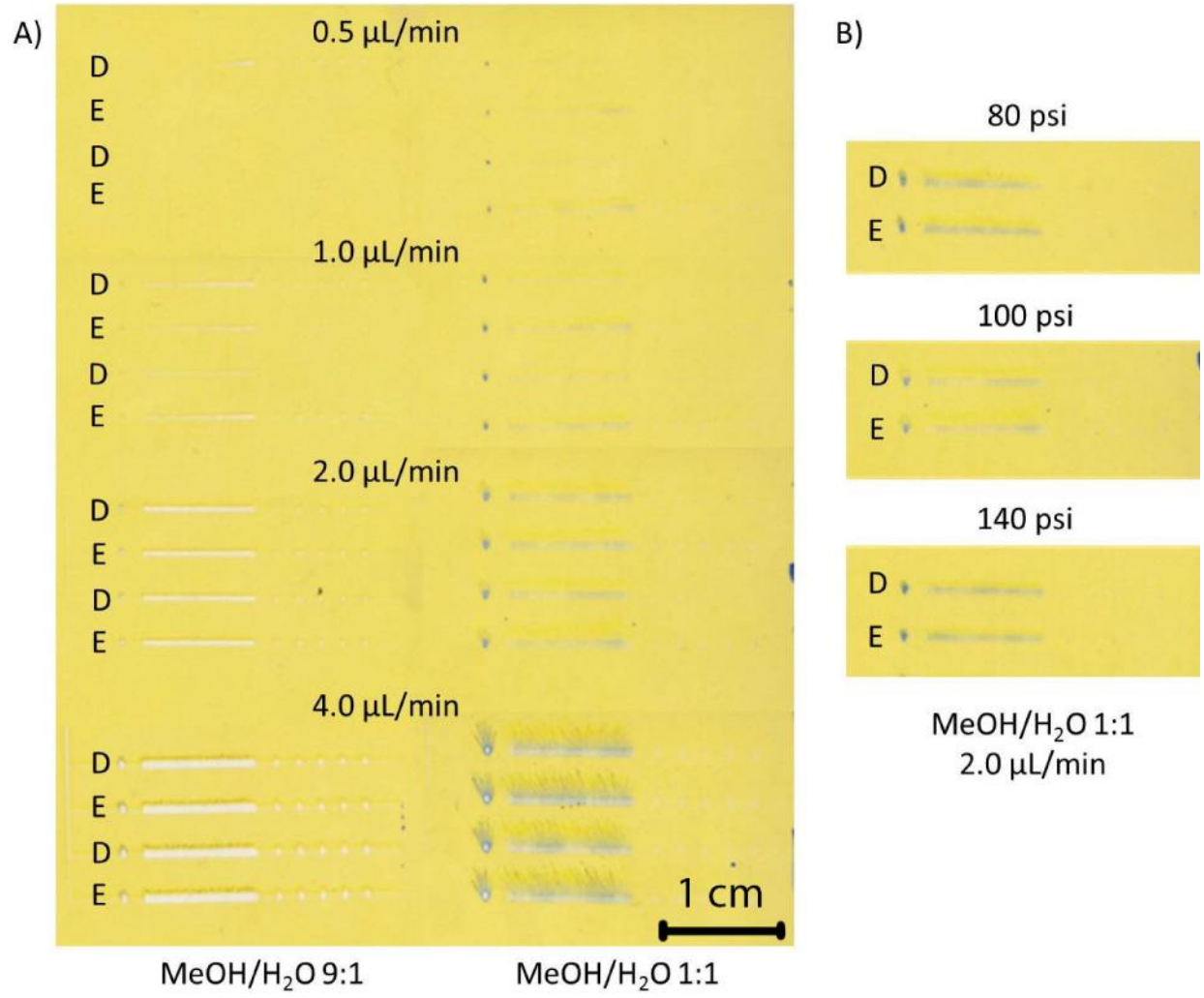

Figure 11. Spots and lines produced by desi (D) and easi (E) obtained on water sensitive paper using methanol and water at 9:1 and 1:1 ratio. Panel (A) represents spots made with varying solvent flow rates of 0.5 µL/min, 1.0 µL/min, 2.0 µL/min and 4.0 µL/min using both solvent mixtures. Panel (B) represents spots made with varying nebulizing gas (N_2) pressure of 80 psi, 100 psi and 140 psi using methanol and water (1:1) at 2.0 µL/min flow rate.

At first the impact between DESI and EASI using two different solvent compositions at varying solvent flow rate was analyzed. A solvent with 9:1 MeOH/H_2O composition was compared with a solvent of 1:1 MeOH/H_2O, and for both methods the solvent with 1:1 tended to show signs of

sample smearing at 4 µL/min. This is expected since the mixture of 1:1 MeOH/H_2O evaporates slower than the 9:1 MeOH/H_2O, as a result the solvent evaporation rate is lower than the solvent flow rate and this difference leads to buildup of the solvent and smearing across the sample. Smearing effects have a big impact in imaging mass spectrometry because ions get delocalized, losing spatial information, hence the quality of the image will drop proportionally to the amount of smearing. As the solvent flow rate increases the area of the solvent impact increases as well, even though using a higher ratio of methanol prevented sample smearing the 1:1 ratio is comparable in size to the 9:1 MeOH/H_2O solvent. This demonstrates the need for a lower flow rate in order to achieve good resolution when working with spray based imaging mass spectrometry techniques such as DESI-MS or EASI-MS. (Figure 11a). Pressure effects were investigated by varying pressure and keeping the other parameters the same. The pressure was varied however the overall impact on the spray spot area was minimal. No significant change was observed from 80 to 140 psi, also no distinguishable difference between the DESI and the EASI lines. Pressure does not seem to have a big impact on resolution however EASI ionization efficiency is dependent on high pressure compared to DESI. The standard EASI 400 psi pressure would destroy most biological samples being analyzed and is impractical for imaging, therefore studies were limited to a maximum of 140 psi, considered enough for EASI to achieve effective ionization while still maintaining the integrity of samples. [86] From the experiment the voltage applied on a solvent doesn't affect the spray spot size in a significant measure. The major components affecting the spray spot size for both methods are the solvent composition and the solvent flow rate, a smaller impact on the spray spot size is the nebulizing gas backpressure and the spray voltage component seems to have little to no overall effect on spray spot size. As a result the spatial resolution remains the same if operated under similar experimental conditions.

3.3.2 Limits of detection on Porous PTFE

One of the main differences between the techniques is supposed to be that DESI is more sensitive for low abundance compounds. This claim was investigated by spotting standards of various compounds on a porous PTFE surface. The surface is non polar and the small pores size help concentrate the sample. This allows for the stray spot to effectively cover the entire region of the sample. The compounds tested needed to be pipetted onto the surface, however adherence to the surface is difficult for polar solvents such as water. A common issue was the droplet remaining on the pipette tip rather than going on the surface. To overcome this issue a mix such as methanol and water can increase adherence. Another common issue when working with low concentrations is that the spray is most efficient in the very center of the spray spot area and ionization efficiency drops towards the edge of the spray, therefore for consistent results the spray needs to ideally hit the very center of the pipetted sample consistently. A guide line drawn across the porous PTFE surface using a spare inlet and little pressure was used to ensure consistent reproducible results. Geometry is an important factor when analysing with either DESI or EASI, an inlet is made of metal, it is rounded a few millimetres in width, this allows to apply consistent pressure and not to create a sharp depression in the surface, as in the case of a ruller or a pen tip. The shallow groove also increased contact with the droplet pipetted on the surface making the pipetting process easier. The various concentrations of the compounds were then pipetted and monitored using selected reaction monitoring SRM mode. By fragmenting the parent ion and monitoring the main daughter ion this ensures a low level of noise and can be used to confidently identify whether or not a signal of the targeted ion is detected. The lowest limit of detection was reported for cases where it was detected at least three separate runs out of four tries.

A summary of optimum conditions used for each compound and the lowest concentration detected reliably with both DESI and EASI parameters is provided in Table 4. The pKa values were obtained from DrugBank database.

Table 4: Limits of detection of selected compounds using both method conditions on a porous PTFE surface.

					Lowest Conc. Detected (ng/µL)	
Compound	Scan Mode	pKa	Collision Energy	Precursor → product (m/z)	DESI	EASI
Propranolol	+	9.42	27	260.2 $[M+H]^+$ → 183.2	0.1	1
Testosterone	+	19.09	20	289.3 $[M+H]^+$ → 253.2	10	100
Dobutamine	+	9.27	25	302.3 $[M+H]^+$ → 137.2	10	10
Verapamil	+	9.68	23	454.4 $[M+H]^+$ → 303.3	0.01	0.1
Chloramphenicol	-	7.49	27	321.0 $[M-H]^-$ → 257.0	0.01	0.1
Ibuprofen	-	4.85	20	205.2 $[M-H]^-$ → 161.2	1	1
Diazepam	+	2.92	30	285.3 $[M+H]^+$ → 257.1	0.1	1
Roxithromycin	+	9.08	20	837.7 $[M+H]^+$ → 679.2	0.01	0.1
Angiotensin	+	7.76	20	523.8 $[M+H]^{+2}$ → 784.4	1	10

Dobutamine and Ibuprofen were detected at the same concentration in both methods. This event suggests that EASI has the potential to be as sensitive as DESI under certain conditions. Dobutamine has pKa 9.68 and Ibuprofen has pKa of 4.85, as a result both of these compounds are charged when pipetted onto the surfaces and are detected at the same concentrations in both

methods. This result suggests that compounds that do not need ionization are solely dependent on the desorption factor in which case there is little difference between the two techniques. However when other compounds were investigated such as Verapamil or Roxithromicin both with a pKa above 9 these compounds had a lower limit of detection by one factor of magnitude with DESI over EASI parameters. This result suggests that for some compounds even though they are present as ions the highly charged nature of the solvent in DESI can result in more ions being desorbed from the surface and transferred to gas phase. For compounds that require ionization DESI has a higher ionization efficiency as observed in the case of Angiotensin and Chloramphenicol both with a pKa around 7, this is a result of the higher charge density per droplet generating more ions per sample area. Important to note that even though EASI has a lower ionization efficiency it is still able to ionize difficult samples such as Testosterone pKa 19.09, this is a good indication that the ionization is a result of the techniques and not simply the solvent being applied on the surface. As is the experiment does confirm that DESI in general does indeed have more sensitivity than EASI. The difference between DESI and EASI does not exceed one order of magnitude, this is consistent across the sample tested.

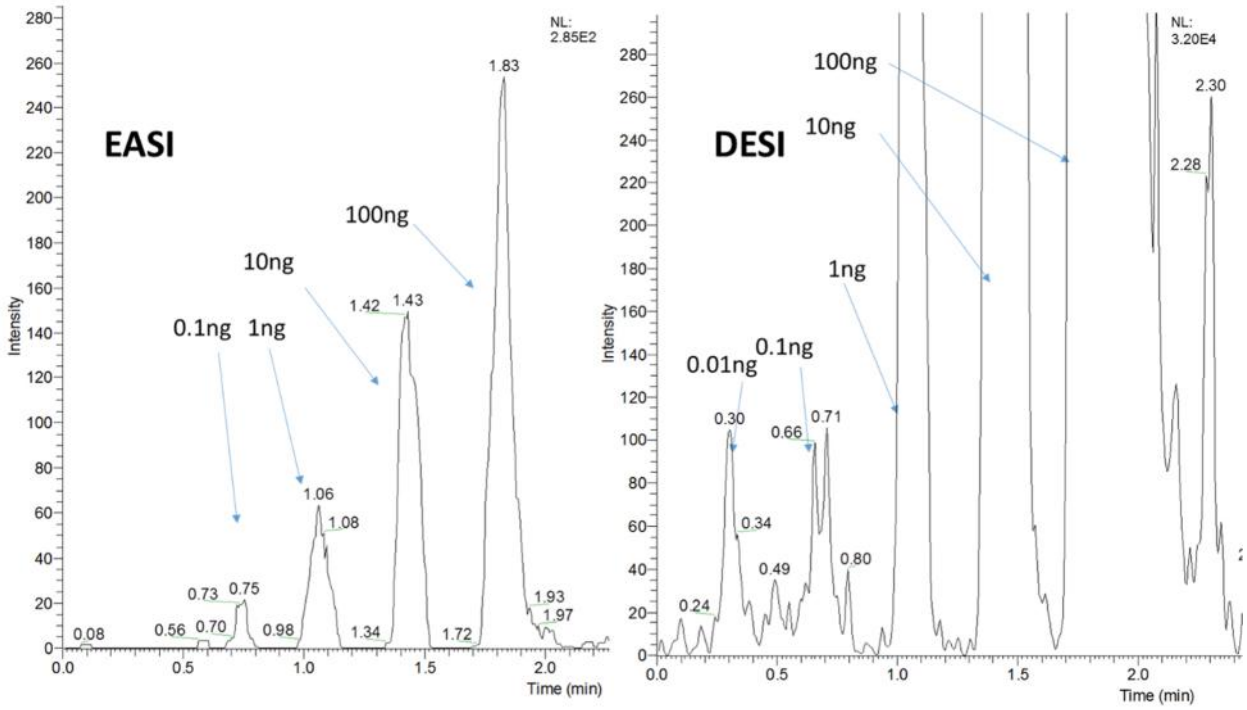

Figure 12. Typical scan of a line with spots of concentrations from 0.01ng to 100ng/spot. SRM scan of Verapamil drug taken with EASI conditions on the left and DESI conditions on the right on an absolute intensities scale versus time.

An example is provided in Figure 12 of a SRM mode scan between DESI and EASI of a line containing increasing concentration of sample. The sample is fragmented and the main daughter ion is plotted on the graph. Detection of lower limit compounds is possible using DESI, however at very low concentrations it doesn't give a linear response. This can lead to ambiguous *in situ* information when imaging very low abundance chemical species.

3.3.3 Tandem mass spectrometry imaging

MS/MS imaging was performed with both DESI and EASI to compare the quality of images and demonstrate their potential for tandem mass spectrometry images. Isobaric species can be a problem for mass spectrometers with a lower resolution, however using tandem mass spectrometry isobars can be differentiated. This experiment tests two red inks that are isobars, the formulation

of the two red inks tested gives the same nuance of red. The principal component for the color red is rhodamine B for one pen and rhodamine 6G for the other, both of these compounds appear at *m/z* 443 in a positive ion mode. A image was obtained using selected reaction mode (SRM) where the *m/z* 443 ion was selected and fragmented and the resulting ion spectra was monitored. The signal mapped at *m/z* 443 is the parent ion remaining after collision, the two rhodamine compounds have slightly different collision energy resulting in a different ion intensity. This can be observed in Figure 13b. Rhodamine B fragmentation has a neutral loss of a CO_2 fragment and the daughter ion can be observed at *m/z* 339, while rhodamine 6G fragmentation has a neutral loss of ethylene resulting in a daughter ion observed at *m/z* 415[87].

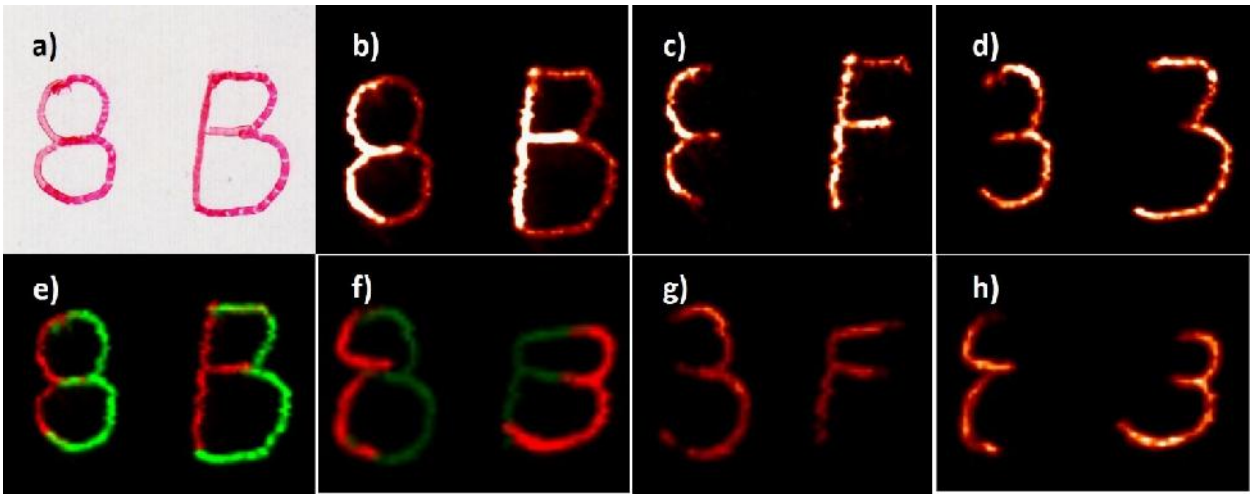

Figure 13. a) Optical image of an 8 and a B made by two different red ink pen formulations to demonstrate an attempt at forging a document. b) DESI image of the 443 m/z ion of the red ink Rhodamine B and Rhodamine 6G c) DESI MS/MS image of the daughter ion 399 m/z of Rhodamine B 443 m/z d) DESI MS/MS image of the daughter ion 415 m/z of Rhodamine 6G 443 m/z e) DESI MS/MS image of the daughter ion 399 m/z, in red, of Rhodamine B 443 m/z ion, and

an overlap of the daughter ion 415 m/z, in green, of Rhodamine 6G 443 m/z f) EASI image of the overlap between ion 399 m/z in green and ion 415 m/z in red. g) EASI MS/MS image of the daughter ion 399 m/z of Rhodamine B 443 m/z h) EASI MS/MS image of the daughter ion 415 m/z of Rhodamine 6G 443 m/z.

Mapping the daughter ions can make it very easy to observe that the red ink comes from two different sources. An overlap of the two daughter ions gives the exact area that was modified and reconstructs an ion image that matches exactly to the optical image, thus demonstrating the use of these techniques for document forensic discrimination. This is observed under both DESI and EASI conditions with similar results. It is important to note that using very high solvent flow rate such as traditional EASI (20µL/min) or very high gas back pressure (400psi) can lead to damage of the document being interrogated, however this study demonstrates that EASI is still a viable alternative if kept at the parameters used in these experiments, namely flow rate 5µL/min and gas back pressure 140psi. These parameters preserved the integrity of the document and had little to no smearing.

3.4 Conclusion

Several new experiments were performed in order to further interrogate the viability of IMS by DESI and EASI. The water sensitive paper demonstrated no significant difference in spray spot size onto a sample when varying voltage, which indicates that both techniques have similar solvent spray distribution. The spatial resolution of both techniques is similar thus we can also conclude that it has similar area of ionization as the DESI experiments. The voltage has virtually no impact on the solvent spray cone distribution, while it may result in different solvent particle sizes it does

not affect the overall area solvent spot or ionization area ionization. For both methods under high flow rate conditions they showed signs of smearing the surface even with increase in pressure; therefore solvents with high volatile composition and low flow rates are desired for imaging purposes. The water sensitive paper experiments revealed that increasing pressure can reduce droplet spread, but not to a significant degree. In imaging experiments high flow rate is undesirable, because it tends to lead to smearing and a larger spray spot area, these results in low quality images with ambiguous ion distribution. EASI had comparable results with DESI even with a low flow rate which indicates it can be practical for IMS use.

The results showed that good chemical images can be obtained by both techniques. DESI was found to be similar or more sensitive than EASI depending on the analyte interrogated.

In the limits of detection experiment when no voltage was applied the detection was in some cases the same or an order of magnitude worse. Similar was the scan of the lipids in the brain tissue which revealed a mirror image in terms of what compounds can be detected in both methods, with a slight drop in overall signal intensity when no voltage was applied. This indicates that both the limit of detection and imaging performance can be enhanced if using a charged solvent. While the ion count is lower in EASI than DESI, both techniques result in similar spatial resolution, can both be used in MS/MS imaging, and have the same sample specificity, hence both can be used to create ion images. Considering that the analyses were conducted using the same experimental conditions (gas pressure, solvent composition and flow rate), further investigation is still necessary to explain the difference in the signal intensity based on physical chemistry properties of the analytes and solvents (proton affinity, solubility, and pKa) and therefore to predict when EASI could replace DESI in IMS without any detriment in terms of analytical sensitivity.

Bibliography

[1] A. El-Aneed, A. Cohen, J. Banoub, Mass Spectrometry, Review of the Basics: Electrospray, MALDI, and Commonly Used Mass Analyzers, Applied Spectroscopy Reviews, 44 (2009) 210-230.
[2] J.J. Thomson, Rays of positive electricity and their application to chemical analyses, Longmans, Green and Company, 1921.
[3] F.G. Kitson, B.S. Larsen, C.N. McEwen, Gas chromatography and mass spectrometry: a practical guide, Academic Press, 1996.
[4] M.S. Munson, F.-H. Field, Chemical ionization mass spectrometry. I. General introduction, Journal of the American Chemical Society, 88 (1966) 2621-2630.
[5] M. Yamashita, J.B. Fenn, Electrospray ion source. Another variation on the free-jet theme, The Journal of Physical Chemistry, 88 (1984) 4451-4459.
[6] D.R. Ifa, J.M. Wiseman, Q. Song, R.G. Cooks, Development of capabilities for imaging mass spectrometry under ambient conditions with desorption electrospray ionization (DESI), International Journal of Mass Spectrometry, 259 (2007) 8-15.
[7] L.A. McDonnell, R.M. Heeren, Imaging mass spectrometry, Mass Spectrom Rev, 26 (2007) 606-643.
[8] G.A. Harris, A.S. Galhena, F.M. Fernandez, Ambient sampling/ionization mass spectrometry: applications and current trends, Anal Chem, 83 (2011) 4508-4538.
[9] E.R. Amstalden van Hove, D.F. Smith, R.M.A. Heeren, A concise review of mass spectrometry imaging, Journal of Chromatography A, 1217 (2010) 3946-3954.
[10] L.A. McDonnell, R.M.A. Heeren, Imaging mass spectrometry, Mass Spectrometry Reviews, 26 (2007) 606-643.
[11] M. Koestler, D. Kirsch, A. Hester, A. Leisner, S. Guenther, B. Spengler, A high-resolution scanning microprobe matrix-assisted laser desorption/ionization ion source for imaging analysis on an ion trap/Fourier transform ion cyclotron resonance mass spectrometer, Rapid Communications in Mass Spectrometry, 22 (2008) 3275-3285.
[12] S. Maharrey, R. Bastasz, R. Behrens, A. Highley, S. Hoffer, G. Kruppa, J. Whaley, High mass resolution SIMS, Appl. Surf. Sci., 231 (2004) 972-975.
[13] R.G. Cooks, Z. Ouyang, Z. Takats, J.M. Wiseman, Detection Technologies. Ambient mass spectrometry, Science, 311 (2006) 1566-1570.
[14] C. Wu, A.L. Dill, L.S. Eberlin, R.G. Cooks, D.R. Ifa, Mass spectrometry imaging under ambient conditions, Mass Spectrometry Reviews, 32 (2013) 218-243.
[15] L.S. Eberlin, A.L. Dill, A.B. Costa, D.R. Ifa, L. Cheng, T. Masterson, M. Koch, T.L. Ratliff, R.G. Cooks, Cholesterol sulfate imaging in human prostate cancer tissue by desorption electrospray ionization mass spectrometry, Anal Chem, 82 (2010) 3430-3434.
[16] M. Morelato, A. Beavis, P. Kirkbride, C. Roux, Forensic applications of desorption electrospray ionisation mass spectrometry (DESI-MS), Forensic Science International, 226 (2013) 10-21.
[17] L.S. Eberlin, R. Haddad, R.C. Sarabia Neto, R.G. Cosso, D.R.J. Maia, A.O. Maldaner, J.J. Zacca, G.B. Sanvido, W. Romao, B.G. Vaz, D.R. Ifa, A. Dill, R.G. Cooks, M.N. Eberlin, Instantaneous chemical profiles of banknotes by ambient mass spectrometry, Analyst, 135 (2010) 2533-2539.
[18] D.R. Justes, N. Talaty, I. Cotte-Rodriguez, R.G. Cooks, Detection of explosives on skin using ambient ionization mass spectrometry, Chemical Communications, (2007) 2142-2144.
[19] M. Nefliu, A. Venter, R.G. Cooks, Desorption electrospray ionization and electrosonic spray ionization for solid- and solution-phase analysis of industrial polymers, Chem Commun (Camb), (2006) 888-890.
[20] Q. Hu, N. Talaty, R.J. Noll, R.G. Cooks, Desorption electrospray ionization using an Orbitrap mass spectrometer: exact mass measurements on drugs and peptides, Rapid Communications in Mass Spectrometry, 20 (2006) 3403-3408.

[21] R. Haddad, R. Sparrapan, M.N. Eberlin, Desorption sonic spray ionization for (high) voltage-free ambient mass spectrometry, Rapid Communications in Mass Spectrometry, 20 (2006) 2901-2905.
[22] W. Rao, D.J. Scurr, J. Burston, M.R. Alexander, D.A. Barrett, Use of imaging multivariate analysis to improve biochemical and anatomical discrimination in desorption electrospray ionisation mass spectrometry imaging, Analyst, 137 (2012) 3946-3953.
[23] R.G. Cooks, N.E. Manicke, A.L. Dill, D.R. Ifa, L.S. Eberlin, A.B. Costa, H. Wang, G. Huang, Z. Ouyang, New ionization methods and miniature mass spectrometers for biomedicine: DESI imaging for cancer diagnostics and paper spray ionization for therapeutic drug monitoring, Faraday Discuss., 149 (2011) 247-267.
[24] C. Wu, D.R. Ifa, N.E. Manicke, R.G. Cooks, Molecular imaging of adrenal gland by desorption electrospray ionization mass spectrometry, Analyst, 135 (2010) 28-32.
[25] Z. Takats, J.M. Wiseman, R.G. Cooks, Ambient mass spectrometry using desorption electrospray ionization (DESI): instrumentation, mechanisms and applications in forensics, chemistry, and biology, Journal of mass spectrometry : JMS, 40 (2005) 1261-1275.
[26] A.B. Costa, R. Graham Cooks, Simulated splashes: Elucidating the mechanism of desorption electrospray ionization mass spectrometry, Chemical Physics Letters, 464 (2008) 1-8.
[27] V. Kertesz, G.J. Van Berkel, Improved imaging resolution in desorption electrospray ionization mass spectrometry, Rapid Communications in Mass Spectrometry, 22 (2008) 2639-2644.
[28] I. Cotte-Rodríguez, Z. Takáts, N. Talaty, H. Chen, R.G. Cooks, Desorption Electrospray Ionization of Explosives on Surfaces: Sensitivity and Selectivity Enhancement by Reactive Desorption Electrospray Ionization, Analytical Chemistry, 77 (2005) 6755-6764.
[29] D.R. Ifa, N.E. Manicke, A.L. Rusine, R.G. Cooks, Quantitative analysis of small molecules by desorption electrospray ionization mass spectrometry from polytetrafluoroethylene surfaces, Rapid Communications in Mass Spectrometry, 22 (2008) 503-510.
[30] Z. Takats, J.M. Wiseman, B. Gologan, R.G. Cooks, Mass spectrometry sampling under ambient conditions with desorption electrospray ionization, Science, 306 (2004) 471-473.
[31] H. Chen, I. Cotte-Rodriguez, R.G. Cooks, cis-Diol functional group recognition by reactive desorption electrospray ionization (DESI), Chem Commun (Camb), (2006) 597-599.
[32] T. Muller, S. Oradu, D.R. Ifa, R.G. Cooks, B. Krautler, Direct plant tissue analysis and imprint imaging by desorption electrospray ionization mass spectrometry, Anal Chem, 83 (2011) 5754-5761.
[33] L. Nyadong, M.D. Green, V.R. De Jesus, P.N. Newton, F.M. Fernandez, Reactive desorption electrospray ionization linear ion trap mass spectrometry of latest-generation counterfeit antimalarials via noncovalent complex formation, Anal Chem, 79 (2007) 2150-2157.
[34] R. Haddad, R. Sparrapan, T. Kotiaho, M.N. Eberlin, Easy Ambient Sonic-Spray Ionization-Membrane Interface Mass Spectrometry for Direct Analysis of Solution Constituents, Analytical Chemistry, 80 (2008) 898-903.
[35] P.M. Lalli, G.B. Sanvido, J.S. Garcia, R. Haddad, R.G. Cosso, D.R.J. Maia, J.J. Zacca, A.O. Maldaner, M.N. Eberlin, Fingerprinting and aging of ink by easy ambient sonic-spray ionization mass spectrometry, Analyst, 135 (2010) 745-750.
[36] E.M. Borges, D.A. Volmer, M.N. Eberlin, Comprehensive analysis of Ginkgo tablets by easy ambient sonic spray ionization mass spectrometry, Canadian Journal of Chemistry, 91 (2013) 671-678.
[37] P.V. Abdelnur, S.A. Saraiva, R.R. Catharino, M. Coelho, N. Schwab, C.M. Garcia, U. Schuchardt, V. de Souza, M.N. Eberlin, Blends of Soybean Biodiesel with Petrodiesel: Direct Quantitation via Mass Spectrometry, J Brazil Chem Soc, 24 (2013) 946-952.
[38] I.B.S. Cunha, A.M.A.P. Fernandes, D.U. Tega, R.C. Simas, H.L. Nascimento, G.F. de Sá, R.J. Daroda, M.N. Eberlin, R.M. Alberici, Quantitation and Quality Control of Biodiesel/Petrodiesel (Bn) Blends by Easy Ambient Sonic-Spray Ionization Mass Spectrometry, Energy & Fuels, 26 (2012) 7018-7022.
[39] A. Hirabayashi, M. Sakairi, H. Koizumi, Sonic spray mass spectrometry, Analytical Chemistry, 67 (1995) 2878-2882.

[40] W. Rao, D. Mitchell, P. Licence, D.A. Barrett, The use of dicationic ion-pairing compounds to enhance the ambient detection of surface lipids in positive ionization mode using desorption electrospray ionisation mass spectrometry, Rapid communications in mass spectrometry : RCM, 28 (2014) 616-624.
[41] M.D. Joshi, J.L. Anderson, Recent advances of ionic liquids in separation science and mass spectrometry, RSC Advances, 2 (2012) 5470.
[42] X. Lin, A.R. Gerardi, Z.S. Breitbach, D.W. Armstrong, C.L. Colyer, CE-ESI-MS analysis of singly charged inorganic and organic anions using a dicationic reagent as a complexing agent, Electrophoresis, 30 (2009) 3918-3925.
[43] C. Xu, D.W. Armstrong, High-performance liquid chromatography with paired ion electrospray ionization (PIESI) tandem mass spectrometry for the highly sensitive determination of acidic pesticides in water, Analytica chimica acta, 792 (2013) 1-9.
[44] Z.S. Breitbach, E. Wanigasekara, E. Dodbiba, K.A. Schug, D.W. Armstrong, Mechanisms of ESI-MS selectivity and sensitivity enhancements when detecting anions in the positive mode using cationic pairing agents, Anal Chem, 82 (2010) 9066-9073.
[45] A. Kawahara, T. Nishi, Y. Hisano, H. Fukui, A. Yamaguchi, N. Mochizuki, The sphingolipid transporter spns2 functions in migration of zebrafish myocardial precursors, Science, 323 (2009) 524-527.
[46] W. Norton, L. Bally-Cuif, Adult zebrafish as a model organism for behavioural genetics, BMC neuroscience, 11 (2010) 90.
[47] Z. Lele, P.H. Krone, The zebrafish as a model system in developmental, toxicological and transgenic research, Biotechnology Advances, 14 (1996) 57-72.
[48] R. Nagel, DarT: The embryo test with the zebrafish Danio rerio - a general model in ecotoxicology and toxicology, Altex-Altern Tierexp, 19 (2002) 38-48.
[49] A.J. Hill, H. Teraoka, W. Heideman, R.E. Peterson, Zebrafish as a model vertebrate for investigating chemical toxicity, Toxicological sciences : an official journal of the Society of Toxicology, 86 (2005) 6-19.
[50] Y.J. Dai, Y.F. Jia, N. Chen, W.P. Bian, Q.K. Li, Y.B. Ma, Y.L. Chen, D.S. Pei, Zebrafish as a model system to study toxicology, Environmental toxicology and chemistry / SETAC, 33 (2014) 11-17.
[51] H. Feitsma, E. Cuppen, Zebrafish as a cancer model, Molecular cancer research : MCR, 6 (2008) 685-694.
[52] M. Konantz, T.B. Balci, U.F. Hartwig, G. Dellaire, M.C. Andre, J.N. Berman, C. Lengerke, Zebrafish xenografts as a tool for in vivo studies on human cancer, Annals of the New York Academy of Sciences, 1266 (2012) 124-137.
[53] D.I. Bassett, P.D. Currie, The zebrafish as a model for muscular dystrophy and congenital myopathy, Human molecular genetics, 12 Spec No 2 (2003) R265-270.
[54] Y.J. Li, B. Hu, Establishment of multi-site infection model in zebrafish larvae for studying Staphylococcus aureus infectious disease, Journal of genetics and genomics = Yi chuan xue bao, 39 (2012) 521-534.
[55] C. Sullivan, C.H. Kim, Zebrafish as a model for infectious disease and immune function, Fish & shellfish immunology, 25 (2008) 341-350.
[56] R.D. Porsolt, G. Anton, N. Blavet, M. Jalfre, Behavioural despair in rats: A new model sensitive to antidepressant treatments, European Journal of Pharmacology, 47 (1978) 379-391.
[57] T. Sakurai, A. Amemiya, M. Ishii, I. Matsuzaki, R.M. Chemelli, H. Tanaka, S.C. Williams, J.A. Richarson, G.P. Kozlowski, S. Wilson, J.R. Arch, R.E. Buckingham, A.C. Haynes, S.A. Carr, R.S. Annan, D.E. McNulty, W.S. Liu, J.A. Terrett, N.A. Elshourbagy, D.J. Bergsma, M. Yanagisawa, Orexins and orexin receptors: a family of hypothalamic neuropeptides and G protein-coupled receptors that regulate feeding behavior, Cell, 92 (1998) 1 page following 696.
[58] M.V. Zoriy, M. Dehnhardt, A. Matusch, J.S. Becker, Comparative imaging of P, S, Fe, Cu, Zn and C in thin sections of rat brain tumor as well as control tissues by laser ablation inductively coupled plasma mass spectrometry, Spectrochimica Acta Part B: Atomic Spectroscopy, 63 (2008) 375-382.

[59] M.L. Reyzer, Y. Hsieh, K. Ng, W.A. Korfmacher, R.M. Caprioli, Direct analysis of drug candidates in tissue by matrix-assisted laser desorption/ionization mass spectrometry, Journal of Mass Spectrometry, 38 (2003) 1081-1092.
[60] Y. Chen, J. Allegood, Y. Liu, E. Wang, B. Cachón-González, T.M. Cox, A.H. Merrill, M.C. Sullards, Imaging MALDI Mass Spectrometry Using an Oscillating Capillary Nebulizer Matrix Coating System and Its Application to Analysis of Lipids in Brain from a Mouse Model of Tay−Sachs/Sandhoff Disease, Analytical Chemistry, 80 (2008) 2780-2788.
[61] J. Pierson, J.L. Norris, H.-R. Aerni, P. Svenningsson, R.M. Caprioli, P.E. Andrén, Molecular Profiling of Experimental Parkinson's Disease: Direct Analysis of Peptides and Proteins on Brain Tissue Sections by MALDI Mass Spectrometry, Journal of Proteome Research, 3 (2004) 289-295.
[62] E.H. Seeley, R.M. Caprioli, Molecular imaging of proteins in tissues by mass spectrometry, Proceedings of the National Academy of Sciences, 105 (2008) 18126-18131.
[63] G.P. Reynolds, S.J. Pearson, J. Halket, M. Sandier, Brain Quinolinic Acid in Huntington's Disease, Journal of neurochemistry, 50 (1988) 1959-1968.
[64] D.P. Hanger, B.H. Anderton, W. Noble, Tau phosphorylation: the therapeutic challenge for neurodegenerative disease, Trends in Molecular Medicine, 15 (2009) 112-119.
[65] L.S. Eberlin, I. Norton, A.L. Dill, A.J. Golby, K.L. Ligon, S. Santagata, R.G. Cooks, N.Y. Agar, Classifying human brain tumors by lipid imaging with mass spectrometry, Cancer research, 72 (2012) 645-654.
[66] L.S. Eberlin, M. Gabay, A.C. Fan, A.M. Gouw, R.J. Tibshirani, D.W. Felsher, R.N. Zare, Alteration of the lipid profile in lymphomas induced by MYC overexpression, Proceedings of the National Academy of Sciences of the United States of America, 111 (2014) 10450-10455.
[67] C. Wu, D.R. Ifa, N.E. Manicke, R.G. Cooks, Rapid, direct analysis of cholesterol by charge labeling in reactive desorption electrospray ionization, Anal Chem, 81 (2009) 7618-7624.
[68] J.L. Anderson, R. Ding, A. Ellern, D.W. Armstrong, Structure and properties of high stability geminal dicationic ionic liquids, Journal of the American Chemical Society, 127 (2005) 593-604.
[69] H. Tadesse, A.J. Blake, N.R. Champness, J.E. Warren, P.J. Rizkallah, P. Licence, Supramolecular architectures of symmetrical dicationic ionic liquid based systems, Crystengcomm, 14 (2012) 4886-4893.
[70] S. Koizumi, S. Yamamoto, T. Hayasaka, Y. Konishi, M. Yamaguchi-Okada, N. Goto-Inoue, Y. Sugiura, M. Setou, H. Namba, Imaging mass spectrometry revealed the production of lyso-phosphatidylcholine in the injured ischemic rat brain, Neuroscience, 168 (2010) 219-225.
[71] C. Lohmann, E. Schachmann, T. Dandekar, C. Villmann, C.M. Becker, Developmental profiling by mass spectrometry of phosphocholine containing phospholipids in the rat nervous system reveals temporo-spatial gradients, Journal of neurochemistry, 114 (2010) 1119-1134.
[72] H.J. Yang, Y. Sugiura, K. Ikegami, Y. Konishi, M. Setou, Axonal gradient of arachidonic acid-containing phosphatidylcholine and its dependence on actin dynamics, The Journal of biological chemistry, 287 (2012) 5290-5300.
[73] A.L. Dill, D.R. Ifa, N.E. Manicke, Z. Ouyang, R.G. Cooks, Mass spectrometric imaging of lipids using desorption electrospray ionization, Journal of chromatography. B, Analytical technologies in the biomedical and life sciences, 877 (2009) 2883-2889.
[74] N.E. Manicke, J.M. Wiseman, D.R. Ifa, R.G. Cooks, Desorption electrospray ionization (DESI) mass spectrometry and tandem mass spectrometry (MS/MS) of phospholipids and sphingolipids: ionization, adduct formation, and fragmentation, J Am Soc Mass Spectrom, 19 (2008) 531-543.
[75] J.M. Wiseman, D.R. Ifa, Q. Song, R.G. Cooks, Tissue imaging at atmospheric pressure using desorption electrospray ionization (DESI) mass spectrometry, Angew Chem Int Ed Engl, 45 (2006) 7188-7192.
[76] M. Girod, Y. Shi, J.X. Cheng, R.G. Cooks, Desorption electrospray ionization imaging mass spectrometry of lipids in rat spinal cord, J Am Soc Mass Spectrom, 21 (2010) 1177-1189.
[77] T. Melo, R.A. Videira, S. Andre, E. Maciel, C.S. Francisco, A.M. Oliveira-Campos, L.M. Rodrigues, M.R. Domingues, F. Peixoto, M. Manuel Oliveira, Tacrine and its analogues impair mitochondrial

function and bioenergetics: a lipidomic analysis in rat brain, Journal of neurochemistry, 120 (2012) 998-1013.
[78] J.A. Hankin, S.E. Farias, R.M. Barkley, K. Heidenreich, L.C. Frey, K. Hamazaki, H.Y. Kim, R.C. Murphy, MALDI mass spectrometric imaging of lipids in rat brain injury models, J Am Soc Mass Spectrom, 22 (2011) 1014-1021.
[79] J.A. Hankin, R.C. Murphy, Relationship between MALDI IMS intensity and measured quantity of selected phospholipids in rat brain sections, Anal Chem, 82 (2010) 8476-8484.
[80] S.N. Jackson, M. Ugarov, T. Egan, J.D. Post, D. Langlais, J. Albert Schultz, A.S. Woods, MALDI-ion mobility-TOFMS imaging of lipids in rat brain tissue, Journal of mass spectrometry : JMS, 42 (2007) 1093-1098.
[81] H.Y. Wang, S.N. Jackson, J. Post, A.S. Woods, A Minimalist Approach to MALDI Imaging of Glycerophospholipids and Sphingolipids in Rat Brain Sections, Int J Mass Spectrom, 278 (2008) 143-149.
[82] D.J. Harvey, Matrix-assisted laser desorption/ionisation mass spectrometry of oligosaccharides and glycoconjugates, Journal of Chromatography A, 720 (1996) 429-446.
[83] S. Sekiya, Y. Wada, K. Tanaka, Derivatization for stabilizing sialic acids in MALDI-MS, Anal Chem, 77 (2005) 4962-4968.
[84] A. Chramow, T.S. Hamid, L.S. Eberlin, M. Girod, D.R. Ifa, Imaging of whole zebra fish (Danio rerio) by desorption electrospray ionization mass spectrometry, Rapid Communications in Mass Spectrometry, 28 (2014) 2084-2088.
[85] S. Milne, P. Ivanova, J. Forrester, H.A. Brown, Lipidomics: an analysis of cellular lipids by ESI-MS, Methods, 39 (2006) 92-103.
[86] C. Janfelt, A. Nørgaard, Ambient Mass Spectrometry Imaging: A Comparison of Desorption Ionization by Sonic Spray and Electrospray, J. Am. Soc. Mass Spectrom., 23 (2012) 1670-1678.
[87] D.R. Ifa, L.M. Gumaelius, L.S. Eberlin, N.E. Manicke, R.G. Cooks, Forensic analysis of inks by imaging desorption electrospray ionization (DESI) mass spectrometry, Analyst, 132 (2007) 461-467.

analytical chemistry

Article

pubs.acs.org/ac

Reactive DESI-MS Imaging of Biological Tissues with Dicationic Ion-Pairing Compounds

Dragos Lostun,[†] Consuelo J. Perez,[†] Peter Licence,[‡] David A. Barrett,[§] and Demian R. Ifa*[,†]

[†]Department of Chemistry, Centre for Research in Mass Spectrometry, York University, Toronto, Ontario M3J 1P3, Canada

[‡]School of Chemistry, University of Nottingham, Nottingham NG7 2RD, U.K.

[§]Centre for Analytical Bioscience, School of Pharmacy, University of Nottingham, Nottingham NG7 2RD, U.K.

Supporting Information

ABSTRACT: This work illustrates reactive desorption electrospray ionization mass spectrometry (DESI-MS) with a stable dication on biological tissues. Rat brain and zebra fish tissues were investigated with reactive DESI-MS in which the dictation forms a stable bond with biological tissue fatty acids and lipids. Tandem mass spectrometry (MS/MS) was used to characterize the dication (DC9) and to identify linked lipid-dication compounds formed. The fragment m/z 85 common to both DC9 fragmentation and DC9-lipid fragmentation was used to confirm that DC9 is indeed bonded with the lipids. Lipid signals in the range of m/z 250−350 and phosphoethanolamines (PE) m/z 700−800 observed in negative ion mode were also detected in positive ion mode with reactive DESI-MS with enhanced signal intensity. Reactive DESI-MS imaging in positive ion mode of rat brain and zebra fish tissues allowed enhanced detection of compounds commonly observed in the negative ion mode.

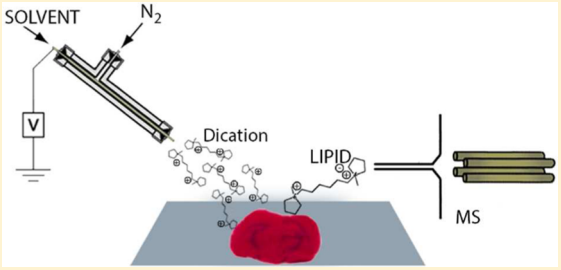

Imaging mass spectrometry (MS) is an established field of mass spectrometry; it is a powerful tool capable of measuring ion distributions over spatial coordinates. Several imaging MS techniques have been used over the years, such as secondary ion mass spectrometry (SIMS), matrix-assisted laser desorption ionization mass spectrometry (MALDI-MS), and desorption electrospray ionization mass spectrometry (DESI-MS), among others.[1−3]

DESI-MS is a versatile ambient technique used for imaging MS since 2006.[1,4−10] DESI-MS works by spraying charged solvent droplets onto a sample. A liquid interface with the surface is created into which the analytes get transferred; subsequent charged droplets impact the surface and desorb droplets containing the analyte via a "droplet pick up" mechanism. Gas phase ions are produced by drying of the droplets containing analyte, which then proceed to the MS inlet to be analyzed by the mass spectrometer.[11] Reactive DESI-MS is a variant of the DESI-MS technique, in which a reactant is included in the spray solvent. When the solution is sprayed on the sample surface it reacts with the sample analyte, the resulting product is analyzed by the mass spectrometer. Reactive DESI has been used when working with samples that are difficult to ionize, typically via simple adduct formation, such as complexation of RDX with the anion CF_3COO^- or TNT with the methoxide anion.[12] However, bond-forming reactions using reactive DESI were also reported.[13] The experiment used cyclization with benzeneboronate anions $PhB(OH)_3^-$ on biomolecules containing aliphatic diols and aromatic diols, compounds which are not ionized efficiently via ESI and MALDI. Reactive DESI is a powerful tool due to its capabilities to be able to target molecules of interest or difficult to ionize compounds, in order to detect and/or enhance the ionization efficiency.[12−16]

Ionic liquids are salts of cations and anions that cannot easily form a crystal and will remain in liquid state at room temperature. Commonly used in organic synthesis, in this work they have been implemented in mass spectrometry to enhance compound detection and boost signal intensity by adduct formation or covalent bonding to targets of interest.[17−21]

In a recent work involving stable dications applied to reactive DESI-MS, nine stable dicationic compounds named DC1-DC9 were synthesized and tested against lipid standards. The dications have two rings of either 5 or 6 atoms, linked by a hydrocarbon chain with varying length and with a positive charge on the nitrogen atom of each ring. The compounds DC2 and DC9 achieved increased signal intensity in the reactive DESI-MS mode when tested on lipid standards compared to negative ion mode control. DC9 attained superior signal intensity over a broader range of compounds than DC2, therefore DC9 has been chosen for the purpose of this study. DC9 has the molecular formula [C6(C1Pyrr)2][Br]2 and is a stable dicationic salt able to bind to a negatively charged compound (Figure 1). It can be detected as a bound ion-pair (DC9-lipid) in the positive ion mode in DESI-MS. DC9 has a mass of 254.4 Da and one positive charge on each nitrogen

Received: November 12, 2014
Accepted: February 12, 2015
Published: February 24, 2015

DOI: 10.1021/ac5042445
Anal. Chem. 2015, 87, 3286−3293

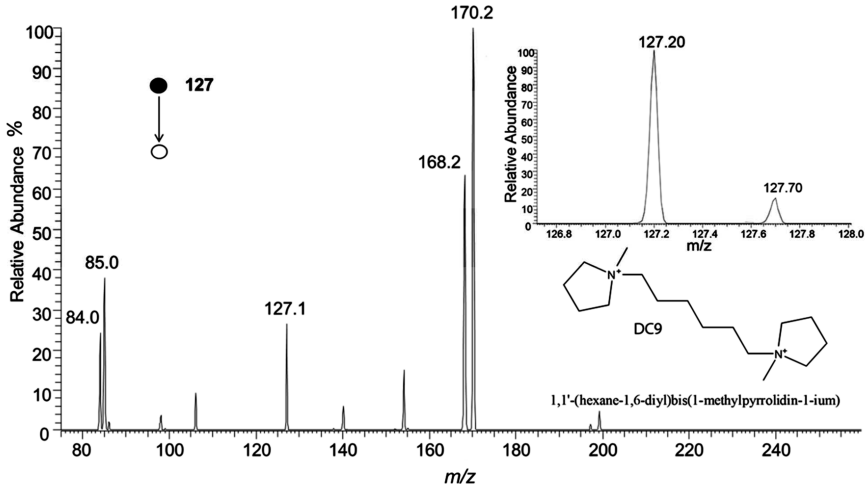

Figure 1. Tandem mass spectrometry (MS/MS) analysis of the dicationic compound DC9 observed at m/z 127. Top inset is a zoom scan (a feature of Thermo Finnigan instrument, a scan with a higher resolution and longer acquisition time) which shows the natural abundance isotope of the doubly charged species, and the bottom inset shows the structure of the DC9 dication with its IUPAC name.

atom, and it can be observed at m/z 127.1 by DESI-MS. Once DC9 binds to the lipid, the net charge of the complex becomes positive, which permits imaging of compounds, more importantly, lipids in the positive ion mode. Fatty acids and certain classes of lipids are detected in the negative ion mode; however, DC9 is capable of creating an ion-pair, changing the polarity of the compounds for DESI-MS analysis. Analyses with DC9 in the positive ion mode allows for a higher signal-to-noise ratio and increased sensitivity for selected lipids when compared to the negative ion mode. It is important to mention that steric hindrance, structural flexibility, and charge localization seem to be the main factors affecting binding of the ionic liquid to the targeted lipid for detection in the positive ion mode.[17]

The aim of this work is to evaluate the performance of the dicationic compound DC9 in biological tissue samples in the positive ion mode by DESI-MS. Enhancements of the lipid signal intensity and/or signal-to-noise levels due to a change in polarity can allow improved imaging of biological samples. Zebra fish were selected here since it is an important biological model commonly used to study genetics,[22,23] environmental toxicology,[24−27] cancer,[28,29] and other diseases.[30−32] Rat brain is another important biological model generally used to study behavioral patterns,[33,34] cancer,[35,36] and disease.[37−41]

We introduce applications for imaging of lipids in the positive ion mode from rat brain and whole body zebra fish tissue with enhanced intensity and ionization efficiency using reactive DESI-MS. DESI-MS has been employed in negative ion mode to discriminate normal from cancerous tissue based on lipid profiles;[42−44] we foresee this application to open new avenues into cancer research and lipidomics studies on complex tissues.

MATERIALS AND METHODS

Materials and Biological Samples. The HPLC-grade methanol, tricainemesylate and carboxymethyl cellulose sodium (CMC), were purchased from Sigma-Aldrich (Oakville, ON, CA). Porous PTFE sheets 1.5 mm thick with an average porous size of 7 μm was purchased from Berghof (Eningen, Germany). Microscope slides 26 × 77 mm with a thickness of 1 mm single frosted were purchased from Bionuclear diagnostics Inc. (Toronto, ON, Canada). Rat brains were purchased from Rockland Immunochemicals Inc. (Gilbertsville, PA). Zebra fish were donated by Dr. Chun Peng (York University, Toronto, ON, CA). H&E staining kit was purchased from American Master Tech Scientific (Lodi, CA).

Dicationic Compound Synthesis and Preparation. The compound DC9 investigated in this study was synthesized using previously reported literature.[17,45,46] A stock solution of 1 mM was prepared by dissolving DC9 in methanol. A diluted 10 μM DC9 solution was prepared from DC9 stock solution and diluted into a 20 mL sterilized vial with methanol. All DESI-MS, imaging, and tandem mass spectrometry (MS/MS) experiments with DC9 were conducted with 10 μM DC9 methanol solution in the solvent spray. For the purpose of this study, the dicationic compound DC9 was investigated against biological tissue samples.

Rat Brain Sample Preparation and Cryosectioning. Rat brain was stored in a −80 °C freezer. The brain was sectioned into 20 μm size coronal cross section slices on a Shandon cryotome FE (Thermo Fischer Scientific, Nepean, ON, Canada). The sections were placed onto microscope glass slides and kept frozen in a −18 °C freezer. Prior to DESI-MS analysis, the rat brain tissue slices were defrosted and dried for 30 min at room temperature. H&E staining was conducted on adjacent tissue sections after DESI-MS analysis.

Zebra Fish Tissue Sample Preparation and Cryosectioning. Four zebra fish were euthanized in a container with tricainemesylate solution at 300 mg/L. The deceased fish were placed into flexible molds to provide support and prevent deformation while cryosectioning. A 5% CMC solution was prepared with distilled water and poured into each mold containing a whole body zebra fish. The molds were immediately frozen at −18 °C overnight before sectioning. For cryosectioning, the plastic mold was removed and CMC frozen zebra fish blocks were used to prepare 20−50 μm sagittal tissue sections. The fish slices were placed on glass microscopic glass slides and kept in −18 °C freezer until use. Prior to DESI-MS analysis, the zebra fish slices were defrosted and dried for 30 min at room temperature. H&E was conducted on adjacent tissue sections after DESI-MS analysis.

Tandem Mass Spectrometry (MS/MS) Analysis. For the DC9 characterization, 2 μL of a 10 μM solution was spotted on a PTFE surface and sprayed with pure methanol. For the

DOI: 10.1021/ac5042445
Anal. Chem. 2015, 87, 3286−3293

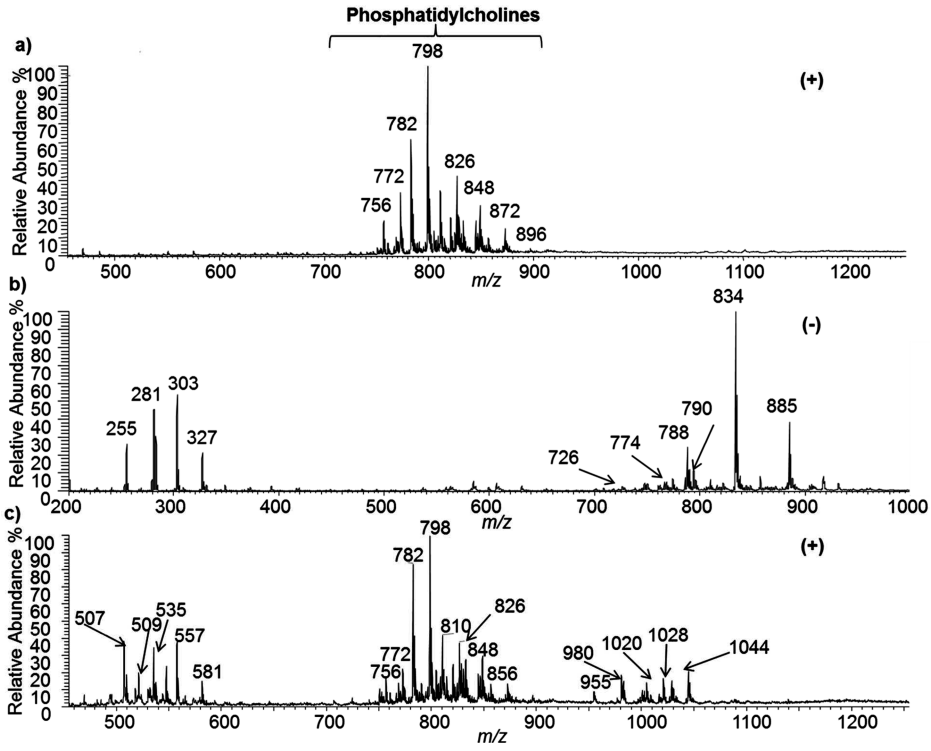

Figure 2. Representative DESI-MS mass spectra of lipids in rat brain. (a) Phosphatidylcholines present in rat brain in positive ion mode control (b) Lipids in rat brain in negative ion mode control. (c) Reactive DESI-MS spectrum of enhanced intensity DC9-lipid ion pairs in rat brain in the positive ion mode.

characterization in reactive DESI-MS, 10 μM DC9 in methanol was sprayed directly onto the biological tissue samples. The MS/MS collision energy was set to 90 (arbitrary units) for the DC9 and 12 (arbitrary units) for the DC9-lipid compounds.

DESI-MS Parameters for Rat Brain and Zebra Fish Tissue. The nebulizing nitrogen gas back pressure was 120 psi, the solvent voltage was set at 5 kV, the spray capillary to surface angle was 52°, the spray capillary to surface distance was ~0.5−2 mm, and the spray capillary to inlet distance was 4−5 mm. The solvent flow rate was set at 3 μL/min, and solvent composition was pure MeOH for negative ion and positive ion modes control, and MeOH spiked to 10 μM DC9 for reactive DESI-MS positive ion mode. The injection time was set at 30 and 40 ms for rat brain and zebra fish, respectively. Imaging spatial resolution was set at 150 μm for both rat brain and zebra fish. The mass in the negative ion mode was scanned in the range of m/z 200−800. In the positive ion mode and the reactive DESI-MS positive ion mode control the mass was scanned in the range of m/z 454−1245. The data was acquired on a Thermo Finnigan LTQ using Xcalibur and was processed using Biomap (freeware, www.msi.maldi.org) to generate ion images of signal intensity versus spatial coordinates.

DISCUSSION

The identity of DC9 was confirmed by spotting 2 μL of 1 mM DC9 sample on a PTFE surface and spraying the spot with pure methanol solvent. Moreover, DC9 was subjected to MS/MS analysis from the spotted sample on a PTFE surface. One common fragment at m/z 85 corresponds to *N*-methyl pyrrolidine radical cation from the alpha cleavage of the nitrogen ring. Its complementary radical cation at m/z 169 is not observed. Instead, the peak at m/z 168 can be associated with the loss of a hydrogen radical in order to form a carbon−carbon double bond at the end of the chain. This double bond could help in the stabilization of the remaining positive charge. The fragment observed at m/z 84 corresponds to the methyl heterocyclic ring cation with a double bond. Its complementary cation can be observed at m/z 170 (Figure 1).

Rat Brain DESI-MS Analysis. Different solvent systems were investigated briefly in a previous study.[17] It was found that pure methanol gave a superior signal over a chloroform methanol 1:1 mix. These findings were confirmed for imaging experiments conducted on rat brain and zebra fish tissues. Reactive DESI-MS was attempted in a chloroform:methanol 1:1 (v/v) mix on rat brain and zebra fish tissues; it was found to have a decreased intensity compared to a pure methanol solvent system (data not shown). All experiments involving DESI-MS in negative and positive ion mode controls were performed under optimum solvent conditions of pure methanol. The rat brain tissue was submitted to three analyses for comparison: DESI-MS in positive ion mode control, DESI-MS in the negative ion mode, and reactive DESI-MS with DC9 in the positive ion mode.

In the positive ion mode control (Figure 2a) and in the reactive DESI-MS experiments on the rat brain tissue (Figure 2c), a cluster of phosphatidylcholines between m/z 700−900 was observed. MS/MS analysis was conducted on the peaks in the cluster and several of the highest intensity compounds, m/z 782, 798, and 848, were identified as phosphatidylcholines. Phosphatidylcholines have a main fragment neutral loss of 59 Da associated with trimethylamine and a neutral loss of 183 Da corresponding to the choline head group which was observed in the peaks between m/z 700−900 (Figure S1 of the Supporting Information).[47−49]

In the negative ion mode, two distinct clusters of ions were observed in the rat brain tissue (Figure 2b). In the first cluster

DOI: 10.1021/ac5042445
Anal. Chem. 2015, 87, 3286−3293

of ions, between m/z 250−350, palmitoleic acid (16:1) at m/z 253, palmitic acid (16:0) at m/z 255, oleic acid (18:1) at m/z 281, and arachidonic acid (20:4) at m/z 303 were identified. Another cluster was observed between m/z 700−900 consisting of phosphoethanolamine (PE 36:1) at m/z 700 (not shown), phosphoethanolamine (PE 36:2) at m/z 726, phosphoethanolamine (PE 38:4) at m/z 766 (not shown), phosphoethanolamine (PE 40:6) at m/z 774, and phosphoethanolamine (PE 40:6) at m/z 790 (Figure 2b).

Figure 2 has a mass shift of m/z 254 for the positive ion mode in order to align the ions bound to DC9 with the observed negative ions. DC9 has a permanent charge and a very strong signal intensity; the mass range around 254 displays a very strong peak suppressing the signal and leads to broad peeks and unstable signal, therefore it is necessary to choose a mass range above this peak to acquire quality data with DC9.

Several fatty acids and lipids present in the DESI-MS negative ion mode can be observed with DC9 in positive spectra. In the positive ion mode reactive DESI-MS with compound DC9, three distinct clusters of ions can be observed (Figure 2c). The first cluster of ions between m/z 500−600 corresponds to the first cluster in the negative ion mode. DC9-palmitoleic acid (16:1) at m/z 507 was enhanced compared to the negative ion mode spectra, while other fatty acids in that range maintained their previous profile. The second cluster observed between m/z 700−900 is the phosphatidylcholines species in similar abundance to the DESI-MS positive ion mode control. The third cluster of ions between m/z 950−1050 is where the most increase in terms of both the relative and absolute intensity is observed when compared to the negative ion mode spectrum. Several lipids had enhanced relative intensity; for instance, PE (34:1) m/z 700 cannot be reasonably detected in the negative ion mode since it is in the noise level, and PE (36:2) m/z 726 has very low intensity in the negative ion mode. However, in the reactive DESI-MS spectrum with DC9, the relative intensity increased and became easily distinguishable from the noise level (Figure 2c). PE (34:1) and PE (36:2) can be observed in the positive ion mode as their mass plus the DC9 mass at m/z 955 and m/z 980, respectively (Figure 2c). The very intense peaks in the negative ion mode at m/z 834 and m/z 885 correspond to a phosphatidylserine (PS 40:6) and a phosphatidylinositol (PI 48:4) that are not observed in the reactive DESI-MS spectrum. As a result, the use of this technique can provide information complementary to the negative ion mode spectra and enhance the signal of low intensity ions that might be available in the sample but difficult to ionize or desorb. Table 1 summarizes the effect of reactive DESI-MS on specific fatty acids or lipids compared to the negative ion mode results. To determine how the DC9 compound affects detection, the signal-to-noise was used as an indicator. Signal intensity does not necessarily correlate with better detection, in our case DC9 compounds detected in the positive mode were seen to have higher intensity but also higher noise levels. Thus we report the change in signal-to-noise ratio in order to have normalized data comparison. Three average spectra taken across the entire rat brain samples were compared between positive ion mode scans with DC9 and negative ion mode scans. The three spectra chosen targeted gray and white matter and were taken from the widest section of the brain. Table 1 reports whether the signal-to-noise levels of each compound increased or decreased compared to their native detection in the negative ion mode. These values are provided in order to help the understanding of the signal change using DC9; however, variations between and within samples based not only on the chemical nature of this reaction but also by the small variation of the spray geometry features of DESI can occur.

Table 1. Lipids and Dicationic Compound DC9 Forming Ion-Pairs in DESI-MS Spectrum in Positive Ion Mode of Rat Brain (DC9 MW 254.4 Da)

rat brain lipids in negative ion mode	observed m/z negative ion mode	DC9-lipid ion pair in rat brain in positive ion mode	signal to noise change (DC9 vs negative ion mode)
palmitoleic acid (16:1)	253[50,51]	507	512%
palmitic acid (16:0)	255[50−52]	509	26%
oleic acid (18:1)	281[50−53]	535	37%
arachidonic acid (20:4)	303[50−53]	557	37%
phosphoethanolamine (PE 34:1)	700[54]	955	127%
phosphoethanolamine (PE 36:2)	726[54]	980	107%
phosphoethanolamine (PE 38:4)	766[54]	1020	153%
phosphoethanolamine (PE 40:6)	774[54]	1028	124%
phosphoethanolamine (PE 40:6)	790[54]	1044	119%
phosphatidylserine (PS 40:6)	834[50,52,53]	1088	not detected
phosphotidylinositol (PI 38:4)	885[50−53]	1139	not detected

Using tandem mass spectrometry, we identified several compounds to be linked with DC9: m/z 507, 535, 557, 980, 1020, 1028, and 1044 consisting of DC9-lipid ion pairs. A common loss of 85 was observed for all ions mentioned above upon fragmentation of the DC9-lipid ion pairs (Figure S2 of the Supporting Information). The loss of 85 corresponds to the DC9 nitrogen ring cleaved at the α position Figure 1. From these results, DC9 creates a stable ion-pair compound with lipids which cannot be easily fragmented. The collision energy used to obtain the fragmentation data was set to 12 (arbitrary units), from this we can infer that DC9 becomes easier to fragment rather than dissociate from the lipid adduct but also that it can have the effect of reducing or preventing in source fragmentation. This stabilizing effect could be a factor in the overall increase of signal. This opens the possibility that DC9 could be used for other techniques to increase signal intensity and stabilize lipids. For example, the MALDI technique has been used to map rat brain lipids,[55−58] and DC9 could potentially be incorporated in the matrix application step to stabilize certain labile lipids, such as gangliosides, a family of glycosphingolipids, prone to lose sialic acid group upon MALDI measurement.[59,60]

Selected ions in Figure 3 illustrate the imaging of lipids using reactive DESI-MS in the positive ion mode. In reactive DESI-MS, it is clear that some lipids are present only in the gray matter, such as PE (36:2) at m/z 980, whereas other lipids are only in the white matter of the brain, such as at PE (40:6) at m/z 1044; when the two ions are overlapped a clear image of the structural features in white matter and gray matter can easily be distinguished (Figure 3j). Negative ion mode images of arachidonic acid (20:4) at m/z 303 and phosphoethanolamine (PE 36:2) at m/z 726 were added to Figure 3 (panels k and l) for comparison. Other negative ions, namely oleic acid (18:1), palmitoleic acid (16:1), phosphoethanolamines, and phosphatidylserine (PS 40:6) of corresponding reactive DESI-MS

DOI: 10.1021/ac5042445
Anal. Chem. 2015, 87, 3286−3293

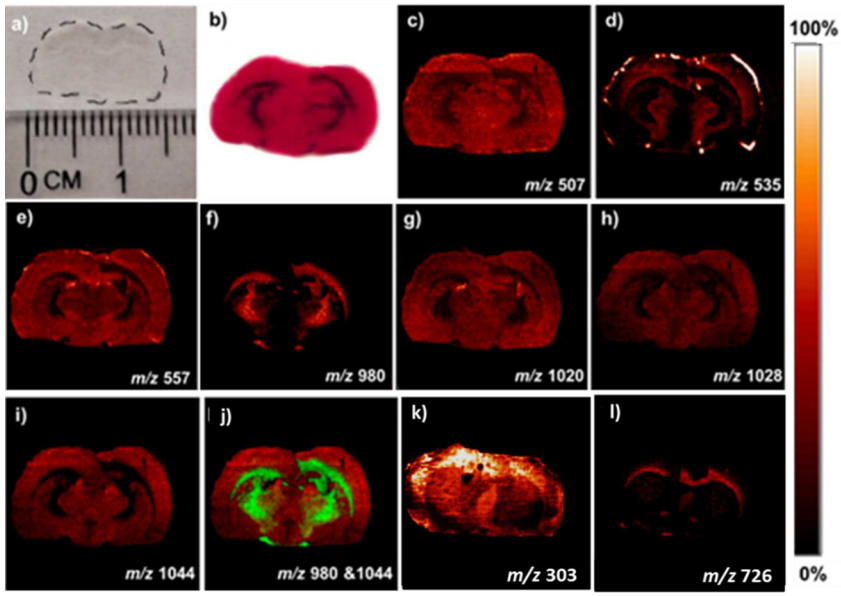

Figure 3. Panel of rat brain images analyzed by reactive DESI-MSI with compound DC9 in the positive ion mode. (a) Optical image of rat brain tissue slide with outline. (b) H&E stained rat brain tissue slide. (c–i) DESI-MS images of lipids with DC9 ion pairs in the positive ion mode. (c) *m/z* 507: DC9 and palmitoleic acid (16:1). (d) *m/z* 535: DC9 and oleic acid (18:1). (e) *m/z* 557: DC9 and arachidonic acid. (f) *m/z* 980: DC9 and PE (36:2). (g) *m/z* 1020: DC9 and PE (38:4). (h) *m/z* 1028: DC9 and PE (40:6). (i) *m/z* 1044: DC9 and PE (40:6). (j) Overlay image of *m/z* 980 and *m/z* 1044. (k and l) DESI-MS images of lipids in the negative ion mode. (k) Arachidonic acid (20:4) at *m/z* 303. (l) Phosphoethanolamine (PE 36:2) at *m/z* 726.

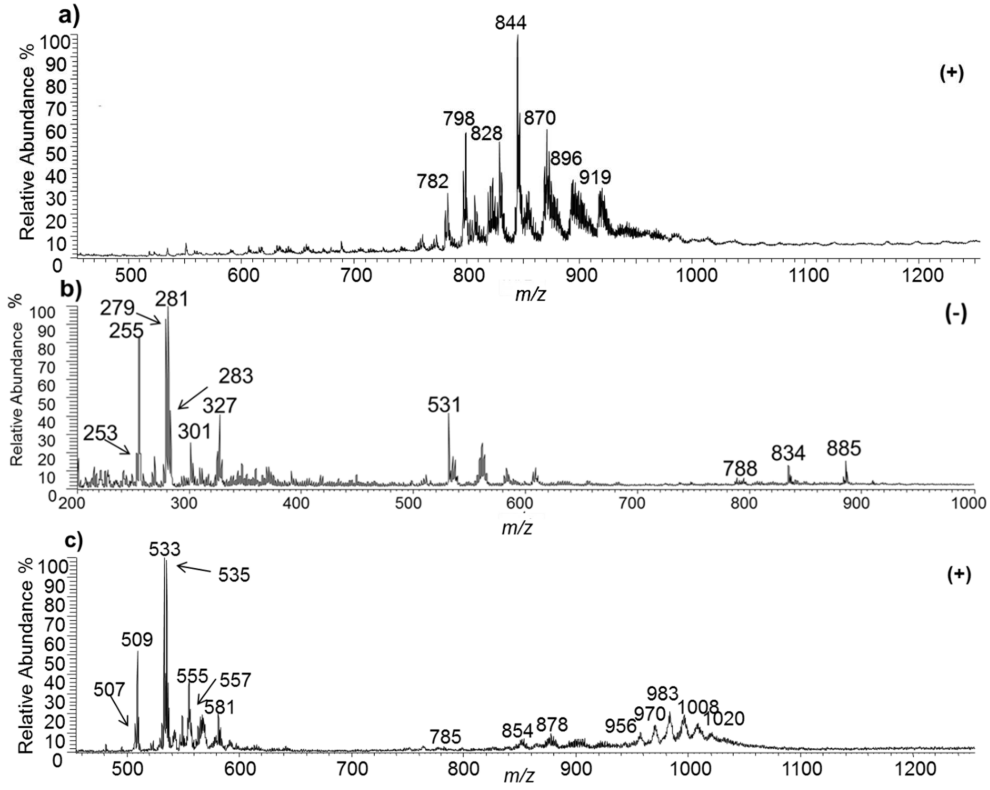

Figure 4. DESI-MS spectra of characteristic metabolites in whole body zebra fish tissue sections. (a) Phosphatidylcholines in zebra fish in DESI-MS positive ion mode control. (b) Control DESI-MS spectrum of zebra fish tissue in the negative ion mode. (c) Positive reactive DESI-MS spectrum of enhanced intensity between DC9-metabolite ion pairs in zebra fish compared to DESI-MS spectrum negative ion mode control.

selected ions, are in Figure S3 of the Supporting Information. With reactive DESI-MS, one can visualize the same distribution of the same compounds, such as phosphoethanolamine (PE 36:2) which has a strong intensity, while in the negative mode the signal intensity is low, resulting in a poor quality image. There seems to be a slight variation of the distribution of ion intensity when comparing DC9 to the negative mode; this can be observed when comparing phosphoethanolamine (PE 36:2)

DOI: 10.1021/ac5042445
Anal. Chem. 2015, 87, 3286–3293

in Figure 3 (panels f and l). The signal intensity difference could be attributed to the ionization efficiency difference, due to matrix effects from the tissue, leading to a different ionization pattern when comparing the negative ion mode ionization to the reactive DESI ionization. DC9 forms a stable complex and could have a stabilizing effect on certain compounds, thus leading to a more intense signal by reducing or eliminating in source fragmentation. It is difficult to definitively determine the process which gives rise to this variation, and further research on reactivity needs to be performed. Figure 3d exhibits a border effect, which was later identified to be a result of the mounting glue polymer used in the tissue sectioning.

Zebra Fish DESI-MS Analysis. Spectra of zebrafish whole body were acquired in the negative ion mode, in positive ion mode control, and reactive DESI-MS with DC9 positive ion mode for comparison. Figure 4 has an m/z shift of 254 for the positive mode in order to align the negative ions with the positive DC9 ions.

Similarly to the rat brain, the positive ion mode control of the zebra fish in the range of m/z 700−900 has a cluster of phosphatidylcholines, Figure 4a. These lipids were also confirmed via tandem mass spectrometry as described in the rat brain section (see Figure S1 of the Supporting Information).[47,48]

In the negative ion mode, the range between m/z 250−350 contains ions such as palmitic acid (16:0), linoleic acid (18:2), oleic acid (18:1), and others (Figure 4b and Table 2). 5α-Cyprinol 27-sulfate, a bile salt produced in the intestinal system, was detected at m/z 531.[61] Two phosphatidylserines (PS 36:1 and PS 40:6) identified at m/z 788 and 834, a phosphatidylinositol (PE 38:4) at m/z 885, and a sulfatide (ST 24:0) at m/z 890 were also observed.[61]

Table 2. Zebra Fish Metabolites and Dicationic Compound DC9 Ion Pairs in DESI-MS Spectrum in the Positive Ion Mode (DC9 MW 254.4 Da)

zebra fish metabolites in negative ion mode	observed m/z negative ion mode[61]	DC9-metabolite ion pair in positive ion mode	signal to noise change (DC9 vs negative ion mode)
myristic acid	227	481	64%
palmitic acid (16:0)	255	509	79%
linoleic acid (18:2)	279	533	101%
oleic acid (18:1)	281	535	88%
stearic acid (18:0)	283	537	115%
eicosapentaenoic acid (20:5)	301	555	354%
docosahexaenoic acid (22:6)	327	581	118%
5α-cyprinol 27-sulfate	531	785	7%
phosphatidylserine (PS 36:1)	788	1042	not detected
phosphatidylserine (PS 40:6)	834	1088	not detected
phosphatidylinositol (PI 38:4)	885	1139	not detected
sulfatide (ST 24:0)	890	1144	not detected

In reactive DESI, Figure 4c, all compounds detected in the negative ion mode in the range of m/z 250−350 were confirmed via tandem mass spectrometry. Compounds with a common loss of m/z 85 correspond to DC9 cleavage at the nitrogen ring. The bile salt 5α-cyprinol 27-sulfate was also observed in the reactive DESI-MS ion mode in the intestines region. Lipid compounds including phosphatidylserines (PS), phosphatidylinositols (PI), and phosphatidylglycerols (PG) have a low binding affinity to DC9 and were not detected in our reactive DESI-MS experiment. These results are in accordance with a previous study conducted with lipid standards where enhancement of these types of lipids in the reactive DESI-MS spectrum was not observed.[17]

Higher mass compounds in the reactive DESI-MS in the range of m/z 900 and above were not possible to identify via tandem mass spectrometry due to overlapping signals of multiple ions and/or low signal intensity. Fragmentation was possible when the isolation window was open to m/z 10. The fragmentation energy required was 7 (arbitrary units), and the fragments obtained are provided in Table S1 of the Supporting Information. The fragments obtained are very broad, indicating that a cluster of ions is being formed with DC9. This pattern of ions is only observed with DC9. Signal intensity was too low to perform MS^3 analysis, and although positive identification was not possible at the moment, some of these ions were mapped and images are provided in Figure S5 of the Supporting Information. From the analysis of the distribution of these ions, they seem to have the same distribution, indicating that they belong to the same class of compounds. The ions are present throughout the body with the exception of the organs. Further investigations will be performed using a high-resolution mass spectrometer.

As applied before, the signal-to-noise was used as an indicator of the DC9 effect on detection. Three average spectra were taken across the entire zebra fish samples and were compared between positive ion mode scans with DC9 and negative ion mode scans. These spectra were acquired from the eye to the tail of the zebra fish. Table 2 reports whether the signal-to-noise levels of each compound increased or decreased compared to their native detection in the negative ion mode. These values are provided in order to help the understanding of the signal change using DC9. As explained earlier, there is great variation, especially when trying to encompass an entire specimen's body where the various organs will have different composition and may either suppress or enhance the reaction of the DC9 to varying extents.

Selected zebra fish ion images in Figure 5 illustrate the mapping of lipids using reactive DESI-MS in the positive ion mode. Compound distribution can be observed throughout the entire body, such as oleic acid (18:1) (Figure 5e) or with a high abundance in certain organs, such as docosahexaenoic acid (22:6) (Figure 5f) in the eye or spleen, and 5α-cyprinol 27-sulfate found in the digestive system (Figure 5g). Structural features can easily be elucidated whenever using the reactive ion mode with DC9. An overlap between palmitic acid (16:0) concentrated in the fish liver and docosahexaenoic acid (22:6) concentrated in the eye and spleen is shown as an example of how reactive DESI-MS imaging can be used for biological structural differentiation. Negative ion mode images are included in the Figure 5 (panels i−l) for comparison of corresponding reactive DESI-MS selected ions. Additional negative ion mode images of phosphatidylserine (PS 40:6) at m/z 834 and phosphatidylinositol (PI 38:4) at m/z 885 are provided in Figure S4 of the Supporting Information. When comparing the same ions ionized in reactive DESI-MS over the control negative mode, different signal intensity between the two modes can be observed due to different tissue composition which react differently with the reactive DESI-MS. This may prove very advantageous since reactive DESI seems to provide

DOI: 10.1021/ac5042445
Anal. Chem. 2015, 87, 3286−3293

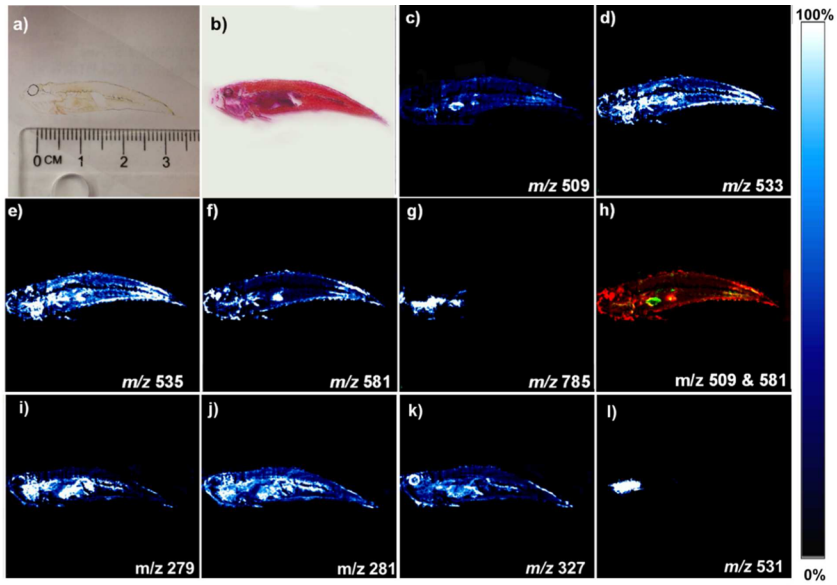

Figure 5. Panel of zebra fish images analyzed by reactive DESI-MSI with compound DC9 in (c–h) positive ion mode and (i–l) negative ion mode. (a) Optical image of zebra fish tissue on a microscopic glass slide. (b) H&E stained zebra fish tissue on a microscopic glass slide. (c–h) DESI-MS metabolite images with DC9 ion pairs in the positive ion mode. (c) m/z 509: DC9-palmitic acid (16:0). (d) m/z 533: DC9- linoleic acid (18:2). (e) m/z 535: DC9-oleic acid (18:1). (f) m/z 581: DC9- docosahexaenoic acid (22:6). (g) m/z 785: DC9-5α-cyprinol 27 sulfate. (h) overlay image of ion pairs m/z 509 and m/z 581, DESI-MS metabolite images in the negative ion mode (i–l). (i) Linoleic acid (18:2) at m/z 279. (j) Oleic acid at m/z 281. (k) Docosahexanoic acid (22:6) at m/z 327. (l) a-Cyprinol 27-sulfate at m/z 531.

different imaging than the negative mode, thus offering new information and not redundant information. This phenomenon is observed strongly in the whole zebra fish body images than in the rat brain images. Since the tissue slices are serial slices, this phenomenon is indicative that the DC9 coupling reaction could be suppressed to a varying degree in different organs. It is difficult to definitively attribute this effect to matrix suppression or facilitated reactivity from compounds in organs. This is a new compound, and its general reactivity is not fully understood yet. Future reactivity work will help to better understand this phenomenon. It can be helpful to distinguish different morphological features such as the case of palmitic acid (16:0) seen distributed in many organs, such as the gills, liver, intestinal system, in the negative mode (Figure S4c of the Supporting Information) and localized to the liver (Figure 5c).

CONCLUSION

Reactive DESI-MS with compound DC9 in the positive ion mode was successful in increasing the signal-to-noise ratio of certain low mass lipids in the range of m/z 250–350 and of phosphoethanolamines (PE) m/z 700–800 in rat brain and zebra fish biological tissues. These DC9-lipid ion pairs have shown an increase in intensity in comparison to the conventional DESI-MS analysis of lipids in the negative ion mode. This method allows the mapping of ions present in the positive ion mode and ions present in the negative ion mode in one single spectrum, decreasing imaging time and the amount of sample required to run an analysis; this can be useful when there is limited sample, for example biopsy samples. Positive ion mode images using reactive DESI are different than in the negative ion mode for the same compound using standard DESI; this opens the possibility of providing new information about the sample rather than redundant information when looking at a complex sample. Reactive DESI-MS using dicationic compounds can generate targeted ionization techniques opening new avenues into cancer research, drug development, and metabolism studies.

ASSOCIATED CONTENT

Supporting Information

Tandem MS/MS spectra of selected phosphatidylcholines, selected DC9-lipid ion pairs, panel of control rat brain and control zebra fish images analyzed by DESI-MS in the negative mode, panel of zebra fish images analyzed by reactive DESI-MS with compound DC9 in the positive ion mode, and zebra fish MS/MS using dicationic compound DC9 on unidentified broad peaks. This material is available free of charge via the Internet at http://pubs.acs.org.

AUTHOR INFORMATION

Corresponding Author

*E-mail: ifadr@yorku.ca. Tel: +1 416 736-2100, ext. 33555.

Notes

The authors declare no competing financial interest.

ACKNOWLEDGMENTS

We thank the Natural Sciences and Engineering Research Council of Canada (NSERC) for financial assistance.

REFERENCES

(1) Ifa, D. R.; Wiseman, J. M.; Song, Q.; Cooks, R. G. *Int. J. Mass Spectrom.* **2007**, *259*, 8–15.
(2) McDonnell, L. A.; Heeren, R. M. *Mass Spectrom Rev.* **2007**, *26*, 606–643.
(3) Harris, G. A.; Galhena, A. S.; Fernandez, F. M. *Anal. Chem.* **2011**, *83*, 4508–4538.
(4) Morelato, M.; Beavis, A.; Kirkbride, P.; Roux, C. *Forens. Sci. Int.* **2013**, *226*, 10–21.
(5) Eberlin, L. S.; Haddad, R.; Sarabia Neto, R. C.; Cosso, R. G.; Maia, D. R. J.; Maldaner, A. O.; Zacca, J. J.; Sanvido, G. B.; Romao, W.;

DOI: 10.1021/ac5042445
Anal. Chem. 2015, 87, 3286–3293

Vaz, B. G.; Ifa, D. R.; Dill, A.; Cooks, R. G.; Eberlin, M. N. *Analyst* **2010**, *135*, 2533−2539.
(6) Justes, D. R.; Talaty, N.; Cotte-Rodriguez, I.; Cooks, R. G. *Chem. Commun.* **2007**, 2142−2144.
(7) Nefliu, M.; Venter, A.; Cooks, R. G. *Chem. Commun. (Cambridge, U.K.)* **2006**, 888−890.
(8) Hu, Q.; Talaty, N.; Noll, R. J.; Cooks, R. G. *Rapid Commun. Mass Spectrom.* **2006**, *20*, 3403−3408.
(9) Haddad, R.; Sparrapan, R.; Eberlin, M. N. *Rapid Commun. Mass Spectrom.* **2006**, *20*, 2901−2905.
(10) Rao, W.; Scurr, D. J.; Burston, J.; Alexander, M. R.; Barrett, D. A. *Analyst* **2012**, *137*, 3946−3953.
(11) Costa, A. B.; Cooks, R. G. *Chem. Phys. Lett.* **2008**, *464*, 1−8.
(12) Cotte-Rodríguez, I.; Takáts, Z.; Talaty, N.; Chen, H.; Cooks, R. G. *Anal. Chem.* **2005**, *77*, 6755−6764.
(13) Chen, H.; Cotte-Rodriguez, I.; Cooks, R. G. *Chem. Commun.* **2006**, 597−599.
(14) Ellis, S. R.; Wu, C.; Deeley, J. M.; Zhu, X.; Truscott, R. J.; in het Panhuis, M.; Cooks, R. G.; Mitchell, T. W.; Blanksby, S. J. *J. Am. Soc. Mass Spectrom.* **2010**, *21*, 2095−2104.
(15) Muller, T.; Oradu, S.; Ifa, D. R.; Cooks, R. G.; Krautler, B. *Anal. Chem.* **2011**, *83*, 5754−5761.
(16) Nyadong, L.; Green, M. D.; De Jesus, V. R.; Newton, P. N.; Fernandez, F. M. *Anal. Chem.* **2007**, *79*, 2150−2157.
(17) Rao, W.; Mitchell, D.; Licence, P.; Barrett, D. A. *Rapid Commun. Mass Spectrom.* **2014**, *28*, 616−624.
(18) Joshi, M. D.; Anderson, J. L. *RSC Adv.* **2012**, *2*, 5470.
(19) Lin, X.; Gerardi, A. R.; Breitbach, Z. S.; Armstrong, D. W.; Colyer, C. L. *Electrophoresis* **2009**, *30*, 3918−3925.
(20) Xu, C.; Armstrong, D. W. *Anal. Chim. Acta* **2013**, *792*, 1−9.
(21) Breitbach, Z. S.; Wanigasekara, E.; Dodbiba, E.; Schug, K. A.; Armstrong, D. W. *Anal. Chem.* **2010**, *82*, 9066−9073.
(22) Kawahara, A.; Nishi, T.; Hisano, Y.; Fukui, H.; Yamaguchi, A.; Mochizuki, N. *Science* **2009**, *323*, 524−527.
(23) Norton, W.; Bally-Cuif, L. *BMC Neurosci.* **2010**, *11*, 90.
(24) Lele, Z.; Krone, P. H. *Biotechnology Advances* **1996**, *14*, 57−72.
(25) Nagel, R. *Altex-Altern Tierexp* **2002**, *19*, 38−48.
(26) Hill, A. J.; Teraoka, H.; Heideman, W.; Peterson, R. E. *Toxicological Sciences: An Official Journal of the Society of Toxicology* **2005**, *86*, 6−19.
(27) Dai, Y. J.; Jia, Y. F.; Chen, N.; Bian, W. P.; Li, Q. K.; Ma, Y. B.; Chen, Y. L.; Pei, D. S. *Environmental Toxicology and Chemistry (SETAC)* **2014**, *33*, 11−17.
(28) Feitsma, H.; Cuppen, E. *Mol. Cancer Res.* **2008**, *6*, 685−694.
(29) Konantz, M.; Balci, T. B.; Hartwig, U. F.; Dellaire, G.; Andre, M. C.; Berman, J. N.; Lengerke, C. *Ann. N.Y. Acad. Sci.* **2012**, *1266*, 124−137.
(30) Bassett, D. I.; Currie, P. D. *Hum. Mol. Genet.* **2003**, *12* (Spec No 2), R265−R270.
(31) Li, Y. J.; Hu, B. *J. Genet. Genomics* **2012**, *39*, 521−534.
(32) Sullivan, C.; Kim, C. H. *Fish Shellfish Immunol.* **2008**, *25*, 341−350.
(33) Porsolt, R. D.; Anton, G.; Blavet, N.; Jalfre, M. *Eur. J. Pharmacol.* **1978**, *47*, 379−391.
(34) Sakurai, T.; Amemiya, A.; Ishii, M.; Matsuzaki, I.; Chemelli, R. M.; Tanaka, H.; Williams, S. C.; Richarson, J. A.; Kozlowski, G. P.; Wilson, S.; Arch, J. R.; Buckingham, R. E.; Haynes, A. C.; Carr, S. A.; Annan, R. S.; McNulty, D. E.; Liu, W. S.; Terrett, J. A.; Elshourbagy, N. A.; Bergsma, D. J.; Yanagisawa, M. *Cell* **1998**, *92*, 697.
(35) Zoriy, M. V.; Dehnhardt, M.; Matusch, A.; Becker, J. S. *Spectrochim. Acta, Part B* **2008**, *63*, 375−382.
(36) Reyzer, M. L.; Hsieh, Y.; Ng, K.; Korfmacher, W. A.; Caprioli, R. M. *J. Mass Spectrom.* **2003**, *38*, 1081−1092.
(37) Chen, Y.; Allegood, J.; Liu, Y.; Wang, E.; Cachón-González, B.; Cox, T. M.; Merrill, A. H.; Sullards, M. C. *Anal. Chem.* **2008**, *80*, 2780−2788.
(38) Pierson, J.; Norris, J. L.; Aerni, H.-R.; Svenningsson, P.; Caprioli, R. M.; Andrén, P. E. *J. Proteome Res.* **2004**, *3*, 289−295.
(39) Seeley, E. H.; Caprioli, R. M. *Proc. Natl. Acad. Sci. U.S.A.* **2008**, *105*, 18126−18131.
(40) Reynolds, G. P.; Pearson, S. J.; Halket, J.; Sandier, M. *J. Neurochem.* **1988**, *50*, 1959−1968.
(41) Hanger, D. P.; Anderton, B. H.; Noble, W. *Trends Mol. Med.* **2009**, *15*, 112−119.
(42) Eberlin, L. S.; Norton, I.; Dill, A. L.; Golby, A. J.; Ligon, K. L.; Santagata, S.; Cooks, R. G.; Agar, N. Y. *Cancer Res.* **2012**, *72*, 645−654.
(43) Eberlin, L. S.; Gabay, M.; Fan, A. C.; Gouw, A. M.; Tibshirani, R. J.; Felsher, D. W.; Zare, R. N. *Proc. Natl. Acad. Sci. U.S.A.* **2014**, *111*, 10450−10455.
(44) Wu, C.; Ifa, D. R.; Manicke, N. E.; Cooks, R. G. *Anal. Chem.* **2009**, *81*, 7618−7624.
(45) Anderson, J. L.; Ding, R.; Ellern, A.; Armstrong, D. W. *J. Am. Chem. Soc.* **2005**, *127*, 593−604.
(46) Tadesse, H.; Blake, A. J.; Champness, N. R.; Warren, J. E.; Rizkallah, P. J.; Licence, P. *CrystEngComm* **2012**, *14*, 4886−4893.
(47) Koizumi, S.; Yamamoto, S.; Hayasaka, T.; Konishi, Y.; Yamaguchi-Okada, M.; Goto-Inoue, N.; Sugiura, Y.; Setou, M.; Namba, H. *Neuroscience* **2010**, *168*, 219−225.
(48) Lohmann, C.; Schachmann, E.; Dandekar, T.; Villmann, C.; Becker, C. M. *J. Neurochem.* **2010**, *114*, 1119−1134.
(49) Yang, H. J.; Sugiura, Y.; Ikegami, K.; Konishi, Y.; Setou, M. *J. Biol. Chem.* **2012**, *287*, 5290−5300.
(50) Dill, A. L.; Ifa, D. R.; Manicke, N. E.; Ouyang, Z.; Cooks, R. G. *J. Chromatogr. B: Anal. Technol. Biomed. Life Sci.* **2009**, *877*, 2883−2889.
(51) Girod, M.; Shi, Y.; Cheng, J. X.; Cooks, R. G. *J. Am. Soc. Mass Spectrom.* **2010**, *21*, 1177−1189.
(52) Wiseman, J. M.; Ifa, D. R.; Song, Q.; Cooks, R. G. *Angew. Chem., Int. Ed.* **2006**, *45*, 7188−7192.
(53) Manicke, N. E.; Wiseman, J. M.; Ifa, D. R.; Cooks, R. G. *J. Am. Soc. Mass Spectrom.* **2008**, *19*, 531−543.
(54) Melo, T.; Videira, R. A.; Andre, S.; Maciel, E.; Francisco, C. S.; Oliveira-Campos, A. M.; Rodrigues, L. M.; Domingues, M. R.; Peixoto, F.; Manuel Oliveira, M. *J. Neurochem.* **2012**, *120*, 998−1013.
(55) Hankin, J. A.; Farias, S. E.; Barkley, R. M.; Heidenreich, K.; Frey, L. C.; Hamazaki, K.; Kim, H. Y.; Murphy, R. C. *J. Am. Soc. Mass Spectrom.* **2011**, *22*, 1014−1021.
(56) Hankin, J. A.; Murphy, R. C. *Anal. Chem.* **2010**, *82*, 8476−8484.
(57) Jackson, S. N.; Ugarov, M.; Egan, T.; Post, J. D.; Langlais, D.; Albert Schultz, J.; Woods, A. S. *J. Mass Spectrom.* **2007**, *42*, 1093−1098.
(58) Wang, H. Y.; Jackson, S. N.; Post, J.; Woods, A. S. *Int. J. Mass Spectrom.* **2008**, *278*, 143−149.
(59) Harvey, D. J. *J. Chromatogr. A* **1996**, *720*, 429−446.
(60) Sekiya, S.; Wada, Y.; Tanaka, K. *Anal. Chem.* **2005**, *77*, 4962−4968.
(61) Chramow, A.; Hamid, T. S.; Eberlin, L. S.; Girod, M.; Ifa, D. R. *Rapid Commun. Mass Spectrom.* **2014**, *28*, 2084−2088.

DOI: 10.1021/ac5042445
Anal. Chem. 2015, 87, 3286−3293

International Journal of Mass Spectrometry 377 (2015) 736–743

Contents lists available at ScienceDirect

International Journal of Mass Spectrometry

journal homepage: www.elsevier.com/locate/ijms

Comparisons of ambient spray ionization imaging methods

Tanam S. Hamid, Dragos Lostun, Elaine C. Cabral, Rafael Garrett, Diethard K. Bohme, Demian R. Ifa *

Centre for Research in Mass Spectrometry, York University, Toronto, Ontario M3J 1P3, Canada

ARTICLE INFO

Article history:
Received 7 April 2014
Received in revised form 10 July 2014
Accepted 17 July 2014
Available online 8 August 2014

Keywords:
Ambient ionization
Imaging
Mass spectrometry

ABSTRACT

Ambient ionization methods allow for the examination of surfaces in their native conditions at atmospheric pressure with minimal or no preparation. Spray-based ambient ionization methods such as desorption electrospray ionization (DESI) and easy ambient sonic-spray ionization (EASI) have been successfully applied to imaging mass spectrometry. In 2012, a comparative study between DESI and EASI on spatial resolution and sensitivity was published by Janfelt and Nørgaard (J. Am. Soc. Mass Spectrom., 23 (2012) 1670–1678). We expand on that work by comparing DESI and EASI techniques for the assessment of the limit of detection (LOD) of several drugs on a PTFE surface and for the determination of the spray spot size varying flow rate and solvent composition for imaging purposes. MS/MS imaging was also done with both methods for performance comparison. The results showed that good ion images can be obtained by both techniques in the MS or MS/MS mode. No significant difference was observed in the spray spot size produced by DESI and EASI. DESI was found to have similar or higher sensitivity than EASI depending on the analyte interrogated.

1. Introduction

Imaging mass spectrometry (IMS) has established itself as an efficient tool that measures the analytes of interest and their spatial distribution by monitoring their mass to charge ratio (m/z) and spatial position [1]. IMS has been accepted worldwide as an effective system to detect and identify a broad range of molecules, due to high sensitivity, high speed of analysis and high chemical specificity [2,3]. Most mass spectrometry techniques require the introduction of the sample into vacuum; ambient ionization-based IMS methods are drawing popularity due to external ionization of the sample, at atmospheric pressure, outside of the vacuum system [4]. Ambient ionization methods allow introduction of ions, but not the entire sample, into mass spectrometer; in addition, ambient ionization methods require minimal or no sample pretreatment, facilitating rapid analysis of samples [5]. Among several developed ambient ionization methods, spray based techniques such as desorption electrospray ionization (DESI) and easy ambient sonic-spray ionization (EASI) have a wide range of applications. DESI has been successfully implemented in the field of forensics [6–8], imaging [9], metabolomics [10], pharmaceuticals [10], and polymers [11].

DESI adopts a soft ambient ionization technique leading to minimal fragmentation. Gas phase ions are produced from the condensed phase analytes by charged microdroplets. These gas phase ions are generated via a 'droplet pick up' mechanism where initial micron sized droplets wet the surface to be analyzed. Further collisions at the surface produce progeny droplets containing the analytes. Finally, gaseous ions are produced from charged progeny droplets which then undergo desolvation and proceed to the MS inlet [12]. Lateral spatial resolution, which is the capability to clearly distinguish between two adjacent spots on the surface, is typically 200 μm. However, the spatial resolution can be reduced to ~40 μm under specific conditions [13,14]. Typical limits of detection (LOD) have been reported in the range of picograms (pg) to femtograms (fg) making DESI-MS a sensitive method, useful for trace amount detection [15,16].

In 2006, Eberlin and co-workers introduced desorption sonic spray ionization (DeSSI) [17], later renamed in 2008 as EASI (easy ambient sonic spray ionization) [18]. EASI adopts a soft ionization method based on sonic spray that does not require high voltage or heating to produce gaseous ions at atmospheric pressure [19]. The mechanism of ionization involves production of gaseous ions due to unbalanced charge distribution in the resulting solvent daughter droplets induced from higher gas flow rates (>3.0 L/min). At sonic spray gas flow, droplets with less than 100 nm undergo fission and the resulting daughter droplets are charged [19]. These high gas flow rates are generated from the nebulizing gas pressure,

* Corresponding author. Tel.: +1 416 7362100x33555.
E-mail address: ifadr@yorku.ca (D.R. Ifa).

http://dx.doi.org/10.1016/j.ijms.2014.07.035
1387-3806/

generally 2–5 times higher in EASI (around 435 psi or 30 bar nebulizing gas backpressure) than in DESI standard conditions (around 120 psi or 8.2 bar) [17]. The intensity of the ions produced in a 'supersonic spray' strongly depends on gas velocity [19]. EASI has been successfully applied to quality control and forensics [7,17,20,21]. It also has been also applied to check for the purity of biodiesel [22,23].

For IMS purposes one has to take into account not only the ability to ionize a sample, but also the impact of the technique on the sample interrogated. EASI at standard conditions is not fully compatible with IMS because it requires high gas flow rates (>3.0 L/min) and high solvent flow rates (>20 μL/min) in order to promote the ionization. These conditions cannot be applied to all kinds of samples, especially biological tissues, because they damage the sample before it can be entirely mapped. Experiments can be done under specific conditions using low gas flow rates (<3.0 L/min) and low flow rates of volatile solvents (<10 μL/min). However, these conditions eliminate the "sonic spray" effect responsible for the high ionization efficiency. Indeed, ionization under these conditions was investigated in 2005 by the Cooks group [24].

In 2012, Janfelt and Nørgaard published a comparative study between DESI and EASI by producing ion images of tissue sections [25]. In this study, a pixel to pixel comparison was performed as it can distinguish between signal and noise. It was concluded that EASI can be as efficient as DESI for imaging and direct analysis of tissue sections as long as a higher solvent flow rate (10 μL/min) is maintained. Improved EASI signals were observed as long as the pressure was kept at 10 bar which is approximately 145 psi. It was found that DESI is more sensitive than EASI toward analytes that are present at low abundance for both rat brain and plant imprints deriving the fact that there must be a difference in dynamic range for both DESI and EASI.

With these previous reports in mind, the experiments reported here were not performed under the standard conditions for either DESI [24] or EASI [17,21], but rather a single set of conditions which allow a comparison of the results (Table 1). Note that the classification of the techniques (DESI and EASI) based on the gas pressure component is not well established. For instance, EASI was reported using as low as 100 psi for nebulizing gas backpressure [20] and DESI was reported using as high as 170 psi gas backpressure [26]. We chose to compare both techniques at 145 psi or ~10 bar, a pressure that can achieve effective ionization in EASI, but still allows imaging experiments without damaging the sample as reported by Janfelt and Nørgaard [25]. However, we found that an even lower flow rate (5 μL/min) could be used to avoid smearing effects. Both techniques were further compared here in terms of the sensitivity (limits of detection), spray spot size and lateral spatial resolution in order to gauge the capabilities in terms of imaging performance. Spray spot size is one of the main components for creating an image with good resolution. Spot analysis was done by measuring spot size on a water sensitive paper under various conditions. Limits of detection, on a porous PTFE surface, of various compounds were recorded to investigate the ionization and transfer efficiency with both methods. MS/MS imaging experiments were performed in order to illustrate IMS applications for forensic analysis. Finally, the coronal sections of rat brain were analyzed to create ion images allowing us to compare both the ionization profiles and the image quality. All these results obtained from new experiments taken together help us further understand the capabilities of DESI and EASI and to assess the viability of these techniques for IMS.

2. Experimental

2.1. Materials and reagents

The solvents (HPLC grade) and the compounds used in the limit of detection experiments: propranolol, testosterone, dobutamine, verapamil, chloramphenicol, ibuprofen, diazepam, roxithromycin, and angiotensin, were obtained from Sigma–Aldrich Canada. Porous PTFE sheets 1.5 mm thick with a medium porous size of 7 μm were purchased from Berghof (Eningen, Germany). Microscope slides 26 mm × 77 mm thickness 1 mm were purchased from Bionuclear diagnostics Inc. (Toronto, ON, Canada). Rat brains were purchased from (Rockland Immunochemicals Inc., Gilbertsville, PA, USA) and the water sensitive paper, paper that changes its color when exposed to water, was obtained from TeeJet Technologies (Harrisburg, Dillsburg, PA). Red pens containing Rhodamine B and Rhodamine 6G, BIC Company, used in MS/MS experiments were purchased from a bookstore at York University.

2.2. Sample preparation

2.2.1. Water sensitive paper

Water sensitive paper was cut to working size and was secured on the moving stage with tape on all sides.

2.2.2. Rat brain

Frozen rat brains were sectioned into 15 μm thick coronal section (12 mm × 15 mm) using a Shandon Cryotome FE (Thermo Fischer Scientific, Nepean, ON, Canada). These tissue sections were thaw mounted onto glass slides, stored at −40 °C and brought to room temperature before analysis.

2.2.3. Limit of detection

Standards of 1 mg/mL were prepared in methanol solvent. The spotting solutions were created from the 1 mg/mL standards using serial dilution to 100, 10, 1, 0.1, and 0.01 ng/μL prepared in a 1:1 ratio of methanol to water solution. The solvent used to spray was also prepared with methanol to water ratio of 1 to 1.

2.2.4. MS/MS imaging

Two different red pens were used attempt forgery on a piece of paper. The paper was secured to the running stage with tape and MS imaging was performed.

Table 1
Standard DESI and EASI conditions versus experimental conditions.

	Standard conditions		Experimental conditions chosen	
	DESI [24]	EASI [17,18]	DESI	EASI
Nebulzing gas back pressure (psi)	50–120	400	140	140
Solvent flow rate (μL/min)	0.5–5	20–25	1.5/5.0[a]	1.5/5.0[a]
Spray voltage (kV)	2–5	0	5	0

[a] Solvent flow rates used in the limits of detection/rat brain experiments.

3. Instrumentation

All experiments were carried out using an LTQ linear ion trap mass spectrometer (Thermo Fisher Scientific, San Jose, CA, USA) with a lab-built DESI ion source.

3.1. Methods

3.1.1. Water sensitive paper

Experiments were performed with solvent flow rates from 0.5 μL/min to 4.0 μL/min. Methanol to water ratios of 1:1 and 9:1 were used. Nitrogen (N_2) gas was varied within 80–140 psi while keeping the flow rate at 2.0 μL/min 1:1, methanol:water, solvent ratio. The geometry conditions were set as: spray angle 52°, capillary to inlet distance ~3 mm and capillary to surface ~2 mm. DESI conditions used 5 kV, while EASI used 0 kV, all other parameters were kept the same. In order to ensure the absence of residual charge in the syringe when turning off the voltage and switching from DESI to EASI, a ground wire was connected to the syringe metal tip during EASI experiments. The moving stage was programmed to make five distinct spots; the distance between each spot was 1 mm and the spray was held on each spot for 1 s before moving to the next. This was followed by making a 10 mm long line while moving the spray continuously and slowly at a speed of 200 μm/s. Each line ended with a final spot sprayed for 10 s before moving on to the next line. After the experiment the resulting papers were scanned for visual inspection.

3.1.2. Limit of detection (LOD)

Shallow parallel indentation lines were drawn on the porous material. Volumes of 1 μL were pipetted on the line in increasing concentrations of 0.01, 0.1, 1.0, 10, and 100 ng/μL, respectively. The spots were left to dry for about 20 min and analysis was performed by scanning across the line with a speed of 200 μm/s. Distance optimized under EASI conditions with capillary angle at 52°, capillary to inlet distance set at ~3 mm and capillary to surface set at ~2 mm. A solvent flow rate of 1.5 μL/min of MeOH:H_2O mixture (1:1, v/v) and a nebulizing gas (N_2) pressure of 140 psi were used. The limits of detection were established by doing MS/MS on the parent ion and monitoring the main daughter ion.

3.1.3. MS/MS imaging

Two red pens containing Rhodamine B and Rhodamine 6G were used one a piece of paper, one pen to write a 3 and an F and the other to convert the 3 to an 8 and the F to a B. The paper was secured to the moving stage and ion images were obtained. The flow rate was set at 3 μL/min, spray tip to inlet distance 3 mm, and spray tip to surface distance 1 mm, solvent was a 1:1 MeOH:H_2O for both DESI and EASI. Voltage was set at 5 kV and pressure at 100 psi for DESI, while EASI was done at 140 psi and 0 kV. Spatial resolution was set at 150 μm, and the Automatic Gain Control was turned off. Experiment ran in MS/MS mode (daughter ion scan) was used to monitor 443 m/z fragments from 200 to 500 m/z, with collision energy of 19 eV.

3.1.4. Rat brain

EASI experiments were conducted in the negative ion mode using a solvent flow rate of 5.0 μL/min of pure methanol and a nebulizing gas (N_2) pressure of 140 psi (~2.3 L/min). The scan range for the experiment was 150–900 m/z, the ion injection time was 120 ms and 3 ms were averaged for each pixel in the image. The spray angle was set at 52°, the capillary to inlet distance was set at ~3 mm and the capillary to surface distance was set at ~2 mm. The experimental conditions for DESI were different by keeping the spray voltage at 5.0 kV. While scanning the rat brain, 50 lines of coronal section (half of the brain) were analyzed by EASI (0.0 kV) and the other 50 lines were analyzed by DESI (5.0 kV).

3.2. Imaging

Ion images were obtained using a lab-built software named ImgCreator that converted the mass spectra files into a format that is compatible with Biomap (freeware, www.msi.maldi.org).

4. Results and discussion

Several experiments were performed: (i) the water sensitive paper was used to test the spray impact area; (ii) MS/MS imaging was performed to investigate IMS applications for forensics; (iii) imaging of rat brain slices to compare ion images and profiles obtained with or without high voltage; and finally (iv) with limits of detection on porous PTFE were compared.

4.1. Water sensitive paper

The experiment with water sensitive paper was performed to compare the size of the spray impact spots produced by both DESI and EASI. In Fig. 1, the spot areas are produced on water sensitive paper with two different methanol and water solvent mixtures. DESI and EASI lines were alternately created. In Fig. 1A the spots were made with methanol and water at a ratio of 9:1 and 1:1, and the solvent flow rate was varied from 0.5 μL to 4.0 μL/min. In Fig. 1B the lines were generated from a 1:1 solvent mixture at a constant flow rate of 2.0 μL/min and the nebulizing gas (N_2) pressure was varied from 80 to 140 psi.

As the solvent flow rate increases, the size of spots also increases which is evident from Fig. 1. Analysis of the spot shape on panel (A) reveals that shape can be controlled by the solvent composition. Methanol evaporates faster than water; as a result this is why with higher concentration of water in the solvent mixture, solvent impact spots tend to smear. Solvent spots on panel (B) in Fig. 1, made with varying gas pressure, are comparatively similar and almost indistinguishable, indicating that pressure is not as significant as the solvent composition and the flow rate. The size and shape of the solvent spots obtained for both DESI and EASI under the various conditions look similar. An absence of high voltage results in a lower number of charged microdroplets, however, this does not significantly affect the size of the spot. Even without high voltage, high gas velocity leads to an unbalanced distribution of charges in the solvent droplets resulting in generation of gaseous ions. Therefore, imaging lateral spatial resolution stays the same in both DESI and EASI under these experimental conditions. The major factors contributing to the shape of the spots are the composition of solvents and flow rate, with a small contribution by the gas pressure. If the voltage does contribute to a different spray impact distribution, the effect of the gas seems to make the voltage effect negligible under these operating parameters. Based on these results a low solvent flow rate and medium gas pressure could be used for the imaging of the rat brain and the LOD experiments. However, stable signals could not be obtained by EASI using less than 5.0 μL/min and, in order to reach this flow rate without smearing the sample, pure methanol was used. The pressure was 140 psi which is the upper limit of what our setup can handle in order to allow an efficient ionization in EASI to ensure a balanced comparison.

4.2. Rat brain

Ion images of rat brain (Fig. 2) were obtained using both DESI and EASI on the same sample by mapping the spatial distribution of phospholipids which are PE(16:0/22:6) at m/z 746.6,

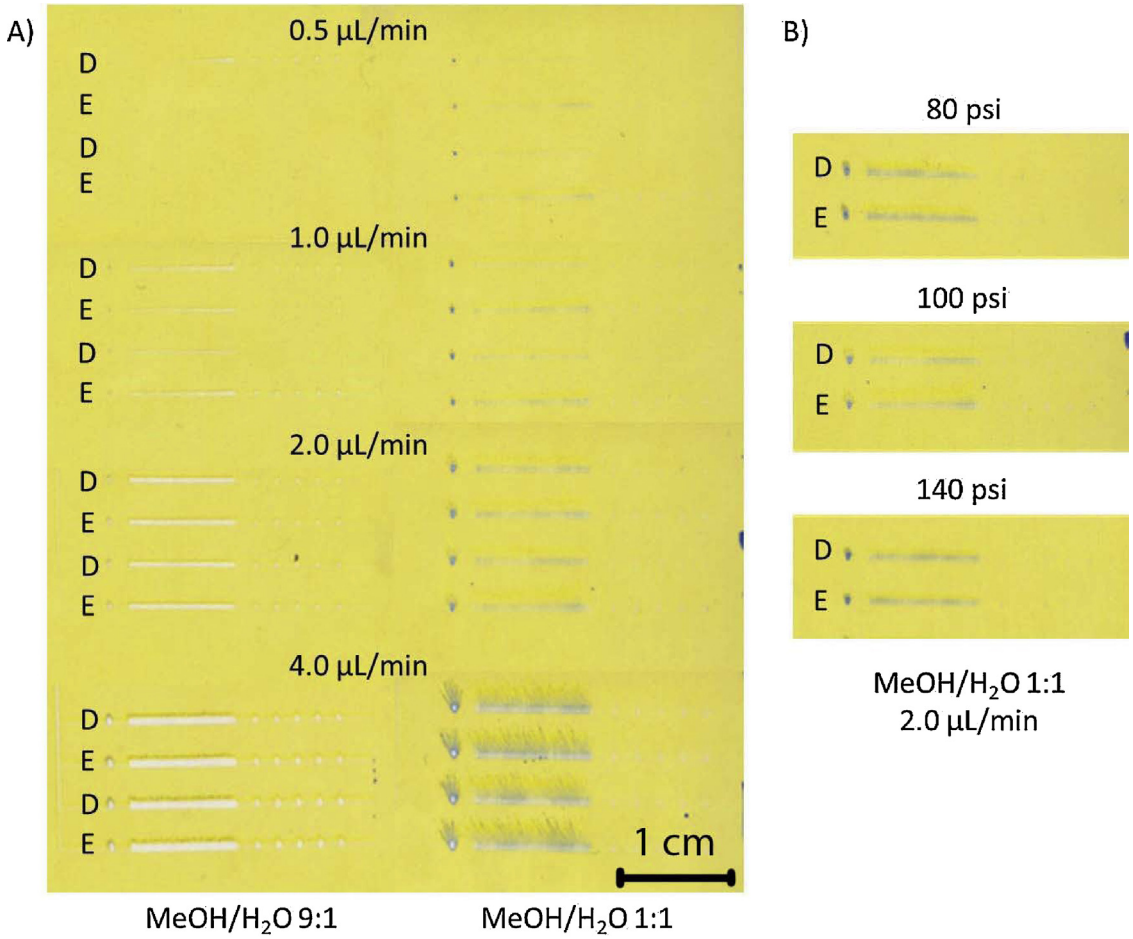

Fig. 1. Spots and lines produced by DESI (D) and EASI (E) obtained on water sensitive paper using methanol and water at 9:1 and 1:1 ratios. Panel (A) shows spots made with varying solvent flow rates of 0.5 µL/min, 1.0 µL/min, 2.0 µL/min, and 4.0 µL/min using both solvent mixtures proportions. Panel (B) shows spots made with varying nebulizing gas (N_2) pressures of 80 psi, 100 psi, and 140 psi using methanol and water (1:1) at 2.0 µL/min flow rate.

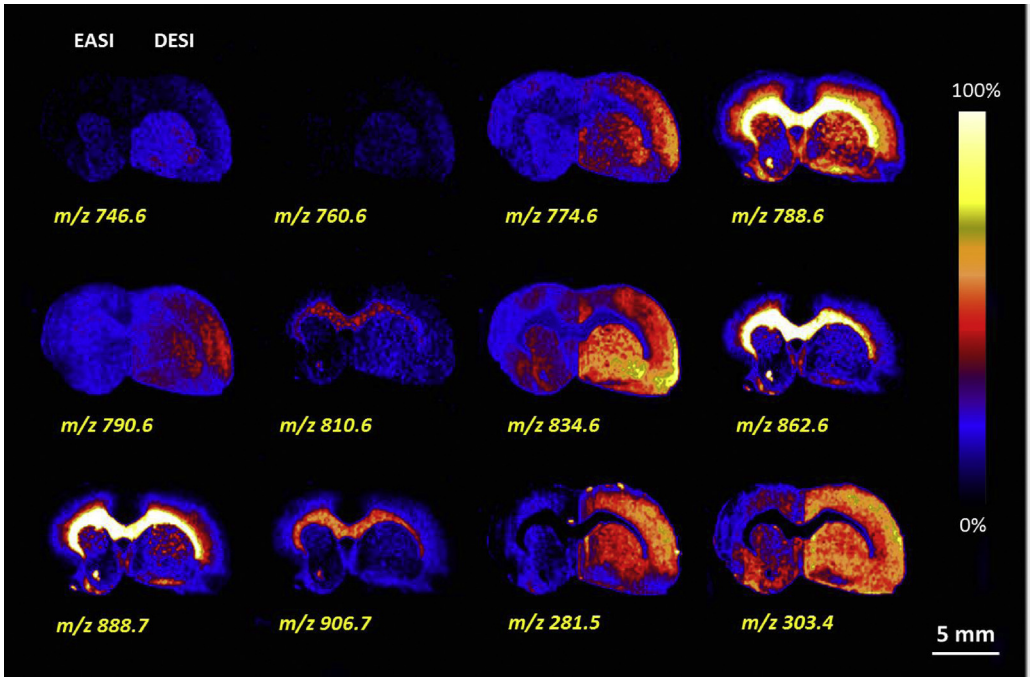

Fig. 2. Images of selected lipid ions from a 15 microns coronal section of rat brain tissue. Half the coronal section (50 lines) is scanned by DESI-MS and the other half is scanned by EASI-MS. Both scans are recorded in the full scan, negative ion mode.

PS(16:0/18:1) at *m/z* 760.6, plasmenyl-PE(18:0/22:6) at *m/z* 774.6, PS(18:0/18:1) at *m/z* 788.6, PE(18:0/22:6) at *m/z* 790.6, PS(18:0/22:6) at *m/z* 834.6, ST(22:0) at *m/z* 863.0, ST(24:1) at *m/z* 888.7, ST(h24:0) at *m/z* 906.7 and fatty acids which are oleic acid (18:1) at *m/z* 281.5 and arachidonic acid (20:4) at *m/z* 303.4 [27]. The mass spectra obtained for gray and white matter contain similar ions except for few of them (Fig. 3A and C).

The white matter (Fig. 3C) contains ions at *m/z* 862.7, *m/z* 888.7 which the gray matter (Fig. 3A) does not contain. This indicates that the white matter of the brain has various forms of sulfatides (ST) which the gray matter does not. The white matter and the gray matter also vary in terms of the relative intensities of ions. For instance, the gray matter contains peaks at *m/z* 281.5 and *m/z* 303.5 that have higher intensities compared to the intensities of the corresponding peaks in white matter. When the mass spectra derived by EASI and DESI-MS are compared, both of them appear to contain similar ions (Fig. 3A and C). Therefore, both DESI and EASI have similar chemical specificity, as both techniques can detect the same type of ions. Both techniques displayed stable signals for phospholipids as well as fatty acids. The only difference lies in the absolute intensity of the ions. The absolute intensity for the ions that are present at both high and low abundance seems to be higher for DESI than EASI. In gray matter (Fig. 3A), the absolute intensity of the peak at *m/z* 834.6 for in the DESI spectrum is higher than the absolute intensity of the corresponding peak for EASI spectrum. The higher voltage in DESI-MS is the key to generating a greater number of charged microdroplets containing analyte ions resulting in such higher spectral intensities. Similarly, in white matter (Fig. 3C), the absolute intensity of the peak at *m/z* 281.5 in the DESI spectrum is higher than the absolute intensity of the corresponding peak with EASI. These results also indicate that DESI is a more sensitive technique than EASI as it consistently produces stable signals with higher intensity. In terms of spatial resolution the two methods are indistinguishable under these conditions. This fact, taken together with the data from the water sensitive paper, seems to suggest that not only the spot size but the effective ionization area seem to be similar for both DESI and EASI experimental conditions.

4.3. Limits of detection on porous PTFE

Limits of detection were investigated on a porous PTFE surface by pipetting the analyte onto the surface in increasing concentrations. This allowed a controlled and reproducible method for determining the lowest concentration detectable under both DESI and EASI parameters. The porous PTFE surface is highly non-polar; this was both a benefit and a challenge. An advantage of using this surface is its ability to concentrate a polar sample onto a small area. A polar solvent, such as water, tends to slide off the surface and not adhere to the surface. Mixing water with methanol improves adherence. Spotting without using guide lines or marks on the surface have led to blank signals along the line. To avoid this issue a shallow line was drawn into surface, this served as both a guide line to ensure all droplets were aligned, but also to facilitate the transfer from the pipette tip to the surface by providing more contact surface between the droplet and the porous material.

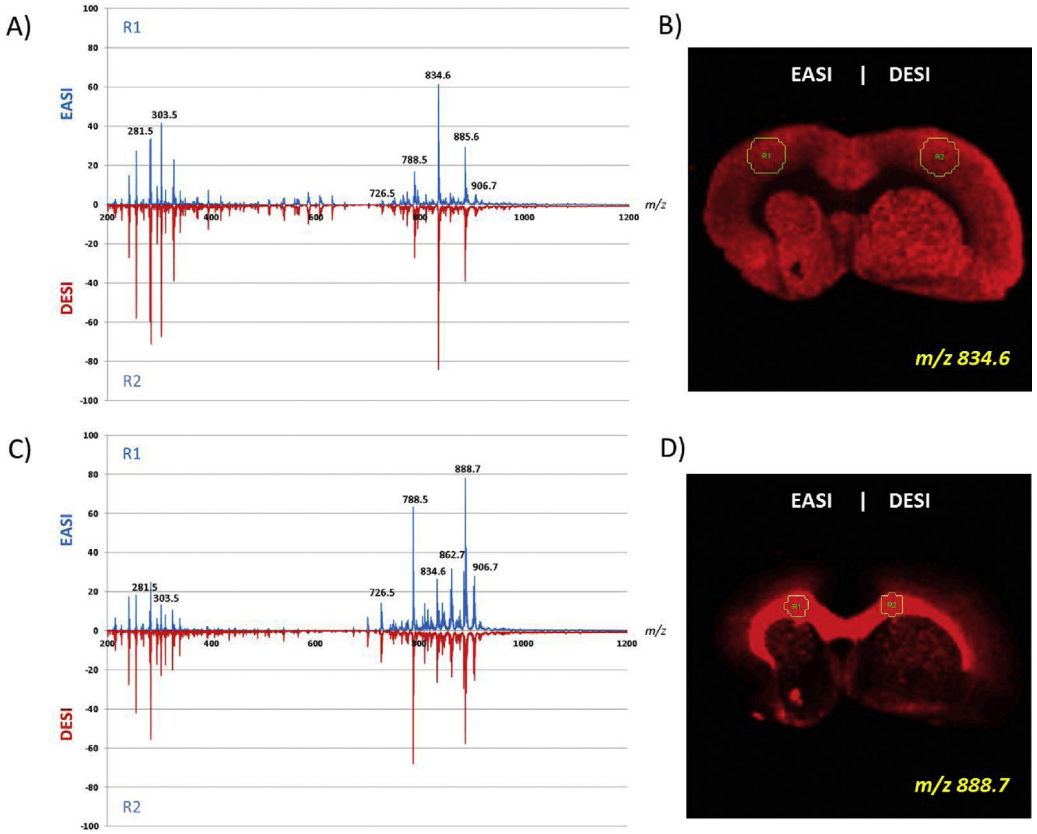

Fig. 3. The averaged mass spectra (A) obtained through EASI (top part) and DESI-MS (bottom part) demonstrate distribution of fatty acids and phospholipids at *m/z* 281.5, oleic acid (18:1); *m/z* 303.4, arachidonic acid (20:4); *m/z* 788.5, PS (18:0/18:1); *m/z* 834.6, ST (22:0); *m/z* 885.6, PI (38:4); and *m/z* 906.7, ST (h24:0) in gray matter of rat brain. The averaged mass spectra (C) demonstrate distribution of all the fatty acids and phospholipids mentioned above in white matter of rat brain. All four spectra are obtained in the negative ion mode. (B) Represents the DESI-MS and EASI-MS ion image showing the distribution of ST (22:0). (D) Represents the DESI-MS and EASI-MS ion image showing the distribution of PS (18:0/18:1).

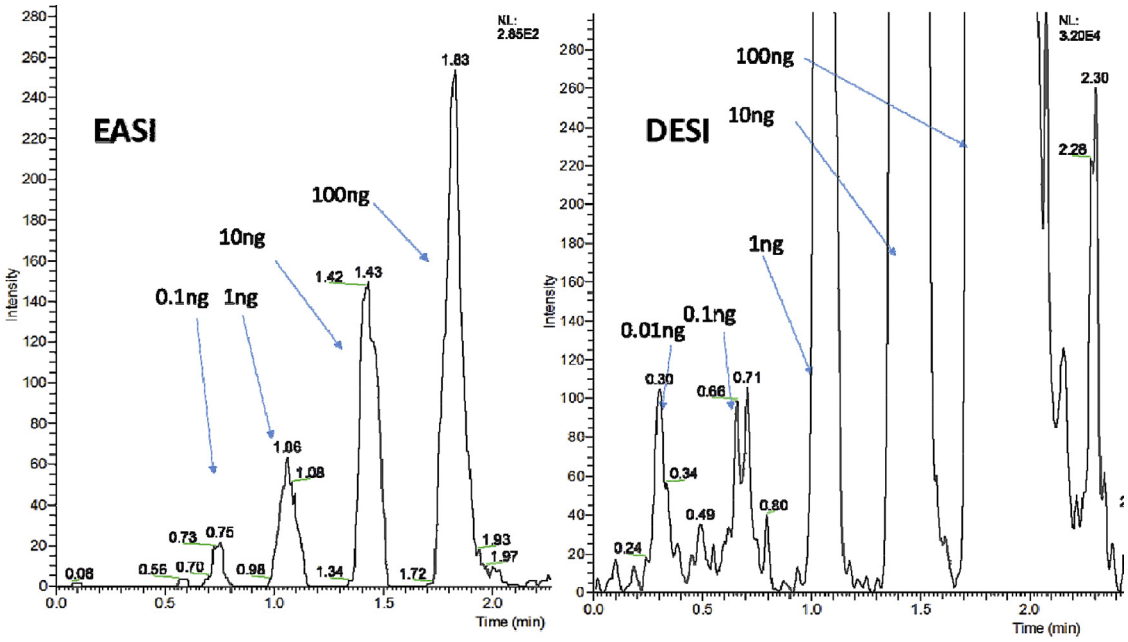

Fig. 4. Typical scan of a line with spots of concentrations from 0.01 to 100 ng/spot. The example above is a scan of verapamil drug taken with EASI conditions on the left and DESI conditions on the right on an absolute intensities scale versus time.

The parent ions of the compounds were selected and the daughter ions were monitored across a line in increasing concentrations using selected reaction monitoring SRM. The limits of detections were reported for consistent detections at the lowest concentration of at least three separate replicates.

The limits of detection for selected compounds reveal a trend. When voltage is applied, it can increase the limits by one order of magnitude. In Fig. 4, the total ion count is 3.20E4 for DESI and 2.85E2 for EASI. Except for dobutamine and ibuprofen, which had similar values for the lowest concentration detected (Table 2), all other compounds showed detection at a lower concentration when voltage was applied.

4.4. MS/MS imaging

The capabilities of DESI and EASI to perform MS/MS images were compared. This is important in order to distinguish isobaric species and for analysis of forged documents and other forensic applications. Fig. 5 shows an example of the use of red inks where "3 F" handmade characters were converted to "8 B" characters by using a different red ink. Both contain the red ink pigment rhodamine with a mass of 443 but one is rhodamine B and the other is rhodamine 6G. These two isobaric compounds fragment distinctively. Rhodamine B produces a fragment at m/z 399 from a neutral loss of CO_2 and Rhodamine 6G produces a fragment at m/z 415 from a neutral loss of ethylene.

Fig. 5 (e) and (f) illustrate how easy it is to distinguish between the two pens by mapping the fragments and the overlap of the fragments.

Both DESI and EASI work very well with our particular compound of interest. This is a charged compound so desorption part of the mechanism becomes important. For DESI the MS/MS image was taken at 100 psi with 5 kV voltage while EASI was taken at 140 psi with no voltage. The signal intensity is higher for EASI in this case showing that desorption at higher pressure would outweigh desorption with a charged solvent after a particular point. To note maximum pressure able to use on a surface greatly depends on the type of sample being used, too much and smearing

Table 2
Limits of detection of selected compounds using both methods on a porous PTFE surface.

Compound	Polarity	Collision energy	Precursor → product (m/z)	Lowest concentration detected (ng/μL)	
				DESI	EASI
Propranolol	+	27	260.2 $[M+H]^+ \rightarrow$ 183.2	0.1	1
Testosterone	+	20	289.3 $[M+H]^+ \rightarrow$ 253.2	10	100
Dobutamine	+	25	302.3 $[M+H]^+ \rightarrow$ 137.2	10	10
Verapamil	+	23	454.4 $[M+H]^+ \rightarrow$ 303.3	0.01	0.1
Chloramphenicol	−	27	321.0 $[M-H]^- \rightarrow$ 257.0	0.01	0.1
Ibuprofen	−	20	205.2 $[M-H]^- \rightarrow$ 161.2	1	1
Diazepam	+	30	285.3 $[M+H]^+ \rightarrow$ 257.1	0.1	1
Roxithromycin	+	20	837.7 $[M+H]^+ \rightarrow$ 679.2	0.01	0.1
Angiotensin	+	20	523.8 $[M+H]^{+2} \rightarrow$ 784.4	1	10

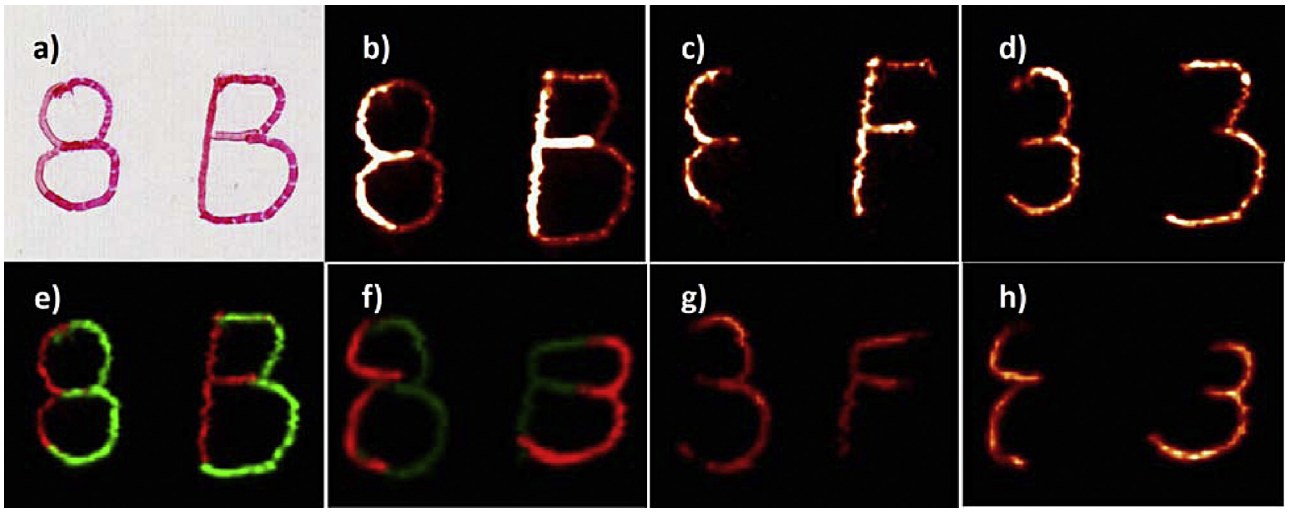

Fig. 5. (a) Optical image of an 8 and a B made by two different red ink pen formulations to demonstrate an attempt at forging a document, (b) DESI image of the m/z 443 ion of the red ink Rhodamine B and Rhodamine 6G, (c) DESI MS/MS image of the daughter ion m/z 399 of Rhodamine B m/z 443, (d) DESI MS/MS image of the daughter ion m/z 415 of Rhodamine 6G m/z 443, (e) DESI MS/MS image of the daughter ion m/z 399, in red, of Rhodamine B m/z 443 ion and an overlap of the daughter ion m/z 415, in green, of Rhodamine 6G m/z 443, (f) EASI image of the overlap between ion m/z 399 in green and ion m/z 415 in red, (g) EASI MS/MS image of the daughter ion m/z 399 of Rhodamine B m/z 443, and (h) EASI MS/MS image of the daughter ion m/z 415 of Rhodamine 6G m/z 443.

can occur creating smudged images, thus making imaging impossible.

5. Conclusion

New experiments were performed in order to further interrogate the viability of IMS by DESI and EASI. The water sensitive paper demonstrated no significant difference in spray spot size onto a sample when varying the voltage, which indicates that both techniques have similar solvent spray distribution. The spatial resolution of both techniques is similar, thus we can also conclude that EASI has a similar area of ionization as the DESI experiments. The voltage has virtually no impact on the solvent spray cone distribution, while it may result in different solvent particle sizes, it does not affect the overall area solvent spot or ionization area ionization. Both methods, under high flow rate conditions, showed signs of smearing the surface even with an increase in pressure; therefore, solvents with high volatile composition and low flow rates are desired for imaging purposes. The water sensitive paper experiments revealed that increasing pressure can reduce droplet spread, but not to a significant degree. In imaging experiments high flow rate is undesirable, because it tends to lead to smearing and a larger spray spot area, these results in low quality images with ambiguous ion distribution. EASI had comparable results with DESI even with a low flow rate which indicates it can be practical for IMS use.

In the limits of detection experiment when no voltage was applied the detection was in some cases the same or an order of magnitude worse than DESI. Similar was the scan of the lipids in the brain tissue which revealed a mirror image in terms of what compounds can be detected with both methods, with a slight drop in overall signal intensity when no voltage was applied. While the ion count is lower in EASI than DESI, both techniques result in similar spatial resolution, both can be used in MS/MS imaging, and both have the same sample specificity, hence both can be used to create ion images. Considering that except for the presence or absence of high-voltage, the analyses were performed under the same experimental conditions (gas pressure, solvent composition, and flow rate), more investigation is necessary to explain the difference in the signal intensity based on phisicochemical properties of the analytes and solvents (proton affinity, solubility, pK_a, etc.) and therefore to predict when EASI can be used for IMS without any detrimental effect in terms of sensitivity.

Acknowledgments

We thank the Brazilian National Council for Scientific and Technological Development (CNPq) and the Natural Science and Engineering Research Council of Canada (NSERC) for financial support.

References

[1] E.R. Amstalden van Hove, D.F. Smith, R.M.A. Heeren, A concise review of mass spectrometry imaging, J. Chromatogr. A 1217 (2010) 3946–3954.
[2] M. Koestler, D. Kirsch, A. Hester, A. Leisner, S. Guenther, B. Spengler, A high-resolution scanning microprobe matrix-assisted laser desorption/ionization ion source for imaging analysis on an ion trap/Fourier transform ion cyclotron resonance mass spectrometer, Rapid Commun. Mass Spectrom. 22 (2008) 3275–3285.
[3] S. Maharrey, R. Bastasz, R. Behrens, A. Highley, S. Hoffer, G. Kruppa, J. Whaley, High mass resolution SIMS, Appl. Surf. Sci. 231 (2004) 972–975.
[4] R.G. Cooks, Z. Ouyang, Z. Takats, J.M. Wiseman, Detection technologies. Ambient mass spectrometry, Science 311 (2006) 1566–1570.
[5] C. Wu, A.L. Dill, L.S. Eberlin, R.G. Cooks, D.R. Ifa, Mass spectrometry imaging under ambient conditions, Mass Spectrom. Rev. 32 (2013) 218–243.
[6] M. Morelato, A. Beavis, P. Kirkbride, C. Roux, Forensic applications of desorption electrospray ionisation mass spectrometry (DESI-MS), Forensic Sci. Int. 226 (2013) 10–21.
[7] L.S. Eberlin, R. Haddad, R.C. Sarabia Neto, R.G. Cosso, D.R.J. Maia, A.O. Maldaner, J.J. Zacca, G.B. Sanvido, W. Romao, B.G. Vaz, D.R. Ifa, A. Dill, R.G. Cooks, M.N. Eberlin, Instantaneous chemical profiles of banknotes by ambient mass spectrometry, Analyst 135 (2010) 2533–2539.
[8] D.R. Justes, N. Talaty, I. Cotte-Rodriguez, R.G. Cooks, Detection of explosives on skin using ambient ionization mass spectrometry, Chem. Commun. (2007) 2142–2144.
[9] D.R. Ifa, J.M. Wiseman, Q. Song, R.G. Cooks, Development of capabilities for imaging mass spectrometry under ambient conditions with desorption electrospray ionization (DESI), Int. J. Mass Spectrom. 259 (2007) 8–15.
[10] Q. Hu, N. Talaty, R.J. Noll, R.G. Cooks, Desorption electrospray ionization using an Orbitrap mass spectrometer: exact mass measurements on drugs and peptides, Rapid Commun. Mass Spectrom. 20 (2006) 3403–3408.
[11] M. Nefliu, A. Venter, R.G. Cooks, Desorption electrospray ionization and electrosonic spray ionization for solid- and solution-phase analysis of industrial polymers, Chem. Commun. (Camb.) (2006) 888–890.
[12] A.B. Costa, R.G. Cooks, Simulated splashes: elucidating the mechanism of desorption electrospray ionization mass spectrometry, Chem. Phys. Lett. 464 (2008) 1–8.
[13] V. Kertesz, G.J. Van Berkel, Improved imaging resolution in desorption electrospray ionization mass spectrometry, Rapid Commun. Mass Spectrom. 22 (2008) 2639–2644.

[14] D.I. Campbell, C.R. Ferreira, L.S. Eberlin, R.G. Cooks, Improved spatial resolution in the imaging of biological tissue using desorption electrospray ionization, Anal. Bioanal. Chem. 404 (2012) 389–398.
[15] I. Cotte-Rodríguez, Z. Takáts, N. Talaty, H. Chen, R.G. Cooks, Desorption electrospray ionization of explosives on surfaces: sensitivity and selectivity enhancement by reactive desorption electrospray ionization, Anal. Chem. 77 (2005) 6755–6764.
[16] D.R. Ifa, N.E. Manicke, A.L. Rusine, R.G. Cooks, Quantitative analysis of small molecules by desorption electrospray ionization mass spectrometry from polytetrafluoroethylene surfaces, Rapid Commun. Mass Spectrom. 22 (2008) 503–510.
[17] R. Haddad, R. Sparrapan, M.N. Eberlin, Desorption sonic spray ionization for (high) voltage-free ambient mass spectrometry, Rapid Commun. Mass Spectrom. 20 (2006) 2901–2905.
[18] R. Haddad, R. Sparrapan, T. Kotiaho, M.N. Eberlin, Easy ambient sonic-spray ionization-membrane interface mass spectrometry for direct analysis of solution constituents, Anal. Chem. 80 (2008) 898–903.
[19] A. Hirabayashi, M. Sakairi, H. Koizumi, Sonic spray mass spectrometry, Anal. Chem. 67 (1995) 2878–2882.
[20] P.M. Lalli, G.B. Sanvido, J.S. Garcia, R. Haddad, R.G. Cosso, D.R.J. Maia, J.J. Zacca, A.O. Maldaner, M.N. Eberlin, Fingerprinting and aging of ink by easy ambient sonic-spray ionization mass spectrometry, Analyst 135 (2010) 745–750.
[21] E.M. Borges, D.A. Volmer, M.N. Eberlin, Comprehensive analysis of Ginkgo tablets by easy ambient sonic spray ionization mass spectrometry, Can. J. Chem. 91 (2013) 671–678.
[22] P.V. Abdelnur, S.A. Saraiva, R.R. Catharino, M. Coelho, N. Schwab, C.M. Garcia, U. Schuchardt, V. de Souza, M.N. Eberlin, Blends of soybean biodiesel with petrodiesel: direct quantitation via mass spectrometry, J. Brazil Chem. Soc. 24 (2013) 946–952.
[23] I.B.S. Cunha, A.M.A.P. Fernandes, D.U. Tega, R.C. Simas, H.L. Nascimento, G.F. de Sá, R.J. Daroda, M.N. Eberlin, R.M. Alberici, Quantitation and quality control of biodiesel/petrodiesel (Bn) blends by easy ambient sonic-spray ionization mass spectrometry, Energy Fuels 26 (2012) 7018–7022.
[24] Z. Takats, J.M. Wiseman, R.G. Cooks, Ambient mass spectrometry using desorption electrospray ionization (DESI): instrumentation, mechanisms and applications in forensics, chemistry, and biology, J. Mass Spectrom. 40 (2005) 1261–1275.
[25] C. Janfelt, A. Nørgaard, Ambient mass spectrometry imaging: a comparison of desorption ionization by sonic spray and electrospray, J. Am. Soc. Mass Spectrom. 23 (2012) 1670–1678.
[26] Y. Zhang, Z.Q. Yuan, H.D. Dewald, H. Chen, Coupling of liquid chromatography with mass spectrometry by desorption electrospray ionization (DESI), Chem. Commun. 47 (2011) 4171–4173.
[27] L.S. Eberlin, D.R. Ifa, C. Wu, R.G. Cooks, Three-dimensional vizualization of mouse brain by lipid analysis using ambient ionization mass spectrometry, Angew. Chem. Int. Ed. Engl. 49 (2010) 873–876.